SOLUBILITY AND PARTITIONING BEHAVIOR OF ORGANIC COMPOUNDS IN COMPLEX NAPL MIXTURES

By

DONGPING DAI

A DISSERTATION PRESENTED TO THE GRADUATE SCHOOL
OF THE UNIVERSITY OF FLORIDA IN PARTIAL FULFILLMENT
OF THE REQUIREMENTS FOR THE DEGREE OF
DOCTOR OF PHILOSOPHY

UNIVERSITY OF FLORIDA

1997

This dissertation is dedicated to

Dr. Richard Hartmann and Mrs. Remy Hartmann

for their love and support

ACKNOWLEDGMENTS

During past several years I received assistance from several people, which I greatly appreciate. First, I would like to thank my committee members, Professors Annable, Rhue, Harris and Kennedy, for their support and helpful comments. I especially thank Dr. Harris for facilitating the Scanning Electron Microscopy and X-ray Diffraction analyses of the soil particles.

I especially want to express my deep gratitude to my advisor Dr. Suresh Rao, for his initial inspiration as I pursued my doctoral study, for many intellectual and challenging discussions, and for his continual contribution to both my personal and professional growth. This work would be impossible without his encouragement and support.

I would like to thank Jim Jawitz , Randy Sillan, Ron Jesssup, Heonki Kim, Steve Trabue and Clayton Clark for their assistance support and friendship. I would like to especially thank Jim Jawitz for modifying the computer code for the model simulation presented in Chapter 3, Randy Sillan for continual assistance in helping with computer software and for scanning color photographs presented in Chapter 4, and Steve Trabue for help in formatting the dissertation.

I would especially like to thank Ms. Gloria Sillan for her assistance in conducting several experiments, help in editing my dissertation draft. Lane Evan for assisting with the UNIFAC simulations, while Claire Shaukla measured pentanol cosolvency. I would like to thank Linda Lee, now on the faculty at Purdue University, for her key role in helping me develop appropriate laboratory skills. I also like to thank my friends Yiqun Ding and Meifeng Zhou for their help and friendship.

It has been a pleasure to be affiliated with the Soil and Water Science Department at the University of Florida through both employment and education, and I would like to acknowledge both staff and faculty for their support for the past seven years. My special thanks go to Bill Reve and John Thomas for their support and friendship.

Finally, my very special thanks go to my parents and to my husband, Xiaokuang Lai, whose love and encouragement gave me strength during my graduate studies, my daughter, Diana, whose understanding and cooperation made this work possible.

TABLE OF CONTENTS

LIST OF TABLES

Table

LIST OF FIGURES

Figure

Abstract of Dissertation Presented to the Graduate School
of the University of Florida in Partial Fulfillment of the
Requirements for the Degree of Doctor of Philosophy

SOLUBILITY AND PARTITIONING BEHAVIOR OF
ORGANIC COMPOUNDS IN COMPLEX NAPL MIXTURES

By
Dongping Dai

December 1997

Chairperson: Dr. P.S.C. Rao
Major Department: Soil and Water Science/Hydrologic Sciences

Many industrial waste disposal sites are characterized by the presence of complex waste mixtures. The multi-component non-aqueous phase liquids (NAPLs) studied here are complex mixtures of environmental concern, and represent industrial wastes such as hydrocarbon fuels, cleaning solvents, and coal/oil tars. Estimation of solubility of organic contaminants from such NAPL into aqueous solutions, and prediction of their partitioning between aqueous and organic phases, are essential for characterizing NAPL contamination at waste disposal sites. This information is also required for remediation of NAPL source areas using aggressive techniques, such as in-situ flushing with cosolvents and surfactants to enhance NAPL solubility. The log-linear cosolvency model has been an effective tool to estimate the aqueous solubility of NAPL components with large molecular weights and low solubilities, and to examine the magnitude of solubility enhancement for given solute-solvent combination. Experimental data for solubilization of single- and multi-component NAPLs

in water and water-alcohol mixtures were collected for several NAPLs. These data were used to evaluate NAPL-water partitioning and cosolvent-enhanced solubilization in cosolvent mixtures. These data provide important information for simulating of aggressive remediation by in situ cosolvent flushing.

The partitioning tracer technique has been recently developed as an effective noninvasive technique for characterizing the amount and distribution of NAPLs in contaminated soils and aquifers. In this study, various assumptions made in the use of this tracer technique were evaluated. The partitioning of alcohol tracers was found to be non-linear in higher relative aqueous concentration range and higher mole fraction in the NAPL. This non-linear partitioning behavior can be predicted using the UNIFAC simulations. The partitioning of alcohol tracers between NAPL and water may exhibit a cooperative behavior in presence of other alcohols. Non-linear partitioning and co-tracer effects may have significant impact on the estimation of residual NAPL saturation using the partitioning tracer method if higher initial tracers concentration or mixed tracers are used.

Cosolvent flushing of coal tar-contaminated soils may alter the tar-water interface by exposing new coal tar coatings, or unmasking soil mineral surfaces that had been coated with tar. An increase in the retardation of alcohol tracers and benzene, and sorption of an ionic organic acid (PFBA) have been found for the methanol-washed coal tar soils. These changes in tracer partitioning behavior as a result of cosolvent flushing have important implications for assessing the extent of soil cleanup based on the partitioning tracer techniques.

CHAPTER 1
INTRODUCTION

Intentional or accidental release of various non-aqueous phase liquids (NAPLs) to the subsurface has resulted in unacceptable health risks based on potential exposure to contaminated soils, sediments and groundwater. The sources of contamination are varied, from simple, single-component NAPL (e.g., chlorinated solvents) to complex, multi-component NAPL mixtures (e.g., gasoline, jet fuel, coal tar, etc.). Constituents of these NAPLs that are of environmental concern, due to their potential carcinogenic nature (Guerin et al., 1978), include: monoaromatic hydrocarbons (MAHs), polycyclic aromatic hydrocarbons (PAHs) and chlorinated aliphatic/aromatic components. Several of these compounds are included in the U.S. EPA list of priority pollutants.

Processes controlling the disposition of the NAPLs in the subsurface include: mobilization, dissolution, phase partitioning, transport, and transformations. The mobilization of the NAPLs in porous media is governed by viscous and capillary forces (Schwille, 1988). Once the bulk fluid phase free NAPL stops migrating either upward or downward through the vadose and saturated zones, globules of residual NAPL trapped by capillary forces are left behind. Removal of the trapped residual NAPLs is dependent on the dissolution process in the soil and ground water systems. For vapor-phase transport in the vadose zone, NAPL-water-gas partitioning needs to be evaluated. Solubility and the

partitioning of the NAPL or NAPL components in the aqueous phase are the primary factors that determine the NAPL dissolution process. For multi-component complex NAPL mixtures, the solubility and partitioning behavior are also governed primarily by the composition of the mixtures.

Solubility and partitioning of organic components

Aqueous solubility of an organic compound is commonly defined as the abundance of the chemical per unit volume in the aqueous phase when the solution is in equilibrium with the pure compound in its actual aggregation state (gas, liquid, solid) at a specified temperature and pressure (e. g., 25°C, 1 atm)(Schwarzenbach, et al., 1992). Generally, the concentration of a saturated aqueous solution of the chemical is the chemical solubility. Solubility of organic chemicals can be modified by the presence of other organic molecules in water. When other organic molecules are present in relatively large abundance (more than 10% by volume), they act as solvent molecules themselves and partially surround the solute of interest approximately in proportion to their volume fraction in the solution (Yalkowsky and Roseman, 1981). For predicting organic chemical chemodynamics, the cosolvent effects on the solubility of organic compounds are of primary interest. The log-linear cosolvency model is one of several theoretical approaches that has been used to examine cosolvent effects on the solubility (Yalkowsky, 1985, 1987) and sorption (Rao et al., 1985). An extensive amount of data has shown that in mixed solvents, solubility of hydrophobic organic compounds (HOCs) increases and the sorption decreases in a log-linear manner as the volume fraction of the organic cosolvent increases (Rao et al ., 1985; Nkedi-

Kizza et al., 1985; 1987; Rubino and Yalkowsky, 1985; 1987a, 1987b, 1987c.). The log-linear models for solubility and partitioning in binary solvent systems are defined as follows:

$$\log S_m = \log S_w + \beta\sigma f_c \tag{1-1}$$

and

$$\log K_m = \log K_w - \sigma\alpha\beta f_c \tag{1-2}$$

where S is the component solubility (mg/L), and K is the component partition coefficient ;σ is defined $\sigma = \log [S_c / S_w]$, the subscripts c, w and m designating neat cosolvent, water and mixed solvent, respectively; and α and β are empirical coefficients that accounts for water-cosolvent and cosolvent-sorbent interactions. For a mixture of water and several cosolvents, assuming that the cosolvent effects are additive, the log-linear cosolvency model is extended as follows:

$$\log S_m = \log S_w + \Sigma\, \beta_j \sigma_j f_c \tag{1-3}$$

where the subscript j=1,2,...n designates the values for the j^{th} cosolvent, and n is the number of cosolvents in the mixture. With these log-linear relationships the aqueous solubility and partition coefficient of more hydrophobic components, which are often difficult to directly measure, can be estimated by log-linear extrapolation. The slope of log-linear relationship between solubility (S) of organic compounds and the volume fraction of organic solvents (f_c) yields the cosolvency power (σ), which serves as an index of the cosolvent's ability to enhance solubility.

At waste disposal sites, mixture of organic chemicals are present both as components of NAPLs and sorbed on to the solid matrix. The dissolution and desorption of organic compounds from an organic mixture may differ from the solubility of a pure organic compound. First, it is possible that the organic chemical of concern does not form an ideal solution in the liquid organic mixture. The more dissimilar (shape, size, polarity) the chemical is from the average nature of the organic mixture, the greater will be this nonideality. Second, the dissolution accounts for the dilution of the compound of interest by the other substances of the organic mixture, since organic mixtures are often made of numerous and unidentified compounds.

Under the assumption of ideal behavior of organic compounds in the organic mixture, the equilibrium partition of a compound between water and an organic mixture can be predicted by Raoult's law:

$$C_{w,i} = X_i^o \, S_{w,i} \tag{1-4}$$

where $C_{w,i}$ is aqueous concentration (mol/L) of component i, $S_{w,i}$ is aqueous solubility of pure liquid chemical (mol/L) of component i, and X^o_i is mole fraction of component i in the organic liquid. The aqueous concentration, $C_{w,i}$, can be estimated in mg/L using measurable parameters in commonly reported concentrations units by:

$$C_{w,i} = (M_i)(MW_{mix})(S_w)(10^{-3}) \tag{1-5}$$

where, M_i is the concentration (mg/kg) of organic compound of interest (i) in the NAPL mixture, MW_{mix} is the average molecular weight (g/mole) of the NAPL mixture. For

chemicals crystalline in their pure form at standard state, super-cooled liquid solubilities, S_{scl}, are used for S_w.

Under ideal conditions, solute concentration in the aqueous phase ($C_{w,i}$) follows Raoult's law (Banerjee, 1984) and is proportional to the mole fraction of solute in the organic phase. Thus $K_{p,i}$ can be stated as (Cline et al., 1991):

$$K_p = \frac{C_{o,i}}{X_{o,i} S_{w,i}} = \frac{(\rho_o / MW_o)}{S_{w,i}} \tag{1-6}$$

where MW_o and ρ_o are the average molecular weight and density of the organic phase, respectively. An inverse relationship between $K_{p,i}$ and $S_{w,i}$ is expected from equation (1-6), and a plot of log $K_{p,i}$ versus log $S_{w,i}$ will have a unit slope and the intercept will vary with the density and the average molecular weight of the organic phase (Cline et al., 1991; Lee et al., 1992b).

Excellent log-log, linear relationships have been reported between K_{oc} , the partition coefficient normalized by the fraction of organic carbon (OC) of the sorbent, and K_{ow} , the octanol-water partition coefficient for several hydrophobic organic compounds. (Karickoff, et al., 1979, Karickoff, 1981, Kenega and Goring, 1980, Rao et al., 1985). K_{oc} values have been used for comparing partitioning relationships between different soils. With varying amounts of organic carbon. K_{oc} is determined from K_w using :

$$K_{oc} = \frac{K_w}{f_{oc}} \tag{1-7}$$

As indicated in this equation, any factors that affect K_w measurement may affect the K_{oc} values, which include: (1) linearity of the sorption isotherm; (2) solids-to-solution ratio; (3) temperature; and (4) presence of other organic chemicals.

Several correlations between log K_{oc} and log K_{ow} have been reported in the literature (Hassett and Banwart, 1981; Karickoff, 1981, Gerstl, 1990, Schwarzenbach and Westall, 1981). Examples are as follow:

$$\log K_{oc} = 0.989 \log K_{ow} - 0.346 \quad (PAHs,\ r^2 = 0.997)(Karickhoff,\ 1981) \qquad (1\text{-}8)$$

$$\log K_{oc} = 0.72 \log K_{ow} + 0.49 \quad (methylated,\ halogenatedbenzenes,\ r^2 = 0.95)\ (Schwarzenbach \wedge Westall,\ 1981) \qquad (1\text{-}9)$$

However, correlations such as equation(1-8) did not give accurate predictions of partition of PAHs in soils at MGP sites (EPRI, 1992). The reasons for such a discrepancy include: (1) The soils used to develop such correlations are typically freshly spiked with the compound of interest, and compounds that have aged in soils for many years often behave differently than compounds freshly spiked onto soil (Sawheny et al., 1988); (2) Small residual amount of NAPL contaminants on the soil may be present either as fine coatings on soil particles or trapped in the interstices of soil particles; (3) Hysteresis between adsorption and desorption isotherms could cause desorption values of K_{oc} (obtained from contaminated soil) different from the adsorption values of K_{oc} (from clean soil and sediment).

The partitioning of organic chemicals from water to an organic (nonpolar) phase depends on the properties of the compounds and the system involved. The octanol-water system has been widely accepted as a reference in comparing the ability of a molecule to partition into defined solvent-water mixtures, because the partition coefficients from this system appears to be best correlated empirically with biological activity(Hansch, 1969, Hansch and Dunn, 1972; Hansch and Leo, 1979). Other environmental partition processes of organic solutes have also been evaluated with respect to octanol-water partition coefficients (Chiou and Block, 1986). Recently, coal tar/water partition coefficients (K_{tw}) were shown to be linearly correlated to octanol-water partition coefficient (K_{ow}). The statistical best-fit relationship is as follow (Lane and Loehr, 1992):

$$\log K_{tw} = 1.13 \log K_{ow} + 0.33 \qquad (1\text{-}16)$$

where K_{tw} is coal tar/water partitioning coefficient. Comparison of the partition behavior in liquid tar contrasted to partitioning from coal tar contaminated soil still needs to be investigated. Coal tar and coal tar components may interact with soil organic matter through physical and chemical processes occurring over long time periods (often decades), and thus alter the tar component partitioning behavior.

Cosolvent flushing for NAPL contaminated soils

Clean up of sites contaminated with NAPL or complex NAPL mixtures is a challenge for the environmental scientists and engineers. Many remediation techniques have been developed and tested at laboratory and field scales (NRC, 1994, 1997).. Cosolvent

flushing is among the emerging technologies (Rao et al., 1997; Sillan et al, 1997 and Jawitz et al., 1997). Cosolvent addition significantly enhances solute solubility as indicated by log-linear cosolvency model, and reduces the interfacial tension (IFT) between NAPL and aqueous or solid phase. IFT measurements for PCE/methanol-/water system (Imhoff et al, 1995) have demonstrated a significant decrease in IFT with increasing methanol/water fraction. By reduction of the interfacial tension between NAPL and the aqueous phase, the residual NAPL can be mobilized and previously trapped NAPL globules can be displaced through pore constrictions. Cosolvent enhances desorption and results in a concomitant reduction in retardation. Therefore, high NAPL removal efficiency is achieved by cosolvent flushing.

Augustijin (1994) has developed several models to simulate the effect of cosolvent flushing on removal of contaminated soils. Among them is the one-dimensional transport model based on the bicontinuum approach and sorption nonequilibrium. This model has been used successfully to simulate the cosolvent flushing of single-component contaminated soil column with a binary cosolvent solution (Augustijn et al, 1994). With some modifications made by Jawitz (1997), this model has been used here to simulate solvent flushing of multi-component NAPL in NAPL contaminated soil for field in-situ cosolvent flushing with binary and ternary solvent.

Partitioning tracers for prediction of NAPL residual saturation

To effectively remediate a contaminated site with any clean up technique, it is important to find the NAPL source and define the spatial distribution of the contaminates.

Recently developed partitioning and interfacial tracers methods have been an effective technique for characterization of NAPL contaminated soils and aquifers (Jin et al., 1995; Wilson and Mackay, 1995; Annable et al., 1995, 1997a) and for assessing the effectiveness and efficiency of cosolvent flushing for remediation of NAPL contaminated aquifer (Annable et al., 1995). There are many important details to consider to successfully apply partition tracer technology to the estimation of NAPLs in the subsurface environment.

Two of the major assumptions for partitioning tracer technique are that the tracer/NAPL partitioning should be linear over the range of the trace concentration, and that adsorption of each tracer on the mineral surfaces of the soil should be negligibly small. Tracer partitioning at liquid-phase mole fraction concentration lower than 0.01 is typically considered dilute in the chemical engineering field, or alternatively, phase equilibrium can be represented by a linear relationship (Henry's law) in this concentration range. As the mole fraction of a tracer increases, its activity coefficient decreases, which indicates that partitioning may be nonlinear. Wise (1997) have simulated the tracer partitioning between NAPL and water using the UNIFAC model. Nonlinear behavior was evident for tracer liquid-phase concentration above 0.1 mole fraction or tracer mole fraction in NAPL above 0.01. In addition, the tracer partition linearity was also a function of the presence of other tracers. Wise (1997) found that for alcohol tracer partitioning between NAPL/water phases, the nonlinearity and nonideality became less significant as concentration of other alcohols tracers increased in the NAPL phase. Here, I will present experimental assessment of these UNIFAC predictions.

Activity coefficient of the solute in the organic phase characterizes the nonideality

and nonlinearity of a compound in most of cases. A number of computational schemes are available to estimate various activity coefficients such that liquid-liquid partitioning for nonideal mixtures can be evaluated. Functional group methods such as UNIFAC provide an enormous flexibility and have been proven to be a fast and reliable tool for predicting liquid-phase activity coefficients. The UNIFAC model has been used to describe many environmentally important properties (Munz and Roberts, 1986, Lee et al, 1992b, Wise, 1997); among these are partition coefficient, water solubility and Henry's constant.

Tracer adsorption on the sand is assumed to be negligibly small compared to the very large retardation due to the residual NAPL saturation. However, for very low residual NAPL saturations (e.g., post-remediation) adsorption of some tracers on soils (especially, the native soil organic matter) may be significant. In addition, if soils have complex mineral background, the partitioning behavior of the tracers may also be altered. For the sorption of organic contaminants by soils containing residual petroleum, Boyd and Sun (1990) hypothesized that the soils may be treated as a three-component system consisting of (1) an inert mineral phase, (2) a sorptive natural soil organic matter phase, and (3) a highly sorptive residual petroleum phase. For accurate prediction of soil-water distribution coefficients in such contaminated soils and sediments, the oil components, along with the natural organic matter component must be measured and accounted for individually (Boyd and Sun, 1990)

. Selective removal of organic components from complex NAPL mixtures during cosolvent flushing may alter the residual NAPL composition, thus, the partitioning behavior of the tracers in post-remediated soil may change. Removing NAPL coatings and exposing the new inorganic or organic components, may have significant effect on the tracer

partitioning behavior, especially for post remediated soils. Therefore, it is important to consider these factors in using partition tracer techniques for evaluating the performance of in-situ flushing techniques.

Dissertation themes:

The focus of my dissertation research work was on understanding the aqueous solubility organic components from environmentally relevant, complex NAPL mixtures. The liquid-liquid partitioning behavior of these organic components between the NAPL and water was investigated. These results were compared with Raoult's law prediction and published data, and discussed in Chapter 2. Cosolvent flushing was evaluated to clean up soils contaminated with complex NAPL mixtures. Both binary solvent (ethanol/water) and ternary solvent (ethanol/pentanol/water) mixtures were used in the study. Effectiveness of the binary and ternary solvent in remediation was evaluated and compared. A solvent flushing model was used to simulate the column effluent profiles, and the model predicted concentration profiles were compared with experimental data (Chapter 3).

To effectively remediate a contaminated site, it is important to characterize the NAPL content and distribution. Partitioning tracer techniques have provided such a tool to quantify the NAPL residual saturation in contaminated soils. However, several factors have to be considered in interpreting the tracer data (Chapter 4), these included: (l) linearity of the tracer on the partition was investigated when high tracer initial concentrations were applied or other components were present; (2) the impact of changing in NAPL composition and the partitioning coefficients for remediated soils on estimation of the NAPL recovery and

flushing efficiency; (3) some special cases of tracer partitioning on post-alcohol solvent flushing for contaminated soils were discussed and the mineral and organic background of the soils were investigated. A synthesis of these finding and suggestions for further work are presented in Chapter 5. Finally, several appendices are included to document some of the data or methods.

CHAPTER 2
AQUEOUS SOLUBILITY AND NAPL-WATER PARTITIONING

Introduction

Solubility is a major factor governing the fate and transport of non-aqueous phase liquids (NAPLs) in geologic media. Such media of environmental interest include soils, sediments, and aquifers. Estimation of solubility of organic contaminants from NAPL into aqueous solutions, and estimation of their partitioning between aqueous and organic phases are essential for predicting the release of organic contaminants from NAPLs in the subsurface environment. This is also important for two distinct scenarios: (1) characterizing contamination resulting from NAPLs at waste disposal sites; and (2) remediation of NAPL source area by aggressive techniques such as in-situ flushing. In the first case, predicting solubility in aqueous solution is necessary for defining the source loading function that controls the characteristics of the dissolved contaminant plume. Aggressive remediation by in situ flushing usually involves addition of cosolvents and surfactants to enhance NAPL solubility. Thus, the effects of these solubility modifiers must be measured, and the

observations matched with predictions based on either empirical or theoretical models. In this chapter, issues related to measuring NAPL component solubility in aqueous and mixed solvent systems is examined. The organic solutes of interest are components of non-aqueous phase liquids (NAPLs), either single-component liquids or complex solute mixtures.

The addition of polar organic solvents that are completely miscible or highly soluble in water (e.g., methanol, ethanol and butanol) to a NAPL-water system results in an increased concentration of the organic constituents of the NAPL in the aqueous-rich phase. The magnitude of such a solubility enhancement depends on the solute-solvent and solvent-solvent combinations. Greater hydrophobicity of the solute and the cosolvent results in larger enhancement of NAPL component solubility in the solvent mixture. Rao et. al (1985) applied the log-linear cosolvency theory, adopted from the pharmaceutical literature (Yalkowsky and Roseman, 1981), to predict the inverse relationship observed between the logarithm of solubility and the volume fraction of cosolvent. This relationship allowed estimation of solubility or NAPL-water partition coefficients for organic compounds with extremely low aqueous solubility for which direct experimental measurement is fraught with difficulties associated with a spectrum of experimental artifacts.

The slope of a log-linear relationship between solubility (S) of organic compounds and the volume fraction of organic solvents (f_c) yields the cosolvency power (σ), which serves as an index of the cosolvent's ability to enhance solubility. Many researchers have developed and emphasized the basic theory for cosolvent enhancement of the solubility of hydrophobic organic compounds (Rao et al., 1990; Pinal et al., 1990; Yalkowsky and Roseman, 1981; Yalkowsky, 1987; Morris et al., 1988; Nkedi-Kizza, et al, 1985). The log-linear cosolvency

model has been used to estimate the solubility and partition coefficients of hydrophobic compounds or components from complex NAPL mixtures (e.g., gasoline, diesel fuel and coal tar) (Cline et al., 1991; Lee et al., 1992a; Lee et., al 1992b).

The research summarized in this chapter focuses on the following primary tasks:

1. Estimate the aqueous solubility of single-component NAPLs and aqueous solubility of specific (target) components in complex NAPL mixtures using the log-linear cosolvency theory;
2. Evaluate the ability of organic cosolvents to enhance the solubility of NAPL components, and estimate the appropriate cosolvency powers;
3. Examine the partitioning behavior of target components of NAPL mixtures in NAPL/water or contaminated soil /water systems; and
4. Evaluate whether the solubility/partitioning behavior of target components in complex NAPL mixture and contaminated soils can be approximated using the theory of ideal mixtures (Raoult's Law).

Solubility and partitioning were examined in batch equilibration experiments involving binary and ternary solvent mixtures used to solubilize components of single- and multi-component NAPLs. Solubility under dynamic flow conditions in packed columns is discussed in Chapter 3.

Materials and Methods

Solutes and NAPLs

Two types of multi-component complex NAPLs were examined in this study: (1) a mixture of jet fuel and chlorinated solvents, collected at a contaminated site at Hill AFB, UT; and (2) Coal tar contaminated soils collected at several former MGP sites. The chemical and physical properties of the solutes (or target analytes) evaluated in this study are listed in Tables 2-1 and 2-2. The solutes listed in Table 2-1 are also major components of the Hill AFB NAPL and the NAPL-contaminated soil collected from the field site. The complex NAPL used in this study was a mixture of JP-4 jet fuel and degreasing solvents found at a chemical disposal site on Hill AFB, Utah; at this site, the University of Florida group conducted an in situ flushing study using cosolvents (Rao et al., 1997) and a second study with surfactants (Jawitz et al., 1997). The multiple waste disposal practices at this site over an extended period (1940-1970) caused an extensive NAPL plume in groundwater. The target components selected for this study represent various chemical classes and mass fractions in the NAPL. These compounds will be referred to as the 'target components" for NAPL and NAPL contaminated soil.

The major polyaromatic hydrocarbons (PAHs) found in coal tar and coal tar contaminated soils are listed in Table 2-2. Coal tar-contaminated soils were provided by Electric Power Research Institute (EPRI) and the Gas Research Institute (GRI), and were collected at former manufactured gas plant (MGP) sites. A broad range of organic contaminants, including primarily polycyclic aromatic hydrocarbons (PAHs) and monocyclic aromatic hydrocarbons (MAHs), are of concern at MGP sites (Guerin et al., 1978). The contaminated soils evaluated and their physical properties are listed in Table 2-3.

Table 2-1. List of physical-chemical properties of selected target components

[1]Compound	[2] MW	[a]Density (g/ml)	[a]Boiling point (°C)	[b]log K_{ow}	[a]Solubility (mg/L, at 20°C)
Tetrachloroethylene	165.16	1.623	121.4	2.53	240
m-Xylene	106.16	0.864	139	3.20	175
p-Xylene	106.17	0.86	138.4	3.09	198*
o-Xylene	106.17	0.88	144.4	3.09	175
1,2-Dichlorobenzene	147.01	1.305	179	3.38	100(154 [c])
1,2,4-Trichlorobenzene	181.46	1.574	213	4.1	19 (49 [c])
1,3,5-Trimethylbenzene	120.19	0.865	164.7	3.55	98 [c]
1,2,4-Trimethylbenzene	120.19	0.88	169	3.55	57
Naphthalene	128.16	1.152	217.9	3.59	20
n-decane	142.28	0.73	173/174	6.00	0.009
n-undecane	156.31	0.7402	196	NA	NA
n-tridecane	184.37	0.755	225.5	NA	0.013**

[a]Verscheren (1983); [b]Abernethy et al., (1988); [c]Chiou and Block (1986).
[1]All compounds were purchased from Aldrich Chemical Co. and used as received.
[2] Molecular weight
* at 25 ^{0}C
NA: not available.

Table 2-2. Physical and chemical properties for selected PAHs found in several coal tar samples collected at former Manufactured Gas Plant sites (Adopted from Lee et al., 1992b)

*Compound	mp[a] (°C)	MW[a] (g/mole)	S_w[b] (mg/L)	log S[d]	log K_{ow}
naphthalene	80.2	128.2	32	-3.05	3.37
1-methylnaphthalene	-22	142.2	27	-3.72.	4.00
2-methylnaphthalene	34	142.2	26	-3.62	4.00
acenapthylene	82	152.2	3.93	-4.02	4.07
acenapthene	93	154.2	3.42	-3.98	3.92
fluorene	116.5	166.2	1.9	-4.03	4.18
phenanthrene	100	178.2	1.0	-4.5	4.46
anthracene	216.3	178.2	0.07	-4.49	4.45
fluoranthene	107	202	0.27	-5.19	5.33
pyrene	150	202	0.16	-4.85	5.18
chrysene	254	228.2	0.006	-5.29	5.61
benz(a)anthracene	156	228.2	0.0057	-6.29	5.61
benzo(a)pyrene	179	252	0.0038	-6.28	5.98

[a]Verschueren (1983). [b]Crystal solubility at 25 [0]C (Little,), unless stated otherwise. [c]Miller et al., (1985). [d]Supercooled liquid solubility calculated by assuming a constant ΔS_f for PAHs (Lee et al., 1992b).

*All compounds were purchased from Aldrich Chemical Co. at >98% purity except for acenaphthene, which was available only at 85% purity.

Table 2-3. Selected physical and chemical properties for the contaminated soils investigated.

Soil ID	Texture	Water Content as reseived (%)(wet basis)	Total Organic Carbon Content (%)	Total PAHs (mg/kg soil)
OU-1	Sand	16	2.54	*S_N = 0.067
UT586	Sand	10	0.62	320
UT690	Sand	12	2.7	3,472
Waterloo	very fine sand	34	9.3	17,600

* residual NAPL saturation, estimated by partitioning tracers method (Annable et al., 1995).
$S_N = \theta_N / \theta_w + \theta_N$, where θ_N is volumetric NAPL content and θ_w is volumetric water content

Solvent selection

Ethanol (absolute, 200 proof) from AAPER Alcohol and Chemical Co, and reagent-grade pentanol from Fisher Scientific Co., were selected as the two main alcohols for this study. NAPL solubility enhancement was examined in both binary solvents (ethanol-water or methanol-water), and in ternary solvent mixtures (ethanol-pentanol-water). These two solvents were also used in the field test cell for *in-situ* cosolvent flushing remediation at Hill AFB, UT (Rao et al., 1997). Lab experiments were conducted using both the binary and ternary solvent mixtures. Reagent-grade methylene chloride from Fisher Scientific Co. was also used in combination with or without ethanol to make standard solutions, to completely dissolve the NAPLs (including coal tar), or to extract the maximum amount of target analytes from the tar-contaminated soils. Deionized and distilled water (DDI water) and Optima-grade water (Fisher Sci. Co.) were used in all solubility experiments.

Preparation of organic solvent solution

Binary solvent mixtures of ethanol and water were prepared as follows: 0, 10, 20, 30, 40, 50, 60,70, 80, and 90 ml of ethanol were mixed with 100, 90, 80,70,60,50,40, 30, 20, and 10 ml of water, respectively. For ternary mixtures of ethanol/pentanol/water, 2, 4, 6 ,8, 10, 12, 15, 20, and 25 ml of pentanol and 28, 26, 24, 22, 20, 18, 15, 10, and 5 ml of water were added to 70 ml of ethanol. The volumes of cosolvent and water were measured separately and combined so that the volume fraction of cosolvent would not change if volume shrinkage occurred upon mixing. Each solvent mixture was stored in a glass bottle with a Teflon lined cap.

NAPL solubilization

Exact amounts of single- or multi-component of NAPL (0.25xx g) were weighed into 5-ml HPLC vials, and 4.5 ml of cosolvent mixture were transferred to the vials for a NAPL/solvent ratio of 1:18. The vials were then capped with Teflon-lined caps. Exact amounts of NAPL contaminated soil (4.5xxxg of moist soil) were weighed into 5-ml HPLC vials, and 1.5 ml of cosolvent mix solution were transferred to the vials; the soil/solution ratio used was 1:3, based on moist soil, or 1:2, based on oven dry soil. All measurements were triplicated. These solutions were then equilibrated on a rotator for 24 hours at room temperature (23 ±2 °C) and were centrifuged at 3000 rpm for 25 minutes (DuPont, Sorvall RT6000 Centrifuge). In all cases, a small excess of NAPL was present at the end of equilibration period. A 2-ml aliquot of the supernatant was removed and placed in 2-ml GC vials with minimal head space, and analyzed by GC-FID. For supernatant with high concentration (beyond concentration of the highest standard), appropriate dilutions were made with appropriate cosolvent mixtures.

Exact amounts of NAPL or NAPL contaminated soil were weighed into 5-ml HPLC vials, and a known volume of 50/50 (v/v) ethanol/methylene chloride solution was added. The NAPLs dissolved completely in this solvent mixture. From the constituent concentrations measured by this method, the total mass (S_o) of the target components in the NAPL mixture was estimated.

Chromatographic analysis

Analysis of NAPL target components A set of standard solutions for target analytes was made from pure chemicals purchased from different suppliers. Their chemical names,

chemical and physical properties, and sources are listed in Table 2-1. Exact amounts of chemicals were weighed into volumetric flasks with methanol/methylene chloride (50/50 v/v) solvent, and diluted sequentially to cover the range of concentrations up to the NAPL solute solubility. Standards were run on the GC-FID with each set of samples.

Target analytes present in the NAPL and NAPL contaminated soil were analyzed by GC/ FID; using a Shimadzu GC-17A Gas Chromatogram with a (30-m long , 0.53 mm ID, and 3 μm film thickness) DB-624 capillary column. The chromatography conditions were as follows: Injector temperature: 220 °C; Detector temperature: 240 °C; Oven Initial temperature: 50 °C, held for two minutes, 50 to 180, ramp at 10 °C /min, 180 to 235, ramp at 20 °C/min, held for 15 minutes. Helium was used as the carrier, set at a pressure of 35-40 kpsi. For analysis of some single-component NAPLs, the runn time was shortened by changing the final holding time to 5 minutes. Each batch of GC-FID analysis included the analysis of five standards of known concentration at beginning of the run, followed by samples of unknown concentration. The standards were also analyzed intermittently during the run.

Each target component in the NAPL mixture was previously identified by GC-MS, and was matched to the component chromatogram of the standard in the GC-FID analysis. In the standard, *p*-xylene and *m*-xylene peaks were overlapped, the 1,3,5-trimethylbenzene and decane peaks did not have baseline separation, but the other solutes had well-resolved, baseline-separated peaks. The concentration of a target analyte in the solution was based on the area determined in the chromatographic analysis by using the standard calibration curve.

Analysis of PAHs Standards of 16 PAH mixtures in methylene chloride were purchased from Ultra Scientific (US-106). 1-methylnaphthalene and 2-methylnaphthalene were added into the standard through serial dilution. Standards of 18 PAH mixtures, with each component concentration ranging from 0.2 to 200 mg/L, were used in quantitative analysis of the supernatant from coal tar contaminated soils.

PAH concentration in the supernatant was determined by using the Shimadzu 14A gas chromatogram (GC) system, equipped with a FID detector and a J&W DB-5 column (30 m x 0.32 mm i.d. 0.5-μm film thickness). Helium was used as a carrier gas at a pressure of 2 kg/cm^2 (at 50 °C), and a flow rate of approximately 1.0 ml/min. Both injector and FID detector temperatures were set at 295 °C. The oven temperature program consisted of an initial temperature of 50 °C, held for one minute; a ramp to 130 °C at 30 °C/min., held for three mins; a ramp to 180 °C at 12 °C/min., held for one minute; a ramp to 240 °C at 7 °C/min.; and a ramp to 300 °C at 12 °C/min., followed by 8 minutes holding.

Data analysis

The solubility of a solute was directly measured by GC-FID analysis or corrected with appropriate dilution factor. For a solute in contaminated soils, the volume of the solvents and the component concentrations were corrected for by the soil water content. All the fractions of the organic solvents were corrected for the soil water content. The solute partition coefficient was estimated by using a mass balance method. An example of the mass balance and partitioning equations follows:

$$S_o M = S_e M + C_w V \qquad (2\text{-}1)$$

then,

$$S_e = S_o - C_w \frac{V}{M} \qquad (2\text{-}2)$$

where $S_o M$ is the initial mass of the components in the NAPL or on the contaminated soil used. On the right hand side of the equation, $S_e M$ is the mass of the components in the NAPL or in the soil; and $C_w V$ is the mass of components in the aqueous phases at the equilibrium. M is the mass of NAPL or soil, while V is the volume of the water or cosolvent . As shown in equation 2-1, C_w values are dependent on both the V/M ratio (the volume of liquid in contact with NAPL or soil) and S_o (the initial component loading in the NAPL or the soil). In order to insure adequate mixing and to meet laboratory handling requirements, V/M ratios used in this research were much higher than those, typical for field conditions.

The partitioning coefficient (K_p) between the NAPL or soil and cosolvent liquid phases for the batch experiments can be defined as:

$$K_p = \frac{S_e}{C_w} = \frac{S_o}{C_w} - \frac{V}{M} \qquad (2\text{-}3)$$

where K_p is the partition coefficient between the NAPL or soil and cosolvent (water), C_w is the equilibrium concentration of the compound in the solution, and S_e is the equilibrium concentration of the compound in the NAPL soil.

The aqueous solubility of target components or the target components NAPL /water partition coefficients were estimated using log-linear cosovlency models as described below. By plotting log measured solubility, or partitioning versus volume fraction of organic solvent, a log-linear relationship is expected:

$$\log S_m = \log S_w + \Sigma \beta\sigma f_c \tag{2-4}$$

$$\log K_m = \log K_w - \Sigma \alpha\beta\sigma f_c \tag{2-5}$$

where σ is a cosolvency power defined previously in Chapter 1; α and β are empirical coefficients that account for sorbent-solute interactions and water-cosolvent interactions, respectively; S and K are the solubility and the partition coefficient of target components with the subscripts w and m designating water and mixed solvent, respectively; f_c is the volume fraction of organic solvents.

When comparing partition relationships between different soils, K_{oc} values were used. K_{oc} is the partition coefficient normalized to the fraction of organic carbon present in the soil (f_{oc}). The purpose of K_{oc} is to compare partitioning behavior in different soils with varying organic carbon content. K_{oc} is determined from K_w using :

$$K_{oc} = K_w / f_{oc} \tag{2-6}$$

K_w is the partition coefficient between the soil and water.

Note that for NAPL (or soil) equilibration with a binary solvent, we have (combining Eqs. 2-1, 2-2, 2-3, and 2-5):

$$S_o M = (K_p M + V) C_e \tag{2-7}$$

$$C_e = \frac{S_o}{(K_p + V/M)}, \quad \textit{for aqueous solutions} \tag{2-8}$$

$$C_e = \frac{S_o}{(V/M + K_w 10^{-\alpha\beta\sigma f_c})}, \quad \textit{for binary cosolvent mixtures} \tag{2-9}$$

where Ce is the equilibrium solute concentration in water or cosolvent mixture, and the cosolvency parameters: α, β, and σ are as defined in Eq (2-5). Also, note that the maximum solution phase concentration is given by:

$$C_{e,\max} = \frac{S_o M}{V} \tag{2-10}$$

where all of the NAPL component dissolves completely in the solution phase. Finally, at $f_c = 0$ (aqueous solution),

$$C_{w,i} \simeq X_i C_{sol,i} \tag{2-11}$$

where $C_{sol,i}$ is the aqueous solubility limit for "pure" component, X_i is the mole fraction in NAPL of the *i*-th component, and $C_{w,i}$ is aqeous concentration of the *i*-th component. (see chapter 1 for further details). When $V/M \ll K_p$, $C_e \simeq S_o / K_p$, or for mixed solvents:

$$C_e \simeq (S_o)\ (10^{\alpha\beta\sigma f_c}) \tag{2-12}$$

or

$$\log C_e = \log S_o + \alpha\beta\sigma f_c \tag{2-13}$$

Results and Discussion

Solubility in binary solvents

Solubility of single-component NAPLs Measured and log-linear extrapolated aqueous solubilities of analytes in single-component NAPL are summarized in Table 2-4. Also shown are the literature-reported aqueous solubility for these analytes. Some examples of solubility plots are shown in Figure 2-1(The rest are in Appendix A). As expected, the analytes' solubility increases log-linearly with the increasing fraction of cosolvent.

In most cases, plots of log (S_m) versus f_c yielded a straight line for ethanol fraction ranging from 0 to 0.8. Thus, mutual miscibility was not significant for $f_c \leq 0.8$. All alkanes showed higher measured aqueous solubility at low cosolvent (<0.3 f_c of ethanol); the plots were linear only from f_c range of 0.3 to 0.8. The log-linear extrapolated aqueous solubilities and the cosolvency power (slope) were based only on of the linear part of the plots.

Solubility of analytes from NAPL mixtures Target analyte solubilities in cosolvents, measured using the OU-1 NAPL mixture, are summarized in Appendix A. Examples of the log (S_m) versus f_c for the NAPL mixture, shown in Figure 2-2, were linear for the range 0 to 0.7. Above 0.7 f_c, the plots tended to level off, especially for those analytes with higher aqueous solubility or lower mass or mole fraction in the NAPL. Similar trends were found for log (S_m) versus fraction of pentanol with 0.7 fraction of ethanol. Only the linear parts of the plots were used to estimate the slope (cosolvency power). The change of mole fraction in some of the components in the NAPL mixture, with a fraction of organic solvent in the system, are also shown in Figure 2-3.

Table 2-4. Summary of measured and log-linear extrapolated aqueous solubility for single NAPL

Compound	[a] log S_1	[b]log S_w	[c]Slope	r^2	range of ethanol f_c
1,3,5-Trimethylbenzene	1.990	1.320	4.767	0.975	(0.3-0.8)
Decane	-2.046	-1.132	6.563	0.987	(0.3-0.7)
1,2,4-Trimethylbenzene	1.756	1.403	4.244	0.975	(0.3-0.8)
1,2-Dichlorobenzene	2.000	1.750	4.100	0.977	(0.3-0.7)
Undecane	NA	-1.872	7.498	0.972	(0.3-0.8)
1,2,4-Trichlorobenzene	1.279	1.037	4.933	0.981	(0.1-0.7)

[a] Log solubility values from Verscheren (1983) and Chiou et al., (1982)
[b] based on linear extrapolated from plot of log S_m vs fc of ethanol in this study.
[c] Slope of the log S_m vs fc of ethanol, slope = $\beta\sigma$

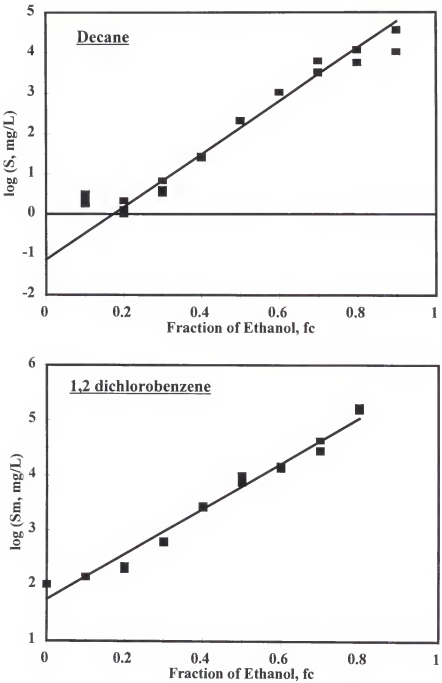

Figure 2-1. Relationship between log solubility of organic chemicals versus volume fraction of ethanol in ethanol/ water solution (single component NAPLs)

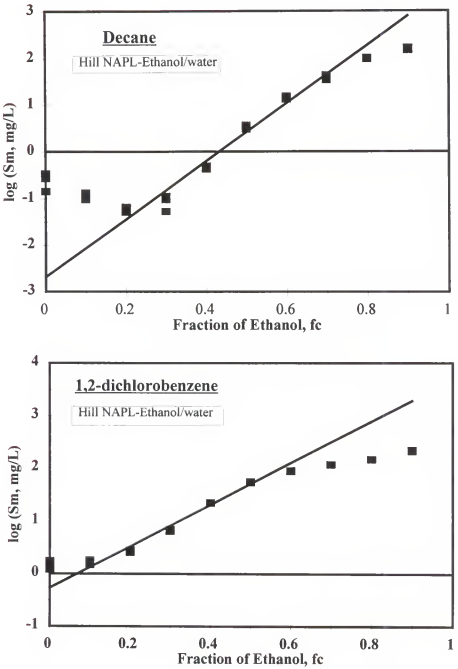

Figure 2-2. Solubility of NAPL target components from Hill AFB NAPL in ethanol/water solution

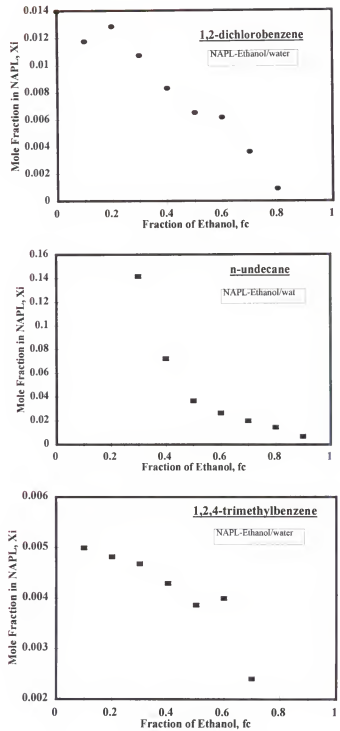

Figure 2-3. Relation beween mole fraction of components in Hill NAPL versus volume fraction of ethanol.

An inverse relationship for the changing mole fraction of a component in NAPL with increased ethanol fraction was obvious.

Most log-linear extrapolations were based on the solubility in ethanol fraction from range 0.2 to 0.8. This range was experimentally chosen because: 1) log S_m versus f_c were linear within this range for most of the components; 2) at low cosolvent fractions (<0.2 or <0.3 for high molecular, low solubility components), the cosolvent effect on solubility was not enough to give reliable measured values; 3) most NAPL components in this study are liquid at room temperature, they are miscible with 100% ethanol and partially miscible with high cosolvent fraction mixture for more soluble single NAPL. Thus, end to end sigma (σ = log (S_c/S_w) value are impossible to obtain; (4) since the solution/NAPL ratio used in the study was about 18:1, complex NAPL mixture components with low mole fraction in the NAPL may be exhausted in higher fraction ethanol solutions (see Eq. 2-12 and Figure 2-4), resulting in an underestimation of the component solubility.

The log-linear solubility equation has been found to be valuable in estimating the solubility of the poorly soluble drugs in binary and ternary mixtures of cosolvents and water (Rubino and Yalkowsky, 1984, 1985, 1987a; and Yalkowsky and Rubino, 1984). For most of the cosolvents tested, some degree of deviation from ideal solubilization behavior exists. The extent of deviation depends upon both the type and amount of cosolvent used. The largest deviation is seen when higher volume fraction (0.7-0.9) of cosolvent are used and is greater for ethanol-water systems than the methanol-water or glycol-water systems (Rubino and Yalkowsky, 1985). The "S" shaped solubilization curve was also found for two organic chemicals in alcohol-water mixtures, and the degree of curvature is much higher for ethanol than for methanol (Rubino and Yalkowsky, 1984, 1985).

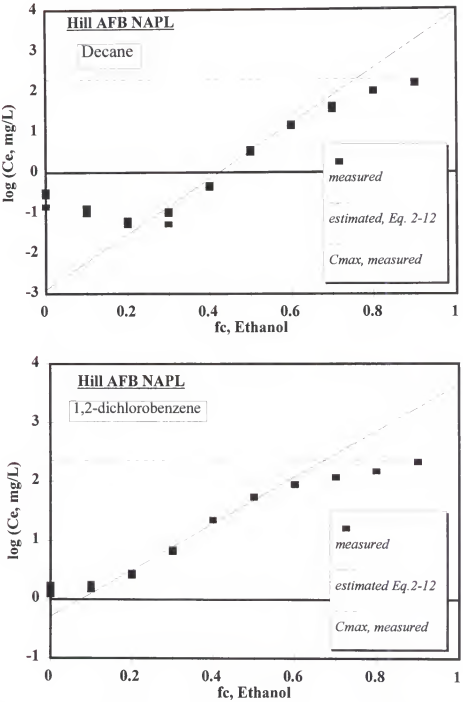

Figure 2-4. Log solubility vs fc for NAPL target components from Hill AFB NAPL in ethanol/water solution, with estimated log S vs fc from Eq. 2-13 and maximum component concentration (Cmax) measured by methylene chloride extraction.

Very few data are available for aqueous solubility of higher carbon number alkanes (C>10). Verschueren. (1983) reported aqueous solubilities of 9 μg/L at 25 °C for decane and 13 μg/L for tridecane at 25 °C. The measured solubilities of n-alkanes were C_{10}, 52 μg/L and C_{11}, 4.4 μg/L (compare with C_{10},74 μg/L and C_{11}, 13.4 μg/L from log-linear extrapolation in this study (Table 2-4)) , and a predicted solubility for C_{12} is 3.4 μg/L by extrapolation (McAuliffe, 1967). The log solubility of n-alkanes in water decreases linearly with increase in carbon number from C_4 alkane through C_9 alkane (McAuliffe, 1967). It has been suggested that if the relation is a continuous function, the solubilities in water of longer-chain n-alkanes could be predicted by extrapolation. However, Baker (1967) found that C_{12} - C_{36}, n-alkanes are solubilized in water at increasingly higher concentrations than anticipated from exptrapolation from data for C_1 to C_{10} alkanes. It appears that a change from a state of true solubility (molecular dispersion) to molecular aggregations occurs at C_{11} (Baker, 1967).

Several methods to estimate aqueous solubility for organic compound have been reported by Yalkowsky and Banerjee (1992). However, for higher carbon number alkanes, estimation of aqueous solubility using these methods is still difficult. For example, the aqueous solubility of higher alkanes can not be estimated using log S_w and log K_{ow} relation because the log K_{ow} for alkanes are also not easy to measure or find in literatures .

Solubility of analytes from NAPL-contaminated soil Target analyte solubilities in the alcohol-water mixtures measured using NAPL-contaminated soil from Hill AFB are summarized in Appendix A. Examples of log (S_m) versus f_c plots, shown for ethanol-water mixtures in Figure 2-5, were linear for the range of 0 to 0.7 for some analytes. The highest

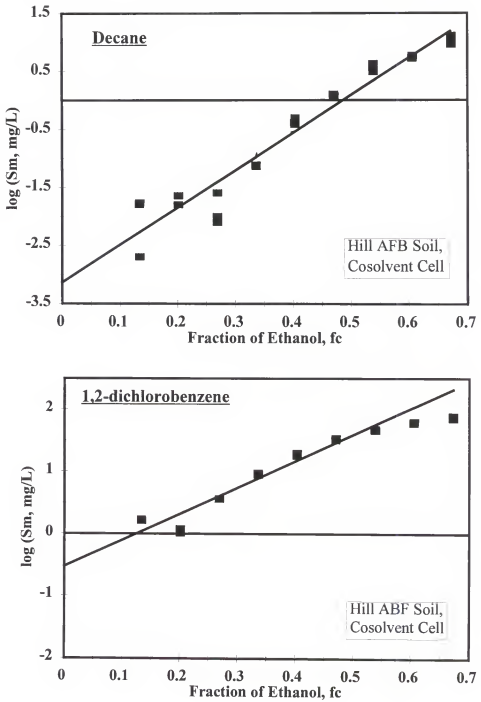

Figure 2-5. Linear relationship between log solubility of target components versus volume fraction of ethanol for NAPL contaminated soil (Hill AFB) in ethanol/water solution

ethanol fraction in the study, with the correction for soil water content, was 0.67 (volumetric basis). The soil:solution ratio used was about 2.5. The log S_m for most of the components increased linearly with ethanol fraction, f_c over the whole range of the ethanol fraction. Only the solubility of 1,2-dichlorobenzene showed a tendency of leveling off with increase of the ethanol fraction. This may due to depletion of the mass at high ethanol f_c for 1,2 - dichlorobenzene. The linear part of the log S_m versus f_c was used for estimating cosolvency powers and extrapolating aqueous solubility for all the target analytes.

Comparison of cosolvency power measured from different systems

The cosolvency power (σ) (i.e., the slope of log-linear plot), estimated from single-NAPL component (σ_{single}) and multi-component NAPL ($\sigma_{mixture}$) were compared by plotting the $\sigma_{mixture}$ versus the σ_{single} (Figure 2-6A). A 1:1 ideal line is included in these plots for easy comparison. Figure 2-6A shows that the points for methyl- or chloro-benzenes fall on the 1:1 line; however, the data for alkanes, especially for undecane, falls significantly below the 1:1 line, which indicate that $\sigma_{mixture}$ value is lower than σ_{single} value. In a similar way, the cosolvency power values estimated from the data for NAPL contaminated soil (σ_{soil}) were also compared with $\sigma_{mixture}$ values (Figure 2-6B). Data for all the components are found above the 1:1 line, except for *o*-xylene. The higher σ_{soil} values indicate that interaction between soil and solvent or soil and solutes are greater (i.e., $\beta > 1$, since the cosolvency power (σ) referred to here is the slope of log-linear plot which includes β (equation 2-4). Over all the cosolvency power (σ) from different systems (single vs mixtures, mixtures vs soil) resulted in less 1 than unit difference for most of components.

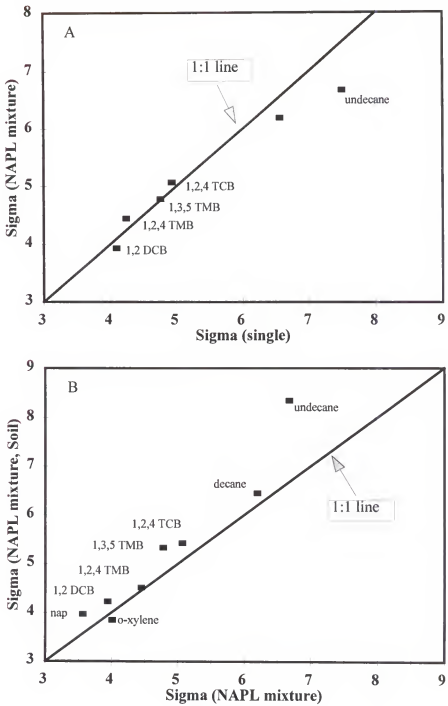

Figure 2-6. Comparison of sigma from NAPL mixture with sigma from single NAPL (A), and sigma from NAPL mixture with NAPL soil (B) for target components.

Morris et al (1988) proposed relationship between σ and log K_{ow} as:

$$\sigma = a \log K_{ow} + b \qquad (2\text{-}14)$$

where *a* and *b* are the slope and intercept of the of the σ vs. log K_{ow} plot. Here, σ is the terminally based slope, i.e., $\sigma = \log (S_c / S_w)$, S_c is the solubility in pure solvent, S_w is aqueous solubility. Equation 2-7 predicts that for a given solvent system, the terminally based slope of the log-linear solubility plot is proportional to the solutes's octanol-water partition coefficient. The *a* and *b* values estimated by Morris et al (1988) for σ in the ethanol-water systems based on solubility data for 11 PAHs were 0.85 and 0.81, respectively. Morris's line is included in the Figure 2-7, where the σ values for the target components from NAPL (Figure 2-7A) and NAPL-contaminated soil (Figure 2-7B) are plotted versus the corresponding log K_{ow} values in ethanol-water systems. The data from this study deviate from Morris's line, several factor may attributed to the deviation: (1) the σ from Morris et al (1988) were estimated from the terminal slopes of the solubility curves, while the σ values in this study are estimated from a more limited range of ethanol fraction, (due to the complete miscibility of the solute, the value of solute solubility data in the pure solvent were unavailable); (2) the compounds used to estimate the *a* and *b* for Morris' line are limited only to a group of PAHs, while in this study, a borader spectrum of components are examined.

Solubility in ternary solvent mixtures

Pentanol is not miscible with water, with an aqueous solubility is about 2.5%. It is difficult to measure the cosolvency power of pentanol itself. Thus, pentanol cosolvency was

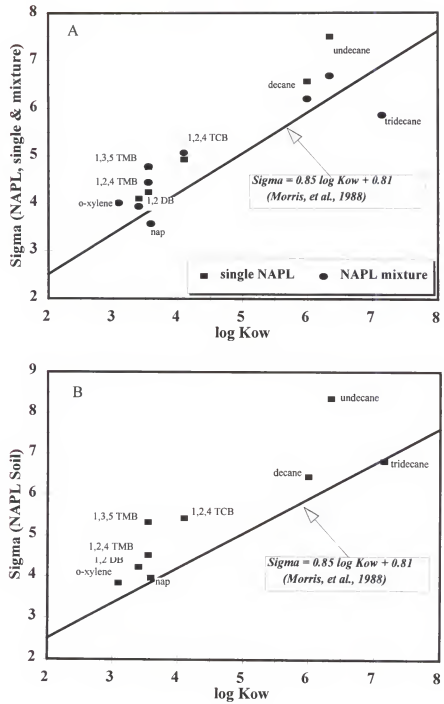

Figure 2-7. Sigma versus log Kow for target components in ethanol/water, from (A) NAPL mixture and single NAPL ; (B) NAPL contaminated soil.

estimated based on solubility measurements in ternary solvent mixtures (ethanol-pentanol-water). This allowed the maximum pentanol concentration to be extended to more than 25 %. Target component solubility, with the ethanol fraction in the cosolvent fixed, increased log-linearly with the increase of pentanol fraction. However, as shown in Figure 2-8, the cosolvency power of pentanol (i.e., the slope of the solubility plots) for undecane solubilization varies from 18.93 for 0.4 f_c ethanol to 7.20 for 0.7 f_c ethanol . This suggests that the solubility of undecane was enhanced dramatically by additional pentanol at low ethanol fraction. Furthermore, these results indicated that the additive effect for the multi-solvent systems described by the log-linear cosolvent model may not be applied in these ethanol/pentanol/water mixed solvent systems.

The plots for log solubility of target components versus fraction of pentanol in ethanol/pentanol/water solution for the Hill NAPL with a fixed ethanol fraction of 0.7 are shown in Figure 2-9; a linear relationship can be seen in these plots. Similarly, the linear relationship was also found for the NAPL contaminated soil at the fixed ethanol fraction of 0.47 (Figure 2-10). However, as described earlier, the slope of log S versus f_c for different based solution of ethanol was different. Therefore, the slope (i.e., cosolvency power) of target components for NAPL was not directly comparable with target components for NAPL contaminated soil in ethanol/pentanol/water solution (Table 2-5).

Solubility of PAH from coal-tar contaminated soil

Solubility of 12 PAHs from three types of coal tar contaminated soils in the methanol/water system are summarized in Appendix A. Examples of the log S versus f_c of

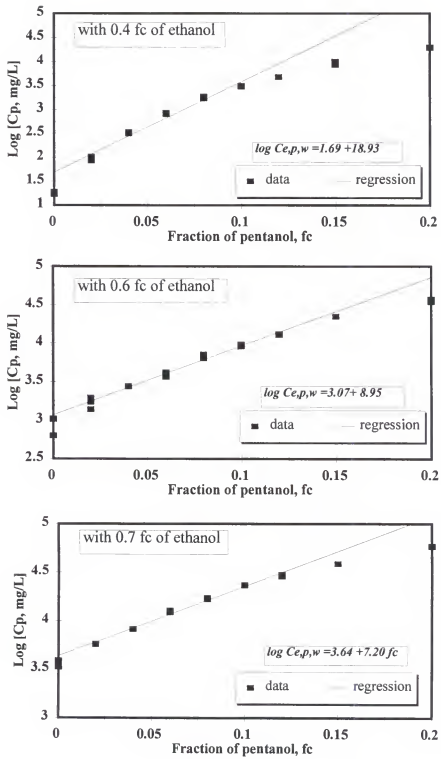

Figure 2-8. Relationship between log undecane solubility versus fraction of pentanol in ethanol/pentanol/water system with different volume of ethanol fraction

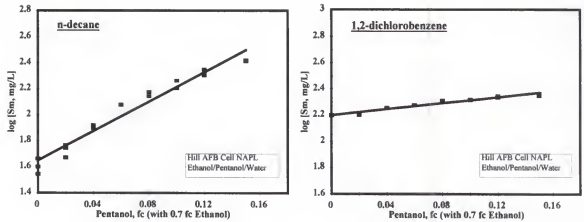

Figure 2-9. log Sm of target components versus pentanol fraction with 0.7 fc ethanol in NAPL-ethanol/pentanol/water system

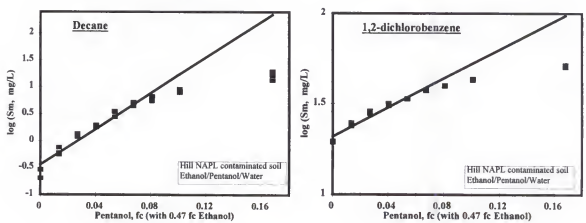

Figure 2-10. Examples of log Sm versus fraction of pentanol with 0.47 fraction of ethanol in the NAPL contaminated soil and ethanol/pentanol/water system

Table 2-5. List of estimated cosolvency powers for NAPL target components in ethanol/pentanol/water systems

Compound	log K_{ow}	Slope *(log $S_{c,p,w}$ vs fc of pentanol)*	
		NAPL (0.6 fc ethanol)	NAPL Soil (0.47 fc ethanol)
p-, m-Xylene	3.09	6.55	11.97*
o-Xylene	3.09	6.51	6.85
1,2-Dichlorobenzene	3.40	3.94	3.97
1,3,5-Trimethylbenzene	3.55	6.65	10.36
1,2,4-Trimethylbenzene	3.55	6.02	14.32
Naphthalene	3.59	4.06	0.79
1,2,4-Trichlorobenzene	4.1	3.61	5.4
Decane	6.00	8.87	16.6
Undecane	NA	9.13	14.46
Tridecane	NA	11.03	16.43

methanol are shown in Figure 2-11. Log-linear relationship between concentration versus fraction of the cosolvent was evident for all of the PAH components.

Ideal behavior

Aqueous solubility values, measured directly or estimated by log linear extrapolation, as well as their cosolvency powers (slope) are complied in Tables 2-6 and 2-7.

Solubility of target analytes for NAPL and NAPL contaminated soil, measured experimentally or estimated by log-linear extrapolation, were plotted with Raoult's law's predicted aqueous solubility values (Figure 2-12). The Raoult's law estimate of the aqueous phase solubility was computed for each solute by using an average molecular weight of 170 for the NAPL and for the NAPL contaminated soil. In each plot, the ideal line (i.e., 1:1 correlation) was included. For aqueous solubilities measured using the field NAPL (Figure 2-12A), data deviate above or below the line. The data that fell below the ideal line resulted in predicted concentrations greater than the aqueous solubility measured or estimated by linear extrapolation. The data that fell below the ideal line were mainly alkanes. Though they were present in reasonable amounts in the NAPL, the aqueous solubilities of these components were so low that direct measurements were not reliable, and were estimated based on log-linear extrapolation. Similar results were found with the aqueous solubilities measured in NAPL contaminated soil (Figure 2-12B). Deviations for a measured solubility of compounds from NAPL with predicted data may attributed to (1) uncertainty of the log linear extrapolated aqueous solubility; (2) existence of nonideal solubility for these NAPL components solubilization from the NAPL mixtures; and (3) depletion of constituent mass in the NAPL.

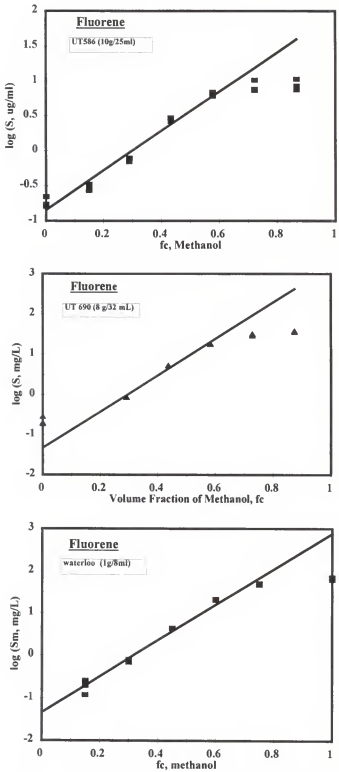

Figure 2-11. Linear relationship between log solubility of PAH versus volume fraction of methanol for coal tar contaminated soils in methanol/water solution

Table 2-6. Complied log-linear extrapolated aqueous solubility of target components and their cosolvency power.

Compound	log S	(log S_w)[a]		[b] Slope	
		NAPL	NAPL soil	NAPL	NAPL soil
p-, *m*-Xylene	2.297	-1.91	-2.98	4.90	6.11
o-Xylene	2.243	-1.79	-1.77	4.01	3.85
1,2-Dichlorobenzene	2.000	-0.27	-0.53	3.94	4.23
1,3,5-Trimethylbenzene	NA	-1.94	-2.39	4.78	5.36
1,2,4-Trimethylbenzene	1.756	-1.13	-1.5	4.45	4.52
Naphthalene	1.500	-1.53	-1.76	3.57	3.97
1,2,4-Trichlorobenzene	1.279	-1.59	-2.01	5.07	5.43
Decane	-2.046	-2.68	-3.14	6.20	6.45
Undecane	NA	-2.78	-3.25	6.68	8.35
Tridecane	NA	-3.06	-3.58	5.86	6.83

[a] Linear extraploated from plot of log S_m vs fc of ethanol.
[b] Slope of the log S_m vs fc of ethanol, slope = $\alpha\sigma$, and $\alpha\beta\sigma$for NAPL and NAPL contaminated soil, respectively.

Table 2-7. Summary of log-linear extrapolated aqueous solubility of PAHs in coal tar mixtures and their cosolvency power.

Compound	[a] log S_l	log S_w			Slope of log S_m vs fc		
		UT 586	UT 690	Water loo	UT 586	UT 690	Waterl oo
naphthalene	-3.05	-0.89 (-0.89)[b]	0.29 (-0.79)	0.79	1.73	1.47	2.55
1-methylnaphthalene	-3.72.	-0.51 (-0.45)	-0.03 (-0.91)	0.68	2.40	1.53	3.07
2-methylnaphthalene	-3.62	-0.44 (-0.39	-0.01 (-0.36)	0.06	2.10	2.29	2.86
acenapthylene	-4.02	-0.49 (-0.46)	-0.68 (-0.58)	-1.32	2.25	2.73	3.45
acenapthene	-3.98	-1.40 (-1.29)	-1.27 (-1.27)	-1.53		2.64	3.87
fluorene	-4.03	-3.36 (-0.73)	-1.33 (-0.54)	-1.33	2.62	4.51	4.22
phenanthrene	-4.5	-4.47 (-0.98)	-1.50 (-0.43)	-1.26	2.82	5.63	4.10
anthracene	-4.49	-5.00 (-1.46)	-0.80 (-0.89)	-1.41	3.77	3.07	4.54
fluoranthene	-5.19	-5.94 (-1.65)	-1.17 (-0.96)	-2.17	3.82	4.00	5.15
pyrene	-4.85	-5.72 (-1.43)	-1.70 (-0.98)	-1.94	4.51	4.53	4.95
chrysene	-5.29		-2.06	-1.66	4.41	4.10	
benz(a)anthracene	-6.29		-1.59				
benzo(a)pyrene	-6.28		-1.11				

[a] Supercooled liquid solubility calculated by assuming a constant ΔS_f for PAHs (Lee et al., 1992b).

[b] the values in the parentheses are directly measured or hexane (methylene chloride) extracted aqueous solubilities.

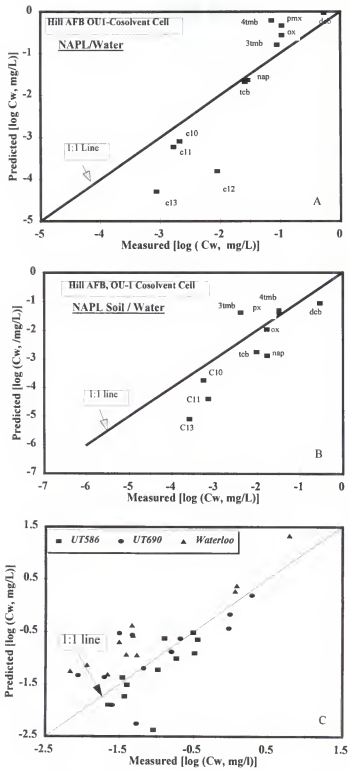

Figure 2-12. Comparison of laboratory measured aqueous-phase concentration with those predicted based on Raoult's law for (A) Hill AFB NAPL (B) NAPL contaminated soil, and (C) PAHs for three types of coal tar contaminated soils.

The predicted log solubility data versus measured aqueous-phase solubility data of PAHs from coal tar contaminated soils are plotted in Figure 2-12C, along with the 1:1 ideal line. All of the predicted data points for the Waterloo tar soil fell consistently above the ideal line. The two other coal tar soils data points were scattered, some deviated a great deal from the 1:1 line.

Lee et al. (1992b) compared laboratory-measured, aqueous-phase concentrations to those predicted by Raoult's law for eight coal tars supplied by EPRI; they reported that the majority of the data lie within a factor-of-two interval about the 1:1 correlation. Good agreement for a majority of PAHs within the factor-of-two suggested that aqueous concentrations of PAHs from coal tar or coal tar contaminated soil may be estimated by using Raoult's law approach.

Peters and Luthy (1993) investigated three ^{14}C labeled PAHs (naphthalene, phenanthrene and pyrene) for their solubility in a coal tar-water system, and predicted their aqueous solubility based on a Raoult's law approximation. The results showed that the experimentally measured aqueous solubility, C_w, agreed well with Raoult's law predictions for naphthalene, but the measured C_w for phenanthrene and pyrene were larger than those predicted by Raoult's law.

The Hill AFB NAPL and the coal tars are both complex mixtures. Coal tars consist of hundreds of components, primarily a group of polycyclic aromatic hydrocarbon components, ranging from single to multiple (4-6) benzene rings, and these PAHs have similar basic structures. The NAPL from the Hill AFB site was a mixture of jet-fuel and cleaning and degreasing solvents, consisting of a group of alkanes and aromatic constituents

like xylenes, trimethylbenzenes and di- and tri-chlorobenzenes. The Hill NAPL is not only complex in composition, but it is also a mixture of structurally different compounds. Solubility of components from a NAPL mixture also is a function of the ideality of the organic phase. Studies by Lee et al (1992b) and Cline et al.(1991) have suggested that NAPL mixtures of structurally similar organic liquids form ideal solutions in the organic phase and the release of these constitutes into air or water may be estimated by Raoul's law. However, mixtures of aromatic constituents, like benzene and toluene, and saturated alkane constituents, like hexane and octane, showed deviations from ideality that resulted in somewhat higher concentrations in the aqueous phase than predicted by Raoult's law (Leinonen and Mackay , 1973; Sanemasa et al., 1987). This nonideality will influence the distribution of solutes from complex NAPL mixtures.

Partitioning of the target components in NAPL/water system

The partition coefficient K_{nw} for all the target analytes and PAHs at different cosolvent fractions were compiled in Appendix A. Figure 2-13 shows a plot of log (K_{nw}) versus fraction of ethanol, f_c, for some of the target analytes from the NAPL-cosolvent system. Similar data for several target analytes from the NAPL-contaminated soil-cosolvent system are shown in Figure 2-14. The NAPL-water partition coefficient for the components with low aqueous solubility was estimated by using the log-linear extrapolation method. K_{nw} values for NAPL target components, estimated by log-linear extrapolation, and their estimated log K_{oc} values, based on the total carbon content of contaminated soil, are compiled in Table 2-8. The K_{nw} values estimated by log-linear extrapolation were used in the studies.

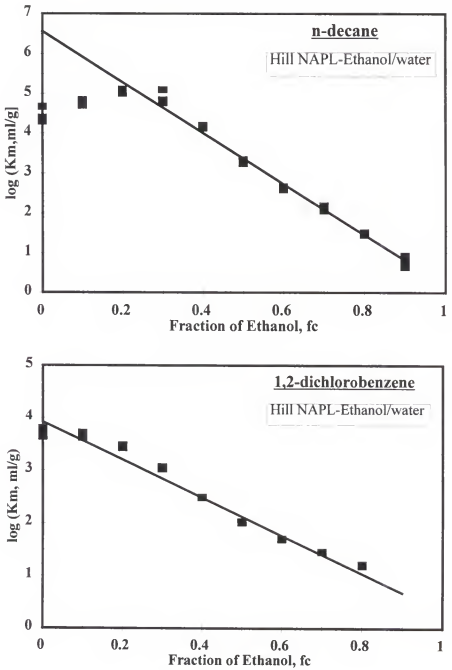

Figure 2-13. Inverse linear relationship between log partition coefficient for target components versus volume fration of ethanol in NAPL-ethanol/water system.

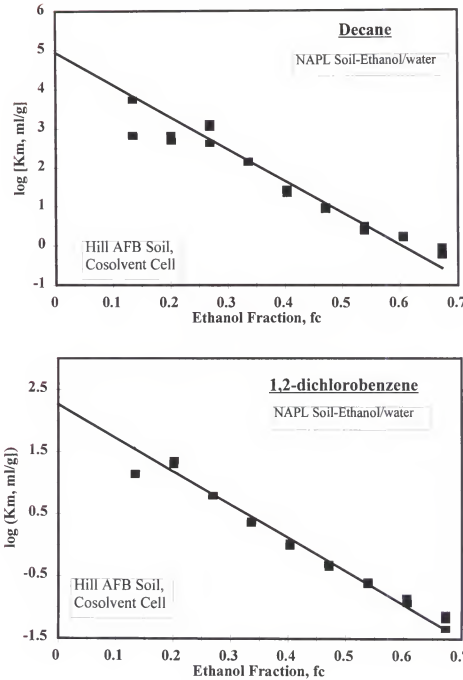

Figure 2-14. Inverse linear relationship between log partition coefficient for target components versus volume fration of ethanol in NAPLcontaminated soil-ethnaol/water system.

Table 2-8. Log-linear extrapolated NAPL-water partition coefficient for target components from ethanol/water cosolvent system

Compound	log K_{ow}	log K_{nw} [a]		-Slope [b]		[c]log K_{oc}
		NAPL	NAPL soil	NAPL	NAPL soil	
p-, m-Xylenes	3.09	5.59	3.02	5.52	6.73	5.46
o-Xylene	3.09	5.10	2.29	4.87	5.11	3.84
1,2-Dichlorobenzene	3.40	3.92	2.27	3.59	5.32	3.81
1,3,5-Trimethylbenzene	3.55	5.32	3.00	5.09	5.96	5.45
1,2,4-Trimethylbenzene	3.55	5.29	3.03	5.24	5.26	4.58
Naphthalene	3.59	4.30	2.29	3.71	6.2	3.94
1,2,4-Trichlorobenzene	4.1	5.09	3.31	6.37	7.86	4.86
Decane	6.00	6.57	4.40	6.38	6.99	5.95
Undecane	NA	6.71	5.22	6.57	8.16	6.82
Tridecane	NA	6.84	4.96	6.31	6.94	6.50

[a] Linear extraploated from intercept of log K_m vs fc of ethanol, [b] Slope of log K_m vs fc of ethanol, i.e., $\alpha\beta\sigma$, [c] Estimates from $K_{oc} = K_{nw} / f_{oc}$

The volume to mass (V/M) ratio used in the laboratory experiments was about 1/2, which is much higher than the field pore water condition at the Hill AFB site. The concentration values obtained from laboratory experiments were not necessarily the same as the concentrations measured in the field due to the difference in V/M ratios (Rao et. al 1997, Sillan et al., 1997).

A log-linear extrapolated coal tar-water partition coefficient, K_{mw}, was estimated by regressing the log partition coefficient versus fraction of methanol (Figure 2-15). The K_{tw} values, estimated by log-linear extrapolation, from these plots are listed in Table 2-9. The estimated log K_{oc} of PAHs from three types of coal tar contaminated soils are also included in Table 2-9.

Relationship between partition coefficient and aqueous solubility Solubility of the solvent in water is small in many lipoidal solvent-water systems. In these cases, the effect of the solvent, dissolved in water, on the solute activity coefficients of the solvent-water mixture was not very significant when solutes have comparable or higher solubility than the solvent in water(Chiou and Schmedding, 1982). Since the extent of solute solubility is an important factor in partition coefficient K, it is convenient to relate K directly to the molar solute solubility in water (Chiou and Schmedding, 1982; Hansch et al., 1969; Chiou and Block, 1986; Yalkowsky and Valvani, 1980; Yalkowsky and Roseman, 1981). If a liquid solute has limited solubility in water, the molar solubility (S_w) is related to the activity coefficient as :

$$S_w = \frac{1}{\gamma_w \overline{V}_w} \qquad (2\text{-}15)$$

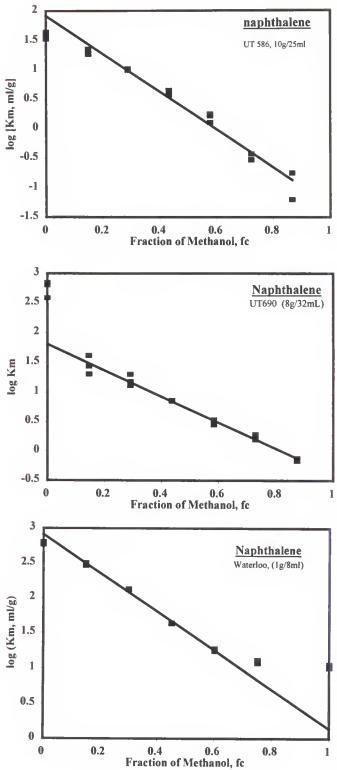

Figure 2-15. Inverse linear relationship between log partition coefficient , log Km, of PAHs versus volumne fraction of methanol for coal tar contaminated soils in methanol/water solution.

Table 2-9 Log-linear extrapolated coal tar-water partition coefficient for selected PAHs from methanol/water cosolvent system

Compound	log K_{ow}	log K_{tw} [a]			log K_{oc} [b]		
		UT 586	UT 690	Water-loo	UT 586	UT 690	Water-loo
naphthalene	3.37	1.62	2.74	2.92	3.83	4.15	3.95
1-methylnaphthalene	4.00	1.97	2.99	3.51	4.15	4.57	4.54
2-methylnaphthalene	4.00	1.61	2.06	3.33	3.82	3.74	4.36
acenapthylene	4.07	1.81	2.83	3.70	4.02	4.40	4.73
acenapthene	3.92	2.0	1.81	4.02	4.31	3.38	5.05
fluorene	4.18	2.67	3.00	4.31	4.99	4.57	5.34
phenanthrene	4.46	2.76	3.45	4.40	5.58	5.02	5.43
anthracene	4.45	2.93	3.31	4.43	5.18	4.88	5.47
fluoranthene	5.33	3.15	3.81	5.34	5.36	5.38	6.37
pyrene	5.18	4.25	4.12	5.22	6.57	5.69	6.25
chrysene	5.61	4.33	4.0	6.27	4.51	5.55	---
benz(a)anthracene	5.61	---	3.87	---	NA	5.44	---

[a] Linear extrapolated from log K_m vs fc of methanol; [b] Estimated from $K_{oc} = K_w / f_{oc}$ relation.

where γ_w is the activity coefficient in pure water saturation and V_w the molar volume of water. Combining equation 2-7 with the previous definition of partition coefficient (K):

$$K = \frac{C_o}{C_w} = \frac{\gamma_w^* \overline{V_w^*}}{\gamma_o^* \overline{V_o^*}} \qquad (2\text{-}16)$$

the relationship between K and S_w for solute in NAPL-water mixtures can be expressed as (Chiou and Schmedding, 1982):

$$\log K = -\log S_w - \log \overline{V_o^*} - \log \gamma_o^* + \log (\gamma_w^*/\gamma_w) \qquad (2\text{-}17)$$

The relative effects of the solute water solubility (γ_w and S_w), the solute and their matrix or solvent compatibility (γ_o*), and the effect of solvent dissolved in water on solute water solubility (γ_w/γ_w*) on partition coefficient, vary from one system to another. To analyze these effects for solutes in a solvent-water system, Raoult's law for ideal behavior (log K' = -log S_w - log V_o*) can be used as a reference. Plot of log K' versus log S_w gives an ideal line, with a slope of -1 and an intercept of -log V_o*. The difference between log K' and log K is equal to log γ_o* + log (γ_w/γ*$_w$). The effect of log ((γ_w/γ_w*) depends on the types of solvnet-water systems and the solutes. In general, this effect is relatively small in lipoidal solvent-water systems for those solute whose solubilities in water are comparable with or greater than the solubility of solvent in water (Chiou and Block, 1986).

The partition coefficient values, measured and estimated by log linear extrapolation, of the target organic compounds in the NAPL/water systems were used together in the

following discussion. A plot of log K_{nw} versus log S (solute crystal solubility) is shown in Figure 2-16. The average molecular weight of 170 g/mole was used to establish the ideal line for the field NAPL, and the NAPL density was measure as 0.9 g/ml. The value of the log V_o^* is calculated based on the average molecular weight and density of the NAPL, i.e.:

$$\log V_o^* = \log \left(\frac{MW_o}{\rho_o}\right) \qquad (2\text{-}18)$$

This gives the intercept of the NAPL-water ideal line as 0.724. The data points in Figure 2-16 show two types of deviation. *p*-xylene and *m*-xylene deviated above the ideal line, while the alkanes all fell below the ideal line. The deviation of a compound in the system measures the sum of the contributions of log γ_o^* and log (γ_w / γ_w^*). In such a complex NAPL system, both the solute-NAPL compatibility (γ_o^*) and the effect of NAPL dissolved in water on solute water solubility (γ_w / γ_w^*) may be significant. Some relatively higher solubility components in the NAPL, dissolved in water, enhanced the solubility of alkanes (generally, alkanes have extemely low solubility in the water); and thus, lowered the partition coefficient. It should be noted that a plot of log K_{nw} versus log S exhibits a nonlinearity for those target components having large differences in their hydrophobicity and solubility.

Chiou and Block, (1986) presented an analysis of the published data to evaluate the relationship between the octanol-water partition coefficient K_{ow} and heptane-water partition coefficient K_{hw}, and aqueous solubility (S_w) for a wide range of liquid and solid organic compounds (mole solubility range -0.4 to -6.7 mole/liter). They noted that measured K_{ow} and

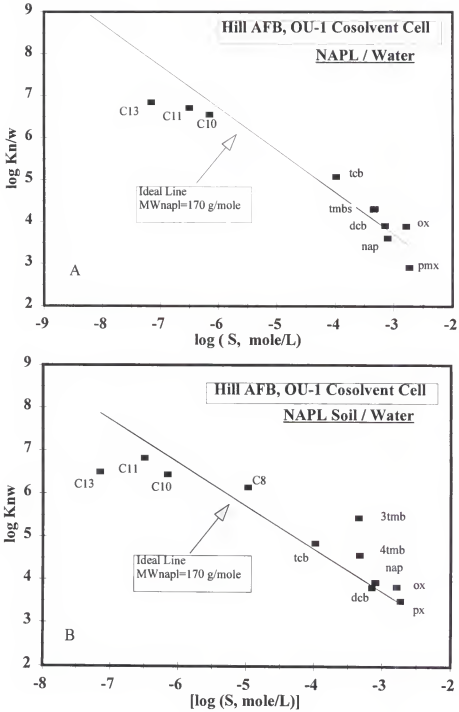

Figure 2-16. Comparison of measured NAPL- water partition coefficients and predicted based on Raoult's law for Hill AFB NAPL (A) and NAPL contaminated soil (B)

K_{hw} values were systematically smaller than those expected, based on the ideal behavior. They suggested that the deviation in the octanol-water system was significantly the effect of log (γ_w/γ_w^*) than log γ_o for solutes that have very low water solubilities. In the heptane-water system the value of log (γ_w/γ_w^*) can be neglected because the solubility of heptane in water is very small (about 3 mg/L) (Leo and Hansch, 1971). Chiou and Block found that the plot of log triolein-water partition coefficient, K_{tw}, versus log S_w or log K_{ow} exhibited a curvature.

A study of fuel-water partition coefficients for the aromatic constituents in gasoline (Cline et al., 1991) found that a plot of log K_{fw} versus log S_w was linear, and fit the line for ideal behavior based on the Raoult's law. However, the compounds included only ranged from -0.26 to -3.2 in their log aqueous solubility, and they all had the same base structure of benzene (Gasoline is a complex mixture of volatile hydrocarbons. The major components are branched-chain paraffins, cycloparaffins, and aromatic compounds). The previously discussed deviation from the ideal behavior was only obvious in those compounds with low solubility.

Chiou and Schmedding (1982) studied the relationship between log K_{ow} and log S for various classes of organic compounds, and they used the ideal line based on the assumption of Raoult's law in the octanol phase, and zero effect of dissolved octanol on water solubility for the octanol-water system(Chiou and Schmedding, 1982). Their results showed that alcohols and ethers approached ideal solution behavior in the octanol phase, because their structure and polarity made them compatible with octanol. Throughout the range of the reported water solubilities, the deviations from the ideal line of alkyl halides, alkynes and

aromatics were fairly comparable with those of alcohols and ethers. By contrast, alkanes and alkenes deviated downward from the ideal line by some 2 orders of magnitude in the partition coefficient. The downward deviations increased systematically with lower solubilities. They suggested that the deviations are caused by liquid solute incompatibility in the water-saturated octanol phase, as measured by the activity coefficient, and by the lesser effect of dissolved octanol on water solubility, both of which increased systematically with decreasing solubility. For such nonideal behavior, the partition coefficient between an organic liquid and aqueous phase can be related to the solubility of the pure liquid as:

$$\log K_p = -\log S_w - \log \overline{V_0^*} - \log \gamma_0^* + \log (\gamma_0^*/\gamma_w) \qquad (2\text{-}12)$$

the last two terms as sources of nonideality as discussed previously, and both usually produce a downward deviation from the ideal line.

Lee et al. (1992a) investigated the applicability of Raoult's law for diesel fuels by interpreting data from Hagwall (Hagwall, 1992), and found that there was good agreement between Raoult's law predictions and measured data for four diesel fuels. Lee et al. (1992b) have also studied eight coal tars collected from different locations in the U.S. The concentration ranges of various target analytes in these carl tars were: monocyclics, 13-25,300 mg/kg; polycyclics, 6,800-218,000 mg/kg for 2 and 3 rings; and 12,00-110,000 mg/kg for >3 rings, and 70-5,000 mg/kg for nitrogen and sulfur substituted polyaromatic hydrocarbons. The eight different coal tars also exhibited a wide range in average molecular weight and density (EPRI, 1992). Of the tars Lee et al. investigated, data points for seven tars were scattered within the factor-of-two error bounds of the ideal line (using Raoult's law

approach, while the data points for one coal tar were consistently above the ideal line.

Three different types of coal tar contaminated soils (EPRI, 1992) were used in this study to evaluate the applicability of Raoult's law in predicting the K_{tw} of PAHs in coal tar soils. The soils were UT 586, a sandy soil (primarily quartz) with total PAHs content of 320 mg/kg soil; UT 690, a sandy soil (very complex mineral background, including a black coal fraction) with total PAHs of 3475 mg/kg; and Waterloo fine sand, with total PAHs of 17,600 mg/kg. The coal tar-water partitioning data for coal tar contaminated soil-water systems is presented in Figure 2-17. Log K_{ctw} values from all three tar soils were plotted against the logarithm of PAHS supercooled solubility (S_{col}), along with the line representing statistically of best fit (Lane and Loehr, 1992) in Figure 2-17. Among all the data only a few of the data points from the Waterloo soil fell on the best fit line. Data points from two other tar soils were all consistently below the line of best fit. The most probable cause for the deviation was the estimated molecular weight. The change in the intercept can be explained by an increase or decrease in the molecular weight and density of the coal tar soils. The interaction of coal tar with original soil organic matter, i.e., may be caused by aging. In this study, Waterloo coal tar soil contained high liquid tar relatively associated with soil as thin coatings.

Relationship between K_{ctw} and K_{ow} High correlation between K_{ctw} and K_{ow} has been demonstrated by earlier other researchers (Lane and loehr, 1992; Picel et al., 1988), as is to be expected given that the correlation between the partitioning of solutes in different immiscible organic/water systems can be descried by a linear free-energy relationship (Campell et al., 1983).

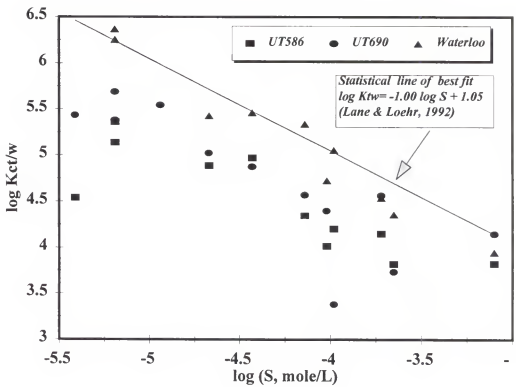

Figure 2-17. Relationship bewteen the log coal tar-water partition coefficient and log solubility for three types of coal tar contaminated soils, and a statistice line of best fit for coal tar-water partition is included for comparison.

The NAPL/water partition coefficient for the target components from NAPL- contaminated soil-water, K_{nw}, and the tar/water partition coefficient for PAHs from coal tar-contaminated soil, K_{tw}, were all normalized to the soil total organic carbon content (f_{oc}). The normalized partition coefficient, log K_{oc} are plotted versus log K_{ow} for all the compounds in this study (Figure 2-18). The plot also includes three regression lines for the following data sets: 1) for soil organic matter-water system (uncontaminated soil)(Karickhoff, 1987); 2) a regression line for the heavily contaminated soil (Waterloo tar soil); and 3) a statistical best-fit linear relationship for coal tar-water partitioning (Lane and Loehr, 1992). All but one of the data points fell between the line for "clean" soil and below the regression line for heavily contaminated soil, with the result that data for the less contaminated coal tar soil UT586 (total PAHs of 320 mg/Kg) fell closer to the "clean" soil line. These results indicate that the partition coefficient for contaminants in soil can be bound at the upper end by their partition coefficients in pure coal tar (or other complex NAPL) and on the lower end by the partition coefficients for a "clean" soil; thus, implying that the native soil organic carbon has considerably less affinity than the tar pitch that constituted much of the contaminates of coal tar. With aging, the partitioning process in contaminated soils apparently becomes less compared to the original contaminated soil.

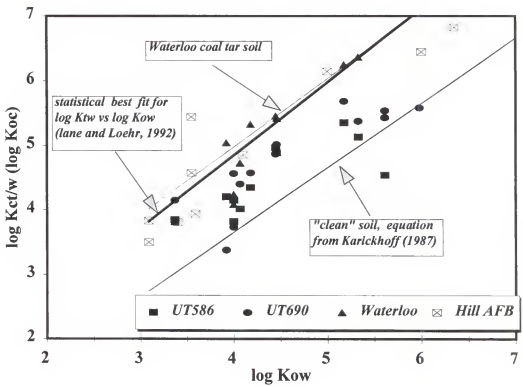

Figure 2-18. Comparison of log Koc vs log Kow for NAPL contaminated soils and that of statistical relationship for coal tars and "clean" soils

Conclusions

1. Aqueous solubility of hydrophobic solutes with large molecular weight and low solubility can be estimated by log linear extrapolation of their solubility measured in cosolvent mixtures. When using Raoult's law approach to predict aqueous solubility from NAPL-mixtures or to predict NAPL/water partitioning behavior, several factors that must be considered are: structural similarity of components in a mixture; the solute-NAPL compatibility; and the effect of NAPL (lower molecular weight solutes) dissolved in water on solute (higher molecular weight, more hydrophobic) water solubility.
2. Addition of higher molecular weight alcohol (pentanol) into ethanol/water mixture significantly increased the NAPL solubility compared to the solubility in ethanol-water. NAPL solubility enhanced by pentanol in ethanol/water mixtures appears more for fraction ethanol at lower basis (0.4) than at higher ethanol basis (0.7).
3. The partition coefficient for contaminants in soil can be bound at the upper end by their partition coefficients in pure coal tar (or other complex NAPL) and on the lower end by the partition coefficients for a "clean" soil in the log K_{oc} versus log K_{ow} plot.
4. Aromatic constituents of complex organic wastes have much stronger affinity to contaminated soils than to soil organic. Implication is that native soil organic carbon is considerably polar than the tar or tar pitch that constitute much of the PAHs; and estimating or simulation using fresh spike contaminants on to soil may not accurate reflect the contaminants partitioning behavior or movement for complex wastes contaminated soils and aquifers.

CHAPTER 3
DISSOLUTION OF NAPL MIXTURES DURING FLOW

Introduction

NAPL transport in the subsurface is a multi-phase flow phenomenon involving physical processes governed by buoyancy, viscous, and capillary forces; and chemical processes such as dissolution and partitioning. NAPLs in the subsurface serve as potential long-term sources of soil and groundwater contamination, and relatively small amounts of NAPLs have the capability of contaminating large aquifer volumes at concentrations above the regulatory limits. The traditional pump-and-treat approach will not be particularly effective in reducing contaminant concentrations for the following reasons: (1) immobility of the residual NAPLs, even at high flushing rates; (2) NAPL is only removed by the slow process of dissolution; and (3) due to subsurface heterogeneity and kinetic limitations to solubilization (Mackay and Cherry, 1989). Since residual NAPL may occupy up to 14-30 percent of the pore space in the source zones (Wilson et al., 1990), it has been estimated that clean up NAPL-contaminated sites by pump-and-treat alone may require years or decades

(Mackay and Cherry, 1989). Several alternate approaches have been developed for enhanced remediation of NAPL-contaminated sites. Several in-situ extraction of enhancing NAPL contaminant removal in the subsurface are under investigation. Examples include in-situ flushing with cosolvents, surfactants and complexing agents (NRC, 1994, NRC, 1997).

The primary criterion upon which the effectiveness of chemical enhancement additives are judged is their solubilization or mobilization potential. The impact of interactions between the additive and the solid phase on the NAPL solubility and mobility enhancement is also an important factor to consider. Alcohol solutions can significantly reduce the interfacial tension (IFT) between NAPL and aqueous or solid phases, thus allowing separate phase displacement of trapped immiscible NAPL ganglia through pore constrictions (Puig, et al., 1982). NAPLs and adsorbed organic contaminants can also be removed through enhanced dissolution or desorption in the solvent-rich cosolvent phase (Augustjin et al., 1994). The miscibility of the low molecular weight alcohols with water allows for nearly complete recovery of alcohol by water flushing. Low concentrations of alcohol remaining in the subsurface after flooding may be readily degraded by the native microorganisms (Novak et al., 1985, Lettinga et al., 1981).

Based on the previous research on cosolvent enhanced solubility (Chapter 2), cosolvent effects on the dissolution of target components of NAPLs and NAPL-contaminated soils were investigated in laboratory columns under 1-D saturated flow conditions. The NAPL sources investigated include: (1) a single-component NAPL, tetrachloroethylene (PCE), which is denser than water (DNAPL); and (2) a multi-component NAPL mixture from Hill AFB. In this chapter, the cosolvent-enhanced dissolution of the NAPLs in

columns under saturated, steady flow conditions were investigated. The flushing efficiency of binary (ethanol/water) and ternary solvents (ethanol/pentanol/water) were compared based on the NAPL constituent mass recovery, mean elution time, and fitted mass-transfer rate coefficients. The experimental data were also fitted using a simulation model developed by Augustijn et al. (1993) and modified by Jawitz (1997).

Theoretical

There are four primary mechanisms responsible for cosolvent-enhanced remediation (Augustijn et al., 1994): (1) reducing the NAPL/water interfacial tension (IFT); (2) increasing the solubility of non-polar organic chemicals; (3) decreasing sorption of non-polar organic chemicals on sorbents; and (4) reducing sorption and dissolution mass-transfer limitations. Cosolvent effects on the solubility and partitioning have been discussed in Chapter 2. Cosolvents reduce the interfacial tension between the solution and NAPL phases, which reduces the capillary forces by which the NAPLs are entrapped in the pore spaces. Therefore, mobilization of residual NAPL is facilitated. The ratio of hydrodynamic and capillary forces acting on the residual NAPL phase is expressed by the capillary number:

$$N_c = \frac{\mu v}{\gamma} \tag{3-1}$$

where μ is the viscosity of the solution phase, v is the groundwater flow velocity, and γ is the interfacial tension between the solution and NAPL phase. In general, residual NAPL is mobilized as the capillary number is greater than 2×10^{-5} , and virtually all NAPL is

displaced when the capillary number exceeds 5 x 10^{-3} (Hunt et al., 1988). High capillary numbers can be achieved by increasing the groundwater velocity and/or decreasing the NAPL-water interfacial tension as indicated in Equation 3-1.

Given the practical limitations on groundwater pumping rates, reducing the interfacial tension by adding cosolvents may be a more viable option. NAPL -water interfacial tension can substantially reduced by addition of cosolvent. Imhoff et al.(1995) found that PCE-water IFT (γ) decreases with increasing methanol/water fraction (f_c), according to the following expression:

$$\gamma = -43.1 f_c^{0.58} + 43.2 \qquad (3\text{-}2)$$

The movement of NAPL and water or cosolvent through porous media can be described at the macroscopic scale by Darcy's law:

$$q_i = -\frac{k_i}{\mu}\left[\frac{\partial p_c}{\partial x_i} + \Delta\rho g \sin\alpha\right] \qquad (3\text{-}3)$$

where q_i is the specific discharge (Darcy's flux) of a particular fluid. k_i is the intrinsic permeability of a particular fluid; μ is the dynamic viscosity of the fluid, $\partial p_c / \partial x_i$ is the pressure gradient in the fluid; $\Delta\rho$ is the density difference of the fluids; g is gravitational accelerates; and α is the angle of flow relative to the horizontal. When the contaminants are not present as a pure phase, but are present only in the solution and sorbed phases, the equation governing the transport of a sorptive constituent is given by the one-dimensional advection-dispersion equation:

$$R\frac{\partial C}{\partial t} = D\frac{\partial^2 C}{\partial x^2} - v\frac{\partial C}{\partial x} \qquad (3\text{-}4)$$

where R is the retardation factor, defined as R= 1+ρK/θ, or $R_i = M_i / \theta C_i$ for multi-component, complex NAPL mixtures; *C* is the concentration in the solution phase; *t* is time; *D* is the hydrodynamic dispersion coefficient; *x* is the longitudinal distance; *v* is the flow velocity; ρ is the dry bulk density of the soil; θ is the volumetric water content; and M_i is the mass of contaminant *i* present in the system.

The solubility enhancement and the reduction of the partition coefficient resulting from cosolvent addition are well established (see Eqs 2-4 and 2-5). The cosolvent effects on the retardation factor can be predicated by the log-linear model (Nkedi-Kizza et al., 1987):

$$\log (R_m - 1) = \log (R_w - 1) - \alpha\beta\sigma f_c \qquad (3\text{-}5)$$

where R_m and R_w are the retardation factors measured in mixed solvent and aqueous solutions, respectively; and α and β are empirical coefficients.

An increase in the mass-transfer rate coefficient (k) with increasing cosolvent content is also expected, based on the log-log linear inverse relationship between k and K (partition coefficient) (Brusseau and Rao, 1989) and the log-linear decrease of K with increasing cosolvent fraction (Eq. 2-5). Combining these two relationships gives::

$$\log k^m = \log k^w - a\Sigma\,\alpha\beta\sigma f_{c,i} \qquad (3\text{-}6)$$

where *a* is the absolute value of the slope for the linear regression between log K and log k.

Materials and Methods

Columns

The experiments reported here were conducted in 25 mm ID × 50 mm length glass columns obtained from Kontes Glass Co. The columns were fitted with Teflon o-rings and Teflon end pieces, containing stainless steel frits (for glass bead packings) or glass-fiber frits (for soil packing). All tubing, fitting and valves in contact with the organic fluids were constructed with Teflon.

Two types of porous media were used in the experiments: (1) glass beads, size < 0.2 mm; (2) sandy subsurface soil from Gainesville, Florida (Eustis #3); this soil has 94 % sand fraction, 3% silt, and 3% clay, and contains 0.47% of organic carbon (OC). The contaminated soils used in the column studies was from the OU-1 site at Hill AFB, UT(Chapter 2).

Reagent-grade tetrachloroethylene (PCE) (Aldrich Chemical CO.) was used as the single-component DNAPL in column studies with packing of glass beads and sandy soil. Methanol (Optima grade) and pentanol (n-amyl alcohol) (Fisher Sci. Co.) and absolute-200 proof ethyl alcohol (AAPER Alcohol and Chemical co.) were used as the organic cosolvents, while the water used in this study was HPLC water (Fisher Sci. Co.) or deionized and distilled water.

Single-component NAPL (PCE) contaminated columns

Columns packed with glass beads or sandy soil were initially saturated with water by pumping 0.01 N $CaCl_2$ DI water upward through the columns at a flow rate of 0.5 ml/min

flow rate (Gilson 302 or 305 pump). Approximately one pore volume of PCE (dyed with a small amount of Sudan III red) was injected into the columns upward, opposite to the water flow direction using a syringe pump(Harvard) at a flow rate of 0.1 to 0.2 ml/min . Subsequently, PCE was flushed from column with 0.01 N $CaCl_2$ DI water at a much higher flow rate (1 ml/min) until displacement of a separate phase PCE was no longer observed in the effluent. The residual PCE saturation in the columns was determined based on the weight difference of the column between water saturation and residual PCE saturation. Assuming that density of aqueous PCE solution (ρ_{sPCE}) equals 1 (g/cm^3), the volume of residual PCE was calculated as follows:

$$\rho_{PCE} V_{PCE} + (PV - V_{PCE})\rho_{sPCE} = W_{(PV)_{PCE}} \qquad (3\text{-}7)$$

where ρ_{PCE} is the density of pure PCE, V_{PCE} is the volume of PCE in the column and $W_{(PV)PCE}$ is the weight of the water-saturated column with PCE. From Eq. (3-7), the volume of PCE in the column were calculated. The residual PCE saturation (S_N) in these experiments ranged from 0.1 to 0.15. Pentafluorobenzoic acid (PFBA)was used as a non-reactive tracer. Nonreactive tracer pulse displacements were performed before and after PCE contamination to determine the hydrodynamic dispersion characteristics of the columns with or without residual PCE saturation.

Contaminated glass bead or soil columns were flushed with methanol/water mixture using two different binary solvent mixtures: (1) 40/60 methanol/water; and (2) 70/30 methanol/water. The cosolvent solutions were introduced at the column inlet at a flow rate

of 0.5 ml/min. Flow interruption method (Brusseau et al., 1989) was applied when appropriate. The column effluent was collected in HPLC vials and analyzed by HPLC (LC-PAH column, UV detector at 230 nm, and 70/30 methanol/water mobile phase at 2 ml/min flow rate). At times when the PCE concentration in the effluent was expected to change rapidly, smaller volume fraction samples were collected.

The effluent samples collected during 0.8 to 2.5 pore volumes displaced appeared cloudy, and the condensed, free PCE droplets settled to the bottom of the sample vials. The effluent samples were initially analyzed without resuspending the free PCE. Then, a known amount of pure methanol was added into the vials to completely dissolve the excess PCE. These samples were also analyzed again for total PCE concentration.

Multi-component NAPL mixture contaminated soil columns

NAPL contaminated soil from OU-1 cell , at Hill AFB, UT, was well mixed and carefully packed into the glass columns. The columns were water saturated by pumping through 0.01 N $CaCl_2$ at 0.5 ml/min for 8 hours, or until the weight of the column remained unchanged. Then, a non-reactive tracer, potassium bromide (Br-), and partitioning tracers (alcohols) were injected, and the residual NAPL content (S_N) was estimated using the partition tracer method (Jin et al., 1995; Annable et al, 1997a). Br- and methanol were used as a non-reactive tracers to determine the hydrodynamic dispersion characteristics of the columns with residual NAPL saturation for pre-flushing and post-flushing.

Residual NAPL content in the columns was estimated with alcohol partition tracers and a non-reactive tracer (Pope et al., 1994, Annable et al., 1997a). The method is based on

measuring the retardation (R) of partitioning tracers relative to a non-reactive tracer, and estimating S_N given the NAPL-water partitioning coefficient (K_{NW}) measured in batch experiments:

$$S_n = \frac{R-1}{K_{NW} + R - 1} \tag{3-8}$$

the retardation factor (R) for the partitioning tracers can be calculated from the normalized first temporal moment for simple 1-D column experiment or calculated as the ratio of average travel times for the partitioning tracer pulse (t_p) and the non-reactive tracer pulse (t_n) introduced and displaced during the flow (Pope et al., 1995; Annable et al., 1995).

In Eq.3-8, K_{NW} is the measure of equilibrium partitioning of the tracers between the aqueous and NAPL phases, i.e., the NAPL-water partition coefficient. The basic assumptions for partitioning tracers used for prediction of NAPL saturations are (Jin et al., 1995; and Annable et al., 1997a): (1) tracer partition between the aqueous and NAPL phase can be represented as a linear and equilibrium processes; (2) residual NAPL in the pore space or on the solid surface has similar partitioning behavior as the free NAPL; and (3) the tracer adsorption is only due to NAPL partitioning.

Binary (70/30 ethanol/water) or ternary (70/10/20 ethanol/pentanol/water) mixtures were used to flush the NAPL contaminated soil columns at a flow rate of 0.5 ml/min. The column effluent was collected into 2 ml GC-vials, and the concentration of the NAPL target components was analyzed by GC-FID. The GC-FID program used for the sample analyses is the same as that described in Chapter 2.

Results and Discussion

Visual observations of NAPL dissolution

PCE movement and dissolution in porous media was observed initially in a simple physical analog of a single pore: by using 0.5 ml analytical pipet as illustrated in Figure 3-1. During water displacement, a PCE globule was initially stabilized in the middle of the pore, but as the methanol front approached the PCE globule, a cloud appeared at the cosolvent and PCE interface. This cloud continued to develop until the globule gradually elongated. The change in shape of the globule is likely due to decreasing interfacial tension between cosolvent and PCE. The formation of the cloud may be caused by the heat of mixing which is generated when the solvent front mixed with water. The cloudy solution condensed in the effluent, became clear and resulted in a small drop of free PCE. The size of the PCE globule decreases as the cosolvent flushing process continued; and, finally the globule was pushed by capillary forces or eventually all of the PCE was solubilized in the cosolvent.

Residual NAPL saturations

PCE residual saturation obtained for three PCE contaminated columns were estimated by a weight difference method (Eq. 3-7), while the residual NAPL saturations for the two NAPL mixture contaminated soil columns were determined using the alcohol partitioning tracer method (Figure 3-2). The values of residual saturation for the columns are listed Table 3-1. The soil bulk density (ρ) and volumetric water content of the column (θ) are included. The hydrodynamic characteristics for the NAPL-(single component or multi-component)

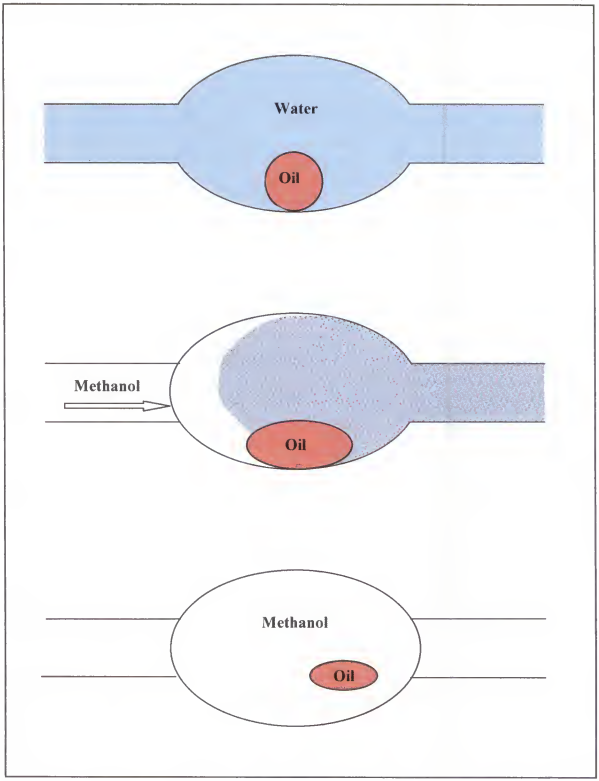

Figure 3-1. Sketches illustrating PCE droplet dissolution through pore body by methanol flushing

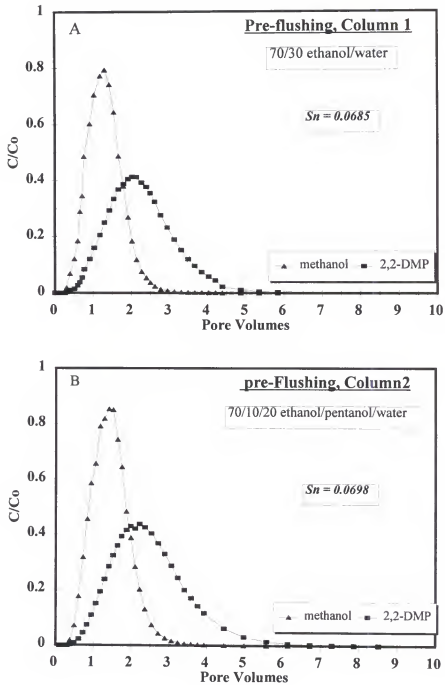

Figure 3-2. BTC of non-reactive and partitioning tracers used for estimation of residual NAPL saturation (Sn) for pre-cosolvent flushing NAPL contaminated soil column: (A) ethanol/water flushing; (B) ethanol/pentanol/water flushing.

Table 3-1. Estimated residual NAPL saturation (S_N) and other column parameters for NAPL contaminated columns

Column	Parameters					
	S_N	ρ_B (g/cm^3)	θ_s	^cP_e	*L(cm)*	*v(cm/hr)*
PCE contaminated glass beads 40/60 MeOH/H_2O	^{a}0.118	1.79	0.41	42	5.0	14.9
PCE contaminated glass beads 70/30 MeOH/H_2O	^{a}0.104	1.70	0.42	42	5.0	14.5
PCE contaminated sandy soil 70/30 MeOH/H_2O	^{a}0.155	1.76	0.42	35	5.0	14.5
NAPL Contaminated soil 70/30 EtOH/H_2O	^{b}0.067	1.89	0.41	15	5.0	14.9
NAPL Contaminated soil 70/10/20 EtOH/PeOH/H_2O	^{b}0.067	1.87	0.43	20	5.0	14.2

[a] S_N were estimated using weight difference method;
[b] S_N were estimated using partitioning tracer method.
[c] P_e is Peclet number, $P_e = vL/D$.

contaminated soil columns, determined from the breakthrough curves of the non-reactive traces(PFBA, Br or methanol) are listed in Table 3-1 as well.

Cosolvent Flushing of PCE Contaminated Columns

PCE contaminated glass bead columns were flushed with 40/60 (v/v) or 70/30 (v/v) methanol/water mixture. Figure 3-3 and 3-4 show plots of fractional recovery of residual PCE and effluent concentrations of PCE as a function of cosolvent pore volumes flushed through the columns. The points which effluent concentration lie above the normal breakthrough curves around 0.8 to 1.5 pore volumes are from those samples with white cloudy "emulsion" like effluent.

When 40/60 methanol/water solution was used for flushing, the white cloudy "emulsion" in the effluent started to appear approximately at 0.9 pore volume and ended at about 1.2 pore volumes displaced. A relatively small amount of the separate-phase PCE was displaced from the column as an "emulsion" during flushing with 40/60 methanol/water. For 70/30 methanol/water flushing, more "emulsion" appeared in the effluent, and the emulsion condensed into a small droplet of clear free PCE in the bottom of the vials. The higher effluent concentration shown at 0.8 to 1.5 pore volumes (Figure 3-4) are total PCE concentrations of effluent (i.e., with methanol-dissolved PCE), including the mass eluted as a cloudy emulsion. The presence of an "emulsion" in the early 0.8 to 2 pore volumes effluent may not be consider as a mobilization of the PCE, because the PCE in the column was initially dyed with Sudan III (red), which is a hydrophobic dye and insoluble in water. If PCE was mobilized during cosolvent flushing, the cloudy or condensed free PCE should be red as the original

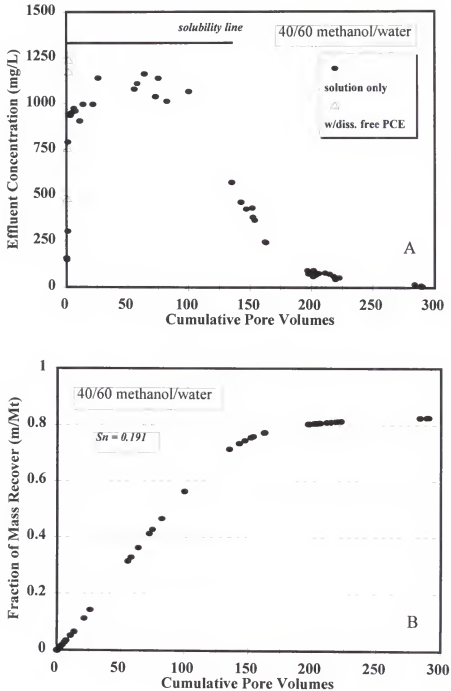

Figure 3-3. Effluent concentration and fraction mass recovery for PCE with 40/60 methanol/water (v/v) flushing on PCE contaminated glass bead column

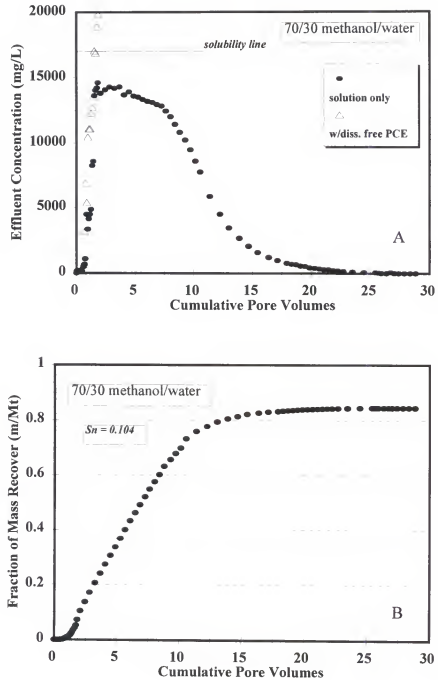

Figure 3-4. Effluent concentration and fraction mass recovery for PCE with 70/30 methanol/water (v/v) flushing on PCE contaminated glass bead column

dyed PCE. Therefore, the "emulsion" like effluent may be the supersaturated PCE, due to the heat generated by the solvent front mixing with water. This local heating increased the solubility of PCE, and flowed out as cloudy fluid due to cooling and condensation. The heat generated by cosolvent and water mixing varied from 3-4^0 C for 40/60 methanol/water mix with water, 7-8 ^{0} C for 70/30 methanol/water mix with water. PCE with heat of change (ΔH) equals 12.056 kcal/K•mol, solubility would increase 1.2 to 2 times if the temperature changes 3 to 10^0 C.

The 70/30 methanol/water flushing of the PCE contaminated soil showed that about 85% of residual mass was recovered within 50 pore volume with two flow interruption (Figure 3-5). The tailing evident in the effluent concentration curve may due to the sorption and desorption of the PCE on the soil organic matter since the Eustis sandy soil contains 0.47% organic carbon. The flow interruption technique indicates mass transfer limitations and may effectively reduce the solvent flushing volume.

Comparison of different cosolvent flushing

As indicated in Figures 3-3 and 3-4, flushing the PCE contaminated glass bead columns with 70/30 methanol/water more efficiently removed the PCE mass from the column than flushing with 40/60 methanol/water. This is not only due to the significantly higher solubility of PCE in 70/30 methanol/water (partially miscible) (Figure 3-6A), the heat generated from the solvent front is also higher. The reduction in the interfacial tension is also greater for 70/30 methanol system comparing to that for 40/60 methanol/water. IFT measurements for the PCE/methanol/water system by Imhoff and his coworkers (Imhoff et al., 1995) demonstrated a significant decrease with increasing methanol/water fraction

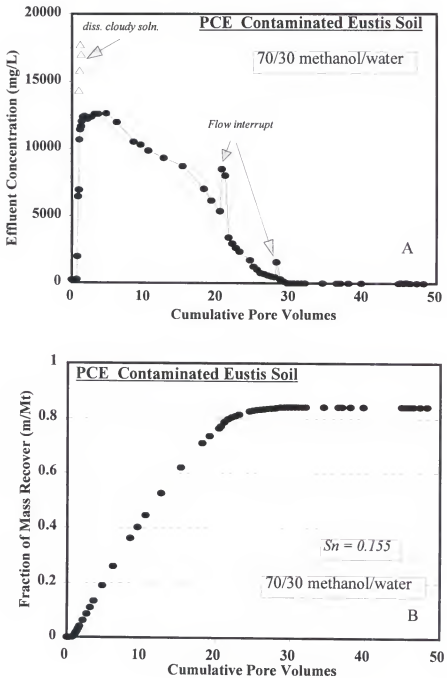

Figure 3-5. Effluent concentration and fraction mass recovery for PCE with 70/30 methanol/water (v/v) flushing on PCE contaminated Eustis soil column.

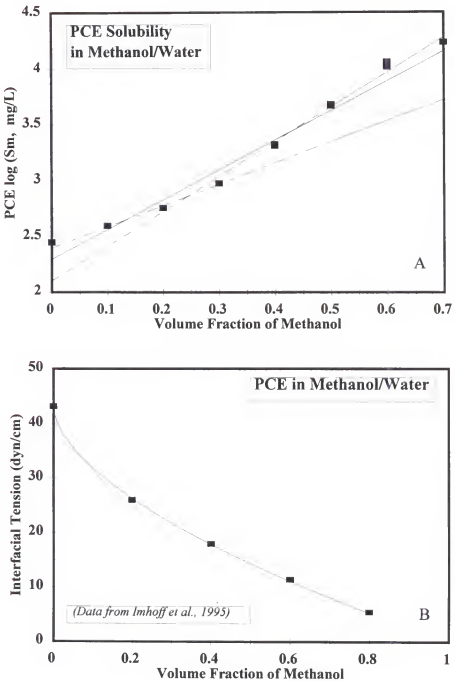

Figure 3-6. Relationship of PCE solubility (A) and interfacial tension (B) to volume fraction of methanol in the solution

(Figure 3-6B). Compare the glass bead packing with the sandy soil packing (Figure 3-4 and 3-5), the front side of the elution profile appears similar in shape. On the back side of the curve, however, the PCE elution from the soil column shows more tailing, and seems rate limited (The flow interruption enhanced the effluent concentration). Since the sandy soil contains organic matter, sorption of PCE on soil organic matter may slow the flushing process. Over all, the residual PCE in glass bead column was removed more efficiently than that in soil column.

Cosolvent Flushing of NAPL Mixture Contaminated Soil Column

Columns packed with NAPL contaminated soil from Hill AFB, UT, were flushed with 70/30 ethanol/water or 70/10/20 ethanol/pentanol/water mixtures. Similar cosolvent mixtures were used in the in situ solvent flushing study at the Hill AFB field site (Rao et al, 1997). The lab column data provided useful information for designing the field test. The effluent concentration and mass recovery of the target NAPL components are plotted versus the cumulative pore volumes of cosolvent mixture flushed through the column (Figure 3-7 to 3-9)(Appendix B. Figure B-1 to B-9). The mass recovery was calculated based on the total mass of each target components, which was estimated by methylene chloride extraction and GC-FID analysis (Table 3-2). The mass recovery estimated for p&m-xylenes and 1,2 4-trimethylbenzene resulted in more than 100 % removal (Figure B-1 and B-5). This may due to the difficulty in chromatographic interpretation for analysis of these components from the complex NAPL mixture. Accumulation of small error from each effluent sample analysis may yield larger difference in comparing with methylene chloride extraction data (total mass).

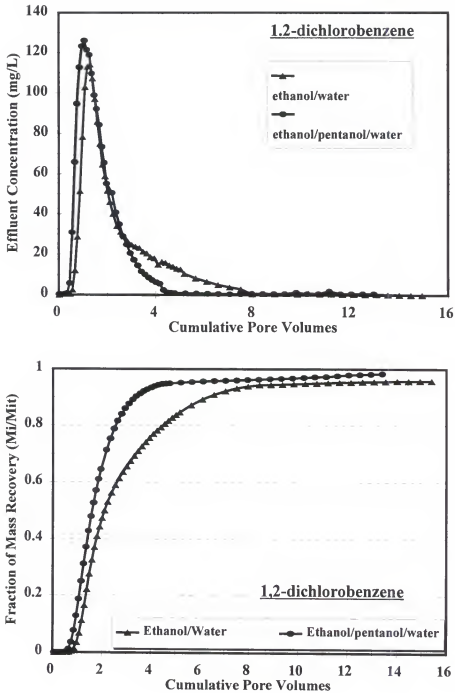

Figure 3-7. Comparison of ethanol/water and ethanol/pentanol/water flushing on effleunt concentration and fraction of mass recovery for 1,2-chlorobenzene on NAPL contaminated soil from Hill AFB, UT.

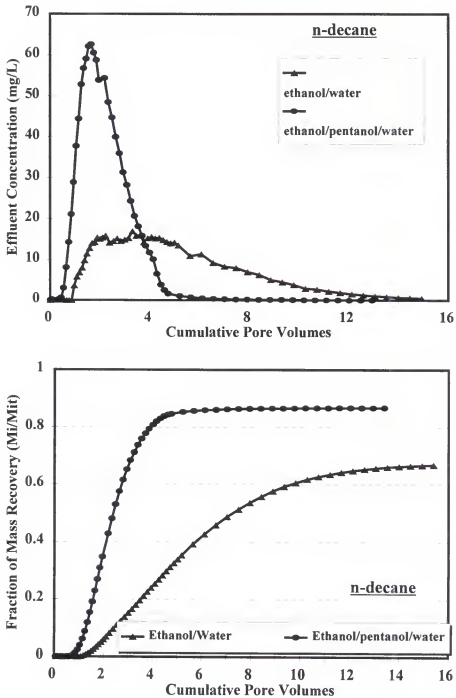

Figure 3-8. Comparison of ethanol/water and ethanol/pentanol/water flushing on effleunt concentration and fraction of mass recovery for Decane on NAPL contaminated soil from Hill AFB, UT.

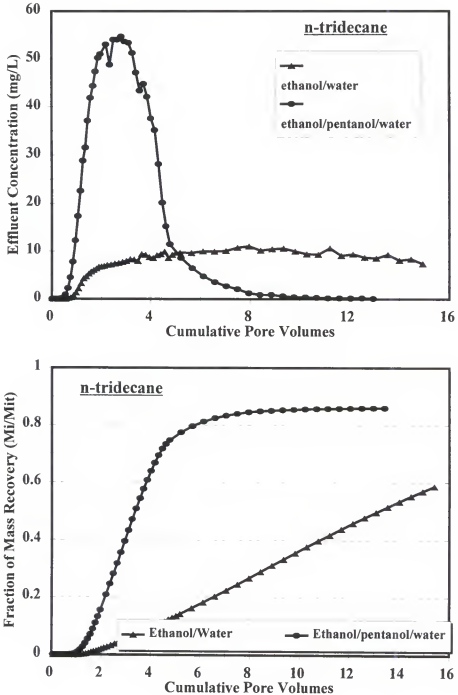

Figure 3-9. Comparison of ethanol/water and ethanol/pentanol/water flushing on effleunt concentration and fraction of mass recovery for n-tridecane on NAPL contaminated soil from Hill AFB, UT.

Table 3-2. Compiled mass of target components for NAPL contaminated soil

Compound	*Mass (µg /g soil)		
	pre-flushing	[a] post-col 1	[b] post- col 2
p-, *m*-Xylenes	5.414	0.071	0.012
o-Xylene	3.318	0.111	0.042
1,3,5-Trimethylbenzene	5.774	0.083	0.000
Decane	34.119	0.353	0.179
1,2,4-Trimethylbenzene	26.667	0.259	0.000
1,2-Dichlorobenzene	43.766	0.581	0.305
Undecane	163.270	8.110	0.597
Dodecane	60.635	16.267	1.121
1,2,4-Trichlorobenzene	14.851	1.389	1.210
Naphthalene	11.995	2.783	0.111
Tridecane	45.998	24.124	1.882

*methylene chloride extraction.
[a] Column be flushed with 17 pore volumes 70/30 ethanol/water mixed solvent;
[b] Column be flushed with 15 pore volumes 70/10/20 ethanol/pentanol/water

For NAPL components with high aqueous solubility (1,2-dichlorobenzene (DCB)), the maximum concentrations in both solvent mixtures (ethanol/water or ethanol/pentanol-/water) were not different (Figure 3-7); within about 8 pore volumes, flushed, about 95% of the DCB mass was removed by both ethanol/water flushing and ethanol/pentanol/water flushing. The mean arrival times, determined from the normalized first moments (μ_1) (Table 3-3), were 3.02 and 2.24 pore volumes for ethanol/water flushing and ethanol/pentanol/water flushing, respectively, Thus, the difference in μ_1 for both cases is less than a pore volume. For NAPL components with low solubility (e.g., decane), ethanol/water flushing with several pore volumes may required for substantial mass recovery. With the addition of a small amount of a high-molecular weight alcohol (pentanol), decane was much more efficiently removed compared with flushing just ethanol/water mixture (Figure 3-8). The normalized first moment (μ_1) for ethanol-water flushing was much greater than that for flushing with ethanol/pentanol/water (6.1 vs 2.7). Cosolvent flushing of other target components also showed similar patterns of more efficient removal with the ternary solvent mixtures (see first moments listed in Table 3-3).

The column data indicate that the Hill AFB NAPL does not completely dissolve in pure methanol or ethanol. Only the higher-molecular-weight alcohols were capable of achieving full miscibility with the NAPL. Pentanol is one of the alcohols that is capable of forming a single-phase mixture with the Hill NAPL (Falta et al., 1996). Addition of pentanol to ethanol/water mixture significantly increased solubility of several hydrophobic components in the NAPL. For example, the solubility of undecane is 3000 mg/L in a binary mixture (70% ethanol), but increase three-fold to 9500 mg/L in a ternary mixture (60%

Table 3-3. Estimated mean arrival time (μ_1) for target components with cosolvent flushing

Compound	*Mean arrival time (μ_1) (pv)	
	70/30 ethanol/water	70/10/20 ethanol/pentanol/water
p-, *m*-Xylenes	4.487	2.349
o-Xylene	4.168	2.877
1,3,5-Trimethylbenzene	4.758	2.317
Decane	6.076	2.681
1,2,4-Trimethylbenzene	5.925	2.806
1,2-Dichlorobenzene	3.056	2.237
Undecane	7.119	2.922
1,2,4-Trichlorobenzene	6.103	3.538
Naphthalene	6.773	3.213
Tridecane	9.385	3.714

*Estimated using first normalized moment.
a. Column be flushed with 70/30 ethanol/water mixed solvent;
b. Column be flushed with 70/10/20 ethanol/pentanol/water

ethanol, 10% pentanol), and increase almost an order-of-magnitude, 23000 mg/L, in 70/10/20 ethanol/pentanol/water mixture (Chapter 2).

In Figure 3-10, measured BTCs for plotted DCB and undecane are plotted versus cumulative pore volumes of effluent. A chromatographic type of separation of DCB and undecane in ethanol/water system (Figure 3-10A) indicated the selective removal of DCB by ethanol/water. The mean arrival times (normalized first moment) for DCB and undecane in this system were 3.07 and 7.12, respectively. For ethanol/pentanol/water flushing DCB and undecane eluted almost together (Figure 3-10B) and both had higher effluent concentrations compared to that in ethanol/water system, and their mean arrival times were different by only less one pore volume (2.24 for DCB, and 2.92 for undecane).

Methylene chloride extraction of soils from columns subjected to cosolvent flushing showed that about 54.13 and 5.46 μg/g of target component mass remained after cosolvent flushing with binary and ternary solvent mixtures (Table 3-2). The average NAPL removal effectiveness was 86.98 % and 98.6%, respectively, for ethanol/water and ethanol/pentanol-/water flushing. The mass recovery calculated from the moment analysis of the elution profiles yielded an average effectiveness of 84.5% and 91.4% for ethanol/water and ethanol/pentanol/water, respectively (Table 3-4). Data summarized in Table 3-4 show that less than 50% of the tridecane was flushed out by ethanol/water mixture. Similar or lower mass removal may be possible for other longer chain or higher molecular weight alkanes. The addition of pentanol in a ethanol/water system has effectively removed tridecane, the recovery of increased to as high as to 95.7 %.

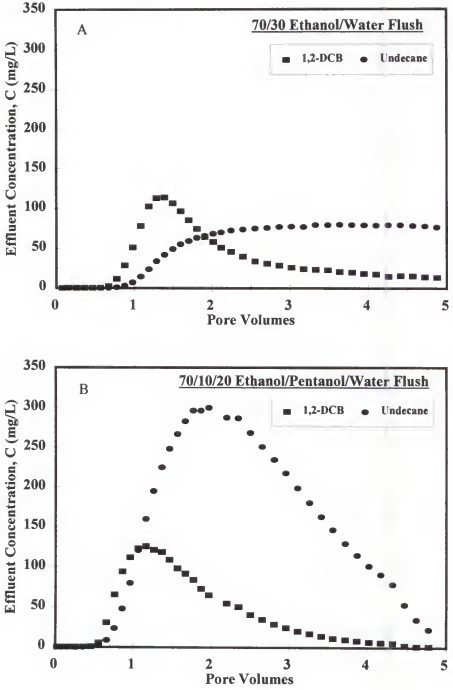

Figure 3-10. Comparison of the degree of separation of 1,2-dichlorobenzene and undecane for ethanol/water with ethanol/pentanol/water flushing of NAPL comtaminated soil from Hill AFB, UT

Table 3-4. Target components mass recovery by cosolvent flushing for OU-1 NAPL contaminated soil

Compound	Effectiveness			
	soil extraction		zeroth moment	
	[a]Col 1	[b]Col 2	Col 1	Col 2
p-Xylene	0.987	0.997	1.160	1.291
o-Xylene	0.966	0.981	0.890	0.994
1,3,5-Trimethylbenzene	0.986	1.000	0.899	0.754
Decane	0.990	0.995	0.669	0.869
1,2,4-Trimethylbenzene	0.990	1.000	1.187	1.322
1,2-Dichlorobenzene	0.987	1.000	0.958	0.984
Undecane	0.950	0.995	0.886	0.994
Dodecane	0.821	0.987	0.507	0.689
1,2,4-Trichlorobenzene	0.906	0.939	1.308	1.025
Naphthalene	0.768	0.996	0.435	0.489
Tridecane	0.476	0.957	0.587	0.860
Average recovery	**0.893**	**0.986**	**0.845**	**0.914**
Partitioning Tracers $S_{N\,post}/S_{N\,pre}$			**0.478**	**0.672**

[a]. Column flushed with 17 pore volumes of 70/30 ethanol/water mixed solvent;
[b]. Column flushed with 15 pore volumes of 70/10/20 ethanol/pentanol/water.

Partitioning tracer tests were also used to estimate the residual NAPL saturation in the columns. Both pre- and post-flushing tracer tests were run on two NAPL contaminated soil columns (for ethanol/water and ethanol/pentanol flush). Similar values of the NAPL residual saturations (S_N), 0.067, were measured for both columns (Figure 3-2). Post-flushing partitioning tracer results indicated that substantial residual NAPL mass still remained in both columns (Figure 3-11), with the S_N values of 0.035 and 0.023 for ethanol/water and ethanol/pentanol/water, respectively. Therefore, the NAPL mass recovery estimated from pre- and post-flushing partitioning tracer tests, were 47% and 67% for ethanol/water and ethanol/pentanol/water, respectively. There is a significant difference in the NAPL mass recovery between the two methods (estimated from partitioning tracers and calculated by soil component extractions) (Table 3-4), which indicated that the target components may only represent a subset of the constituents in the NAPL contaminated soil, remaining part of the NAPL constituents may be high in molecular weight or more strongly associated with soil particles. On the other hand, the partitioning tracer technique, based on several assumptions (stated early in the Chapter), may need to be carefully evaluated. In the next Chapter, partitioning tracer behavior is further evaluated and discussed.

The removal of contaminants by cosolvent flushing is much more effective with addition of small amount of higher molecular weight alcohol, which should make the cosolvent flushing technique more attractive.

Numerical Modeling of Cosolvent Enhanced Dissolution

The simulation model developed by Augustijn et al. (1994) for cosolvent-enhanced

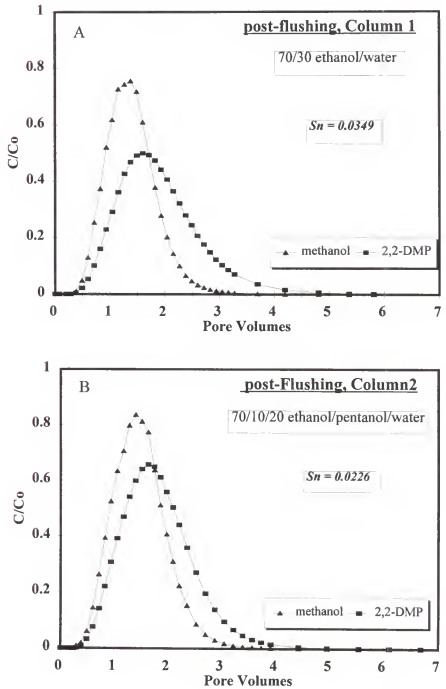

Figure 3-11. BTC of non-reactive and partitioning tracers used for estimation of residual NAPL saturation (Sn) for post-cosolvnet flushing NAPL contaminated soil column

desorption of contaminants was adapted (Jawitz, 1997) to simulate cosolvent-enhanced dissolution of NAPLs. This one-dimensional flow model is based on the bicontinuum approach, where desorption is assumed to occur instantaneously only at a fraction of sorption sites, and is described by a first-order mass transfer model at all other sites. For the work presented here, this bicontinuum approach was also assumed appropriate for NAPL dissolution. Thus, a fraction of the NAPL is dissolved instantaneously, while dissolution of the remaining NAPL is subject to a first-order mass-transfer constraint. In this section, selected experimental data and model simulations are compared to demonstrate the applicability of the model. The dissolution data from single NAPL (PCE) and complex NAPL mixture presented in the earlier sections were fitted with the model predictions. For complex NAPL mixture, four different components, o-xylene, decane, 1,2,4-trimethylbenzene and 1,2-dichlorobenzene were considered to be representative of the behavior of other NAPL constituents of concern. The parameters which were used in the model were estimated as follows:

Peclet Number (*Pe)* The hydrodynamic characteristics of the NAPL-contaminated soil columns were determined by estimating the Peclet numbers from the breakthrough curves of the non-reactive tracer from the partitioning tracer test (Figure 3-2).

Retardation factor (*R*) For transport problems, equilibrium sorption is commonly expressed in terms of a retardation factor:

$$R = 1 + \frac{\rho_B}{\theta} K \qquad (3\text{-}9)$$

where θ is the volumetric water content (ml/cm^3), and ρ_B is the dry bulk density (g/cm^3). The initial mass of contaminant *i*, M_i (g/cm^3), present in the system is given by :

$$M_i = \theta C_i + \rho_B S_i \tag{3-10}$$

where C_i (g/ml) is the aqueous concentration of the contaminant, and S (g/g) is the concentration in NAPL (modeled as sorbed phase). If the mass in the NAPL phase is linearly related to the mass in solution, then combining Equations 3-9 and 3-10 gives the equivalent retardation factor:

$$R_i = \frac{M_i}{\theta C_i} \tag{3-11}$$

Thus, an equivalent retardation factor can be determined from knowledge of the mass of NAPL constituent *i* present in the system and the constituent's aqueous concentration. For a multi-component NAPL, the equilibrium aqueous concentration of an individual component is defined by Raoult's law:

$$C_i = X_i S_i \tag{3-12}$$

where S_i is the aqueous solubility of contaminant i and X_i is the mole fraction of i in the NAPL. Assuming the mole fraction to be approximately equal to the mass fraction and small NAPL saturations and no air, and combining Equations 3-10, 3-11 and 3-12, the equivalent retardation factor can be written as :

$$R = \frac{S_N \rho_N}{S_t 10^{-6}} \qquad (3\text{-}13)$$

Fraction of instantaneous sites (F) The parameter describing sorption nonequilibrium F, generally is unaffected up to 20% cosolvent over a range of different chemicals and then decreases with increasing cosolvent fraction (Brusseau et al., 1991). Augustijn et al.(1994) proposed the following relationship for cosolvent fractions above 20%:

$$F^m = F^w - \frac{(F^w - 0.01)}{0.8} (f_c - 0.2) \qquad 0.2 \leq f_c \leq 1 \qquad (3\text{-}14)$$

where the superscripts *w* and *m* refer to the values of F in water and in the cosolvent mixture respectively, and f_c is the cosolvent fraction. Equation 3-12 assumes an initial constant F, and a linear decrease beyond a cosolvent fraction of 0.2 to an arbitrary value of 0.01 for the neat organic solvent. However, the compilation of F values for different chemicals and soils (Augustijn, 1993) showed no apparent relationship between F and the equilibrium sorption coefficient normalized to the organic carbon fraction (K_{oc}).

Damkohler number (ω) The Damkohler number is a measure of the mass transfer limitations, and is given by:

$$\omega = \frac{k L}{v} \qquad (3\text{-}15)$$

where k is the first-order mass-transfer rate coefficient (hr^{-1}), L is the flow path length (cm), and v is the fluid velocity (cm/hr). Value of k for given constituents can be estimated from the equilibrium sorption coefficient for organic carbon, K_{oc}. Using data for various soil types from Brusseau and Rao (1989) along with more recently compiled data, Augustijn et al.(1994) developed the following log-log, inverse relationship between k and K_{oc}:

$$\log k = 3.53 - 0.97 \log K_{oc} \qquad (3\text{-}16)$$

When the "aging effects" on the mass transfer rates are incorporated process, Augustijn (1993) established the following relationship by using additional data:

$$\log k = 1.74 - 0.69 \log K_{OC} \qquad (3\text{-}17)$$

Rate constants calculated from Equation 3-17 will be approximately one order magnitude lower than those calculated from Equation 3-16. However, the effects of "aging" and different types of NAPL contamination on mass transfer rates are not well understood. Augustijn (1993) hypothesized that due to the effects of aging (e.g., NAPL degradation, oxidation, and polymerization), mass-transfer rates would gradually change from extremely slow rates in freshly contaminated soils, back to an end-point mass-transfer behavior similar to that uncontaminated soils. The log K_{oc} - log K_{ow} relationship presented in Figure 2-17 for four different type soils suggested that the Hill AFB field site NAPL contaminated soil behavior more similar to the original NAPL than to the uncontaminated soils. The physical appearance of the contaminated soil studied by Augustijn (1993) exhibited the effects of aging to a great degree than did the NAPL contaminated soil in this study.

Cosolvency power (σ) The solubility enhancement through cosolvent effects in well established by the Equation 2-4. The cosolvent effects on the retardation factor is modeled by (Nkedi-Kizza et al., 1987):

$$\log (R_m - 1) = \log (R_w - 1) - \alpha\beta\sigma f_c \tag{3-18}$$

for a ternary cosolvent mixture, the solubility enhancement can be modeled by the following equation:

$$\log (R_m - 1) = \log (R_w - 1) - (\alpha_1 \beta_1 \sigma_1 f_{c1} + \alpha_2 \beta_2 \sigma_2 f_{c2}) \tag{3-19}$$

where the subscripts i refer to the cosolvents. For the simulations presented here, the NAPL/cosolvent and water/cosolvent interaction correction factors, α and β respectively, were both assumed to be equal to 1. Equation 3-17 then can be simplified as:

$$\log (R_m - 1) = \log (R_w - 1) - \sigma^* (f_{c1} + f_{c2}) \tag{3-20}$$

where σ^* is a weighted average cosolvency power:

$$\sigma^* = \frac{\sigma_1 f_{c1} + \sigma_2 f_{c2}}{f_{c1} + f_{c2}} \tag{3-21}$$

Brusseau et al. (1991) presented data which indicated that the first-order mass-transfer rate coefficient increased in a log-linear fashion with increasing cosolvent fraction. Using this relationship, and the log-log inverse linear relationship between k and K_{oc}, Augustijn et al.(1994) presented a relationship between Damkohler number and cosolvent effects which

has been modified for a ternary solvent mixture as above:

$$\log \omega_m = \log \omega_w + a \sigma^* (f_{c1} + f_{c2}) \qquad (3\text{-}22)$$

where a is the slope of log k versus log K_{oc} relationship. Thus, it is evident from Equation 20 and 22 that as the cosolvent effect increased (through increasing σ and /or f_c), dissolution or desorption is increased, and mass-transfer limitations are decreased.

Numerical Modeling Results

The dissolution data from single NAPL (PCE) and complex NAPL mixture (Hill AFB) discussed above were fitted with the model predictions. For complex NAPL mixture, four different components, o-xylene, decane, 1,2,4-trimethylbenzene and 1,2-dichlorobenzene were considered to be representative of the behavior of all the NAPL constituents of concern. The model parameters used to predict the dissolution behavior of PCE in different methanol fraction with glass bead and sand packing are listed in Table 3-5, Model parameters which were used for four representative components with both ethanol/water and ethanol/pentanol/water flushing are summarized in Table 3-6.

Single component NAPL dissolution In Figure 3-12 the model simulations for PCE dissolution with methanol (fraction of 0.4 and 0.7) are compared with the experimental data. for both flushing solution. Different sigma σ values were used to best fit the data. As indicated from the batch solubility study (Figure 3-6), log solubility of PCE versus methanol, may be best described by two different regression lines, which result in two estimations of slope (σ) values. The model prediction appears to yield excess mass on the early profile,

Table 3-5. Parameters used to model dissolution of tetrachloroethylene (PCE).

Parameter	Contaminated Glass Bead Column		Soil Column
	40/60 MeOH/H2O	70/30 MeOH/H2O	70/30 MeOH/H2O
Column			
v (cm/hr)	14.90	14.52	14.52
L (cm)	5	5	5
θ	0.41	0.42	0.42
Pe	42	42	35
Dissolution			
R_w	1215	1072	1107
F_w	0.05	0.05	0.05
ω_w	0.05	0.05	0.015
σ	2.37[a]	2.88[b]	2.88
f_c	0.4	0.7	0.7
a	0.69	0.69	0.69

[a] PCE σ value for methanol fraction equal or less 0.4, [b] PCE σ value for methanol fraction higher than 0.4 (see Figure 3-6)

Table 3-6 Parameters used to model dissolution of target components.

Parameter	Value			
	o-xylene	Decane	1,2,4-TMB	1,2-DCB
with 70/30 ethanol/water flushing				
R_w	358	124511	4609	668
F_w	0.05	0.05	0.05	0.05
ω_w	0.006	0.0002	0.002	0.05
σ	3.85	6.45	4.52	4.23
f_c	0.7	0.70	0.7	0.7
a	0.69	0.69	0.69	0.69
with 70/10/20 ethanol/pentanol/water flushing				
σ*	4.18	6.75	4.70	4.19
f_c	0.8	0.8	0.8	0.8
a	0.69	0.69	0.69	0.69

*σ values for 70/10/20 ethnaol/pentanol/water flushing are weighted average cosolvency power

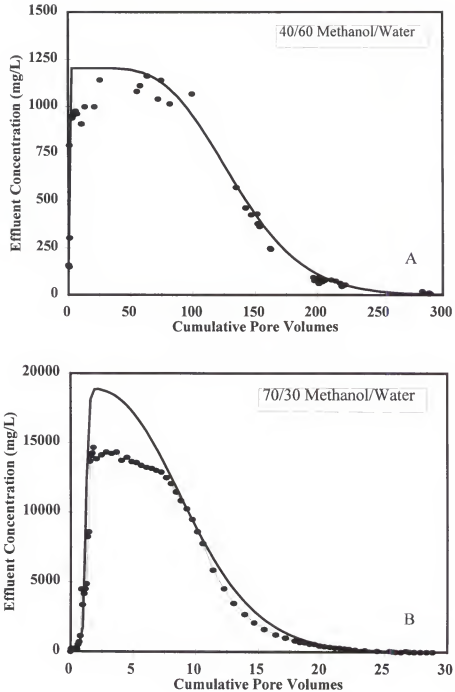

Figure 3-12. Experimental data (symbols) and independent model predictions (lines) for PCE dissolution from glass bead columns at two different cosolvent fractions: (A) 40/60 methanol/water; (B) 70/30 methanol/water

especially for 70/30 methanol/water flushing. However, the extra mass from free PCE which further dissolved with addition of pure methanol (shown as open circle) (Figure 3-12B) may make up the mass in the profile from experimental data. Other than this part of the elution profile, the data match well for the model prediction (Figure 3-12), however, longer tailing than the actual elution data. This may be due to the fact that at low elute concentration, slower mass recovery rate; also at such low level, the concentration may not be accurately measured by GC analytical procedures employed. Furthermore, the model was designed to simulate elution profiles from solvent flushing for contaminated soil with presence of low organic matter content. The model predicted elution profile for PCE contaminated soil (Figure 3-13) appears to be a relatively better fit with the data on the late elution profile. Extra mass on the early profile were due to the effluent containing free PCE. The different ω_w values for predicting of soil packing and glass bead packing may be due to the variation in the NAPL trapping or discontinuous nature of the thin film in these two different porous media, and also presence of small amount of soil organic carbon may decease the mass-transfer rate of PCE dissolution.

Dissolution from multicomponent NAPL mixture Simulated elution profiles for o-xylene, decane, 1,2,4-trimethylbenzene and 1,2-dichlorobenzene along with experimental data for flushing with two solvent mixtures are presented in Figure 3-14 through 3-17, respectively. The model predictions appear to fit the data well (shown in Table 3-6). For two fitted parameters, F_w and ω_w, fixed the F_w value was used for all the components since it is assumed as a constant according to equation 3-14. Variable ω_w values were used to fit the BTCs for different components, but the same value were able to fit the data for different

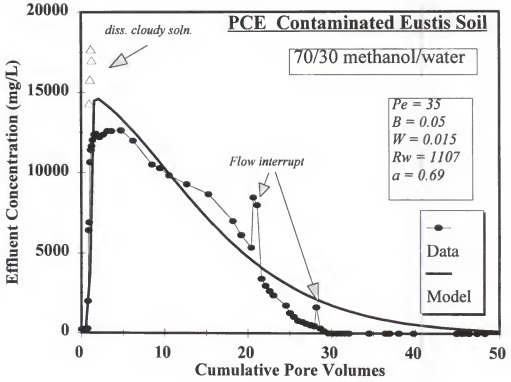

Figure 3-13. Experimental data (symbols) and independent model predictions (lines) for PCE dissolution from Eustis soil column in methanol/water solution.

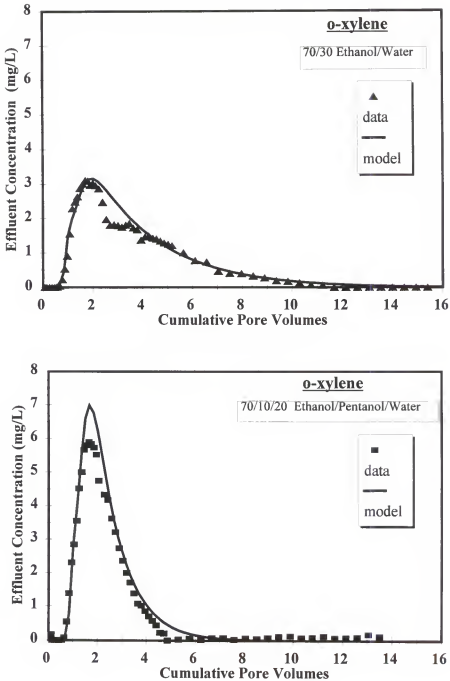

Figure 3-14. Experimental data (symbols) and independent model predictions (lines) for o-xylene dissolution from NAPL contaminated soil with binary and ternary cosolvent systems.

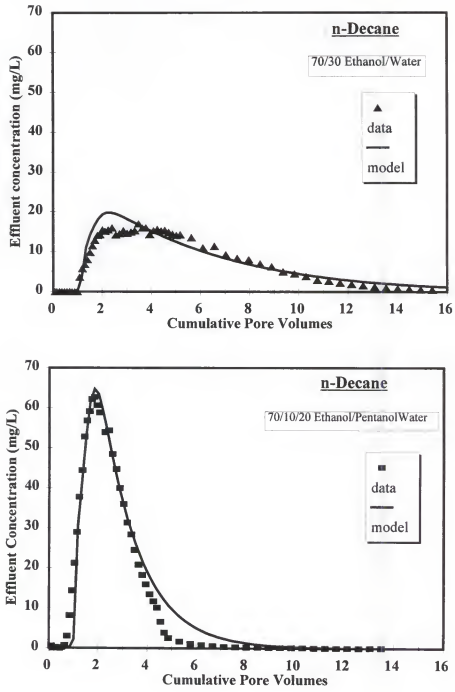

Figure 3-15. Experimental data (symbols) and independent model predictions (lines) for decane dissolution from NAPL contaminated soil with binary and ternary cosolvent systems.

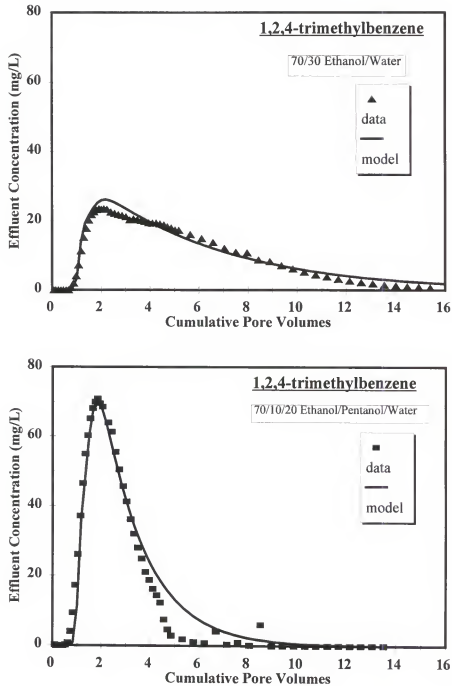

Figure 3-16. Experimental data (symbols) and independent model predictions (lines) for 1,2,4-trimethylbenzene dissolution from NAPL contaminated soil with binary and ternary cosolvent systems.

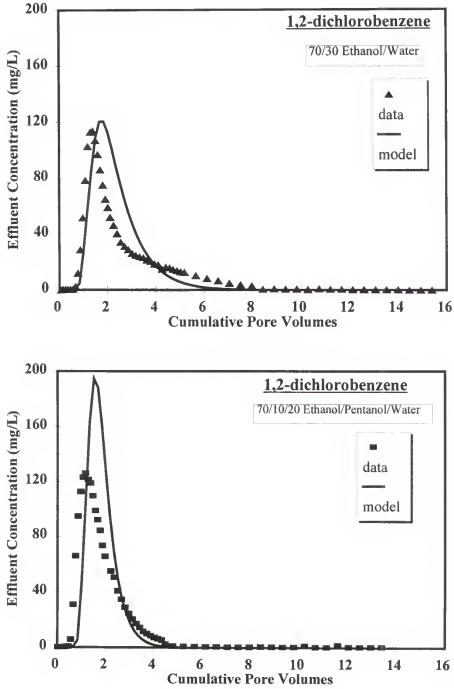

Figure 3-17. Experimental data (symbols) and independent model predictions (lines) for 1,2-dichlorobenzene dissolution from NAPL contaminated soil with binary and ternary cosolvent systems.

cosolvent mixtures (ethanol/water, ethanol/pentanol/water) for the same component. The ω_w values ranged from 0.05 for 1,2 DCB to 0.0002 for decane (Table 3-6), which indicated that the mass-transfer rate decreases with the increase in the molecule size, since the ω_w is directly related to the mass-transfer rate coefficient (equation 3-15) for the same media at fixed flow velocity. NAPL dissolution is an interfacial phenomenon, and the rate is directly proportional to the contact area between the solution and NAPL phase (Augustijn, 1993). For multi-component NAPLs, the constituents first have to diffuse through the organic phase toward the NAPL-water interface under influence of a concentration gradient before dissolution can take place; this process could become the rate limiting step. Therefore, larger molecules with lower diffusing coefficients are characterized by a slower dissolution mass-transfer rate.

Comparison of mass-transfer rate between NAPL dissolution and desorption

The ω_w values used in this NAPL dissolution simulation are about one order of magnitude lower than those used by Augustijn (1993) based on the same a value (0.69). The mass-transfer rate coefficient, k, values for the NAPL dissolution were estimated using equation 3-15, and log k values for the four representative components from NAPL mixture are plotted against their log K_{oc} (Figure 3-18) along with the data from Augustijn (1993) for desorption from three types of tar-contaminated soils. As show in Figure 3-18, data for all four components lie on the line of the 95% confidences interval along with the "aged" tar-contaminated soil. This may suggest that dissolution of contaminants from the Hill AFB NAPL contaminated soil may have a similar behavior as those from aged tar-

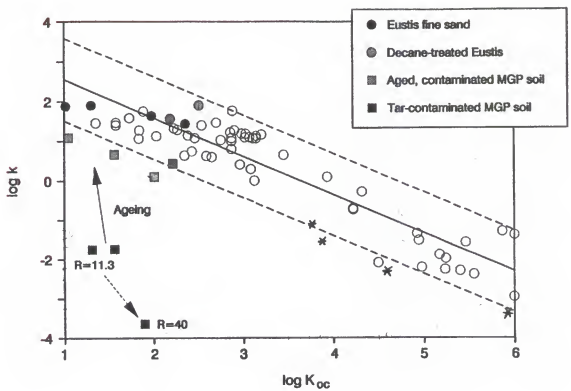

Figure 3-18. Comparison of the mass-transfer rates found for Hill AFB NAPL Contaminated soils (star mark) with the rate coefficients reported for other contaminated soils.

contaminated soils; the dissolution and desorption mechanisms in both cases are similar. Rate limitations for multi-component NAPL diffusion through the organic phase, suggest that the dissolution process is mechanistically very close to desorption and sorption model could be used to describe the phase partitioning of solutes between the immobile NAPL phase and water (Augustijn, 1993).

Conclusions

1. Cosolvent mixtures such as ethanol/water and ethanol/pentanol/water increase the solubility of contaminants, and decease partitioning and sorption on the contaminated source. These are favorable for remediation. Several experiments have showed that cosolvents are very effective additives for removing organic contaminant from complex NAPL contaminated soils;
2. The removal of contaminants by cosolvent flushing is much more effective with addition of a small amount of a higher molecular weight alcohol. The average NAPL removal effectiveness was 98.6% for 70/10/20 ethanol/pentanol/water flushing, and 86.98% for ethanol/water flushing for NAPL contaminated soil columns;
3. The contaminants dissolution from NAPLs by cosolvent flushing can be predicted by numerical model based on the bicontinuum approach. The model simulated effluent profiles for several components agree very well with the column experimental effluent profiles;
4. Dissolution from NAPLs is a rate limited process, For dissolution from multi-

component NAPL and NAPL contaminated soil, diffusion through the organic phase could be the primary rate limiting step. The rate limitations for dissolution from the multi-component Hill AFB NAPL contaminated soil may be described as similar process as those from aged tar-contaminated soils;

5 Removal effectiveness estimated from partitioning tracer method was not comparable with the removal effectiveness estimated from soil extractions. This may due to either that only limited range of components were selected to evaluated mass recovery on the component basis, or that the partitioning trace method used for residual NAPL saturation estimation may need to be examined, especially, on some of the assumptions which the method based on, such as the linear trace partitioning between NAPL/water phase and negligibly small change in partitioning coefficient for pre- and post-flushing soils. These assumptions were evaluated in next Chapter.

CHAPTER 4
TRACER PARTITIONING IN NAPL-WATER SYSTEMS

Introduction

In recent years, remediation techniques have been improved and new technique have been developed to more effectively remove organic contaminates from residual NAPL in source area of contaminated sites. Examples include in-situ flushing with cosolvents or surfactants or combination of cosolvents and surfactants (NRC, 1994, 1997). For efficient site clean up , it is essential that the NAPL source zone be properly characterized, including the delineation of NAPL source zones, and an estimation of the volume and spatial distribution of NAPL within these zones. The partitioning tracers method, introduced by Jin et al.(1995) and tested by Annable et al. (1995, 1997a) in field studies, provides an attractive alternative to the traditional intrusive technique of soil coring and analysis. The partitioning inter-well tracers tests (PITT) permit non-destructive sampling of a much larger volume of the aquifer, and yield more reliable estimation of NAPL saturation (Jin et al., 1995; Annable et al., 1997a).

Partitioning tracers are chemicals that have tendency to selectively partition into NAPLs. At equilibrium, the distribution of the tracer between NAPL and water phases is characterized by the "partition coefficient" (K_{NW}), which is the ratio of tracer concentrations in NAPL (C_N) and aqueous phases (C_w), respectively. When several tracers with different

K_{NW} are injected into a column or an aquifer with residual NAPL, and displaced, the non-partitioning tracers move at the velocity of the water, while the partitioning tracers lag behind. The chromatographic separation of the nonpartitioning and partitioning tracer pulses depends on the fraction of the time the tracer spends in the NAPL phase compared to that in water, Thus, the retardations of tracers is directly influenced by the NAPL saturation (S_N) and the equilibrium partition coefficient (K_{NW}). By selecting tracers that partition into the NAPL phase which have known or measured K_{NW}, the NAPL volume (V_N) or residual saturation in (S_N) the source zone can be quantified (Jin et al., 1995).

The theoretical basis for the use of partitioning tracers has been described in detail by Jin et al. (1995) and field tested by Annable et al. (1995, 1997a). For partitioning tracers to be used to quantify NAPL saturation, the following assumptions are made:

1) Linear, partitioning occurs between the aqueous and the NAPL phases: $K_{NW} = C_N / C_w$; where C is the tracer concentration, with the subscripts N and w denoting the NAPL and water phases, respectively. The partition coefficient (K_{NW}) for each tracer is assumed to be independent of the tracer concentration;
2) Tracer retardation is solely due to partition into NAPL phase; background sorption by all other phases (e.g., mineral surfaces) is negligibly small; and
3) Alteration of NAPL composition does not measurably impact the K_{NW} value.

Aqueous concentrations of the partitioning tracers applied in lab and field tracer tests (Pope et al, 1995 ; Annable et al, 1997) are usually less than 1 % mole fraction. Munz and Roberts (1986) indicated that in the chemical engineering field, liquid-phase mole fraction concentrations $x_i \leq 10^{-2}$ (~ 1 wt%) are typically considered to be dilute. For such systems,

the multi-phase phase equilibrium can be represented by Henry's law and the distribution of partitioning tracers between NAPL and water can be described by a linear isotherm. As the mole fraction of the tracer increases from zero, its activity coefficient decreases, which indicates that the partitioning is likely to be a nonlinear process at higher tracer concentrations (Wise, 1997). The application of the partitioning tracers in laboratory 1-D column or 2-D box experiments and field tests usually involves either frontal or pulse displacement technique (Annable et al., 1995). Though tracer concentrations used in these tests are normally less than 80% of aqueous solubility limit, tracer concentration in the NAPL (most likely in the area close to the inlet) may reach higher than 0.1 mole fraction.

The partitioning tracer test has been used to evaluate the effectiveness of cosolvent or surfactant remediation of NAPL contaminated soil columns (Table 3-4) and field test cells (Annable et al., 1997a, Jawitz et al., 1997). The estimated NAPL recoveries have been compared with that from target NAPL component recovery by extracting pre-, and post-remediated soils. However, there are two major concerns that have caught the attention of researchers. First, the partitioning tracer estimation indicates higher residual NAPL saturation than that based on an analysis of soil cores (Jawitz et al., 1997); Second, the impact of these remediated soils may have on the environment and the application of other techniques such as partitioning tracer and interfacial tracer tests. In this chapter following aspects of partitioning tracers will be discussed:

First, partitioning of tracers between NAPL and water under equilibrium conditions was examined to evaluate: (i) cooperative partitioning in the presence of a co-tracer; (ii) tracer partitioning non-ideality; (iii)tracer partitioning non-linearity; and (iv) the use of the

semi-empirical, thermodynamic model UNIFAC to predict the tracer activity coefficients. Predicted partitioning isotherms were compared to experimental data to validate the UNIFAC model.

Second, the partitioning tracers adsorption by contaminated and remediated soils was investigated using: (i)soils with different types and levels of contamination (i.e., Hill AFB NAPL , coal tar); and (ii) tar-contaminated soils with different mineralogy.

Finally, the post-remediation soils were examine based on: (i) the effect on the partitioning tracer behavior (using alcohol tracers, an aromatic tracer (benzene) and an ionic organic tracer); and (ii) the surface morphology, and the compositional and mineralogical characters of soils.

Materials and Methods

Partitioning tracers in the NAPL/water systems

One of the objectives of the tracer studies was to examine the partitioning behavior not only in a low aqueous concentration region, but also to extend the method for concentration of the tracers at higher mole fraction in the NAPL.

The partitioning tracers used in the study were: methanol: 2,2-dimethyl-3-pentanol; n-hexanol; and 6-methyl-2-heptanol. All of these tracers were obtained from Aldrich Chemical Company, with a purity of 99+%. A synthetic, multi-component NAPL was prepared by mixing reagent-grade *p*-xylene, *o*-xylene, n-nonane, n-decane, n-undecane, n-dodecane, n-tridecane, 1,2-dichlorobenzene, 1,3,5-trimethylbenzene,1,2,4-trichlorobenzene,

n-hexadecane and water in known proportions. This NAPL mixture, and n-decane as the single-component NANPL, were used in the tracer partitioning experiments. n-octanol and eicosane ($C_{20}H_{42}$) were also added as polar or non-polar co-tracers to the NAPL mixture. A sample of the field NAPL from Hill AFB OU-1 cell was also used to compare with the synthetic NAPL mixture whose composition was based on the field NAPL. Field NAPL consists of jet-fuel and degreasing solvent mixture and contains all the previously mentioned components which have been identified and at least 100 or more other unidentified components.

For measuring NAPL/water partitioning at concentrations below tracer's aqueous solubility, saturated tracer solutions (both single or mixtures of 4 tracers) were made in HPLC water. Then 1, 5, 10 and 20 ml of saturated tracer solution were transferred to 50 ml volumetric flasks, and diluted 50, 10, 5 and 2.5 times, respectively. Exact amounts of (0.25xx g) decane or NAPL mixture were weighed into 5-ml HPLC vials; then 4.5 ml each level of concentration of the tracer solution were added to the vials with the NAPL and without NAPL (used as C_0 solution), and capped immediately with Tefol-lined screw-top caps to avoid volatile losses. All measurements were triplicated. These solution were then equilibrated on a rotator for 24 hours at room temperature ($23 \pm 2\ ^0C$). After equilibration, the vials were centrifuged at 3000 rpm for 25 minutes (Dupont, Sorvall RT6000 Centrifuge). The supernatant aliquots were removed and placed in 2 ml GC vials with minimal head space, and the samples were immediately analyzed by GC-FID. The amount of tracers in the NAPL was determined by the difference between the initial and equilibrium tracer concentrations in the aqueous phase.

Partitioning tracer isotherm measured, as described above, can be extended only to less than 0.1 mole fraction of tracer in NAPL phase, since the tracers have limited solubility in aqueous phase. To achieve tracer mole fraction in NAPL higher than 0.1, two different methods were used.

Sequential addition of 80% saturated tracer aqueous solution 4.5 ml of 80% saturated tracer solution were added to the known weight of a 5 ml HPLC vial (at least triplicated) with 0.25xx g of decane or NAPL in the vial. The vials were capped immediately with Teflon-lined caps and rotated on the rotator for 12 to 24 hours. After equilibration, the solution was centrifuged at 3000 rpm for 25 minutes (Dupont, Sorvall RT6000 Centrifuge). The supernatant aliquots were removed, and placed in 2 ml GC vial for analysis. The vials with decane or NAPL and remaining tracer solution were weighed, and the remaining mass and volume of the tracer solution were added into the mass and volume of the second addition of the tracer solution. The original tracer solutions were carried on with each sequence as Co .

Tracers with NAPL at known mole fraction. Various amounts of tracer and decane or lab synthetic multi-component NAPL were weighed and mixed together so that the initial mole fraction of the tracer ranged from 0.1 to 0.9. And, 0.25xx g of the NAPL mixture were added into 5 ml vials containing 4.5 ml HPLC water and capped immediately with Teflon lined caps, then rotated on the rotator for 12 to 24 hours. After equilibration the solution was centrifuged at 3000 rpm for 25 minutes (Dupont, Sorvall RT6000 Centrifuge). The supernatant samples were placed in 2 ml GC vial for analysis. All the points were triplicated.

Analysis of tracer solution

Supernatant tracer solutions were directly injected in the GC-FID system with a 30 m long , 0.53 id, and 1 μm film of DB-624 capillare column. Other GC condition were: injection temperature at 150 ºC, FID detector temperature at 220 ºC, oven temperature program: 50 ºC held for 2 minutes and ramped to 220 ºC at 10 ºC/min; and Helium as the carrier gas, set at a pressure 40 kpsi. Each set of samples run included five standards of known concentration at beginning. One or two standards were also analyzed intermittently during the run.

Data Analysis

The amount of tracers partitioning into the NAPL phase at different tracer concentrations (S_o, in μg tracer/g of NAPL) was calculated as follows:

$$S_e = \frac{(C_o - C_e)V}{M_N} \tag{4-1}$$

where C is the concentration of the tracer, subscripts *o* and *e* donate initial and equilibrium concentrations, respectively; V is the volume of tracer solution; and M_N is the mass of NAPL.

For experiments where the sequential addition of the tracer solution was applied, the initial tracer concentration was modified as:

$$C_{o,i,t} = \frac{(V_{r,i-1}\ C_{e,i-1}) + (V_i\ C_{o,i})}{(V_{r,i-1} + V_i)} \tag{4-2}$$

where $V_{r,i-1}$, $C_{e,i-1}$ and $V_{r,i-1}$ are the tracer mass and volume remaining from the previous equilibrium solution, and ($V_i C_{a,i}$) and V_i is the mass and volume of the tracer at i^{th} addition. Each equilibrium stage, i ,S_e was computed as:

$$S_{e,i,t} = S_{e,i} + S_{e,i-1} \tag{4-3}$$

where $S_{e,i-1}$ is the amount of tracer in the NAPL from the previous equilibrium solution, and ($S_{e,i}$) is the amount of tracer partition in the NAPL at i^{th} equilibrium.

The tracer partitioning between NAPL/water was estimated based on tracer mass balance as:

$$S_{e(M)} = S_{o(M)} - C_e V \tag{4-4}$$

where $S_{(M)}$ is amount of tracer in µg, subscripts *e, o* for the tracer at equilibrium and initially

$$S_e(mole/mole) = \frac{S_e \times 10^{-6} \times MW_{NAPL}}{MW_{Tracer}} \tag{4-5}$$

mixed with NAPL, respectively; and C_e is the concentration of the tracer in the aqueous solution at equilibrium.

Mole-based partition data were generated by normalizing the tracer concentration in the NAPL with molecular weight of tracer and NAPL as:

where MW is molecular weight. The equilibrium concentration of the tracer was also

normalized with the solubility of the tracer, so the data could be directly compared with UNIFAC simulation results.

Tracer partitioning in contaminated and remediated soils

To investigate the partitioning behavior of tracers in remediated soils, experiments were conducted with four types of contaminated soils: 1) NAPL contaminated soils (Pre-, and post- surfactant flushing) from test cell on OU-1 site, Hill AFS, UT; 2) Coal tar contaminated soils with low levels of total PAHs (340 mg/Kg soil), simple mineral background (generally quartz); 3) coal tar contaminated soil with medium levels of total PAHs and complex mineral background; and 4) heavily contaminated coal tar soil with total PAHs as high as 18,000 mg/Kg. Four alcohols methanol, 2,2-dimethyl-3-pentanol (DMP), n-hexanol, and 6-methyl-2-heptanol (6M2Hep) and, an aromatic organic compound, benzene, were used in the column partitioning tracer tests to quantify the residual NAPL atruations for pre-, and post-flushed soils. Potassium bromide (Br^-), pentafluorobenzoic acid (PFBA), and labeled ^3H_2O were also used in the column experiment as non reactive tracers. Methanol was used to remove the contaminants from coal tar contaminated soils.

Alcohol partitioning tracers for pre-, and post- surfactant flushing soil columns

Both contaminated soil and post surfactant flushing soils taken from the OU-1 test cell were sieved and carefully packed into stainless-steel columns (length: 7.4 cm; inner diameter: 1.0 cm). After the column was completely saturated, a miscible-displacement experiment was performed with four alcohol tracers and KBr mixture. Methanol and Br were used as non-reactive tracers, while the three alcohols (DMP, hexanol and 6M2hep) were used as

partitioning tracers to quantify the residual NAPL saturation and to evaluate the partitioning behavior. A pulse of the tracer mixture was pumped through the columns using a Gilson piston pump. Water was then pumped through. The column effluent samples were collected and analyzed as soon as possible using a GC-FID (the same GC method as described early in the Chapter) for measuring the concentration of alcohol tracers. Bromide (Br-) concentrations were analyzed by HPLC (UV at 205, Dionex IONPAC AS4A-SC ion exchange column, 1.2 mM of Sodium Borate as a solvent at flow rate 2 ml/min).

Waterloo coal tar contaminated soil column For the Waterloo soil column experiment, only the middle section of the column (7.4 cm x 1.0 cm stainless steel) was packed with the soil. Clean builders sand (heated in a muffle-furnaced at 550 OC for 24 hours) was packed in both ends the of the column. The column was saturated with water; then alcohol tracer tests were conducted as described previously. After the tracer test, the column was flushed with about 200 pore volumes of 90/10 methanol/water solution until the yellow color effluent became clear. Methanol was displaced by extensive flushing with water. Then, another tracer test (the same as the pre-flushing tracer test) was conducted.

Coal tar contaminated UT soil columns The coal tar contaminated soils (UT 586, UT690) were packed in stainless steel columns (7.4 cm x 1.0 cm), after the column was completely saturated with 0.01 N $CaCL_2$ water, A 1.0-ml stainless steel sample loop was installed between pump and the column, so that, instead of injecting large pulses of organic solution, a small volume was injected to limit radioactive waste and minimize the sample volatilization. One ml, approximately half of the pulse of ^3H_2O, was injected as a non-reactive tracer to determine the pore volume and Peclet number of the columns. Column

effluent was collected in scintillation vials with known volume of ScintiVerse II and ^3H_2O concentration was measured with the scintillation counter (Delta 300, 6890 Liquid Scintillation System, Searle Analytic Inc.). Following the ^3H_2O test, PFBA was also injected as a non-reactive tracer to compare with the ^3H_2O test. The hydrodynamic dispersion characteristics of the packed columns were determined by ^3H_2O and PFBA breakthrough curves. Then, the column was equilibrated with 30/70 methanol/water (v/v) by pumping at a flow rate of 0.2 ml/min. ^{14}C labeled benzene methanol was injected through the loop into the packed column. ^{14}C benzene in 30% methanol was used as a partitioning tracer in this case, because the background of contaminants from the coal tar soil strongly interfered with the ^{12}C benzene detection during the analysis. The ^{14}C benzene tracer test in 30/70 methanol/water system was also done to minimize the volatilization of benzene and decrease the experimental running time. The effluent sample and initial C_0 sample were directly collected into scintillation vials with the known weight of ScintiVerse II cocktail and immediately analyzed on the scintillation counter. A breakthrough curve (BTC) was generated from these analysis results.

After running the ^{14}C benzene BTC experiment in triplicate, the packed column was washed extensively by pumping 1 to 2 liters of 100 % methanol with flow interruptions each for a different duration. Then, the column was re-equilibrated with water; and the ^3H_2O, PFBA and benzene in 30/70 methanol/water were repeated on the "remediated" soil columns. In this case, ^{12}C benzene with frontal input was used for benzene partitioning test.

The partitioning behavior of benzene was also examined using the range of the initial benzene concentration (C_0) for both pre- and post- methanol flushing tar soils in this study.

Soil particle analysis

The treated soil UT690 (after methanol wash) was further treated with particle-size fractionation method. The sandy fraction was obviously very heterogeneous, and was further separated. By use of a small hand magnet, the sandy fraction of the samples was separated into nonmagnetic and relatively magnetic fractions; the latter portion comprising about 5 % of the sandy fraction. The nonmagnetic part consisted of four types of distinct particles. They appear to be: quartz, white-bone like pieces; red-brick like pieces; and black-coal like pieces. Clay size fraction and silt fraction powder were mounted on the XRD ceramic-tile and glass slide, respectively, for X-ray diffraction (XRD) analysis to identify the mineral composition. Quartz was visually identified in the sandy fraction. The other sorted particles were ground. And mounted on the quartz plate for XRD analysis.

Surface morphology and composition of the soils

The surface morphology and composition of contaminated soils and the soil after treatments were examined by use of Optical Microscopy and SEM-EDXA. This was especially done for sorted black pieces from the UT690 coal tar soil.

Results and Discussion

Analysis of tracer isotherms

Linear partition isotherm At very low initial concentration (<0.1 aqueous solubility), linear partition behavior was observed for all three tracers (DMP, hexanol and 6-methyl-2-heptanol) in decane/water and Hill NAPL/ water systems (Figure 4-1 and 4-2). The tracer mole fraction in the NAPL is plotted against the relative aqueous concentration (C_e / C_s), which is calculated as the ratio of equilibrium aqueous concentration (C_e)divided by the aqueous solubility (C_s) of the tracer. The linear relationship was expected based on Henry's law. At such low concentrations the aqueous phase concentration of the tracer represents the activity (i.e., unit activity coefficient). It is in this low concentration range (C_e / C_s) that most of tracer partition coefficients (K_{NW}) have been measured in lab batch equilibrium studies and applied in lab column and field partitioning tracer tests (Annable et al., 1995, 1997a).

Nonlinear partitioning isotherm Figure 4-3 shows the phase partitioning behavior of 2,2-DMP in decane/water and field NAPL-water systems over an extended range of concentrations ($0 \leq C_e / C_s \leq 1$). As the concentration of DMP increases ($C_e / C_s > 0.4$), the isotherms starts to show nonlinear trends for both NAPLs. This nonlinear behavior is especially evident at tracer relative aqueous concentration $C_e / C_s < 0.6$. In this high concentration range (mole fraction in NAPL> 0.7), the partitioning isotherms become more ideal, approaching the Raoult's law prediction line. The non-ideal behavior of DMP can be easily seen (Figure 4-3) by comparing the data with Raoult's law line. It is customary to assume the Raoult's law, activity coefficient , $\gamma_i \rightarrow 1$ as $x_i \rightarrow 1$, such that the pure liquid

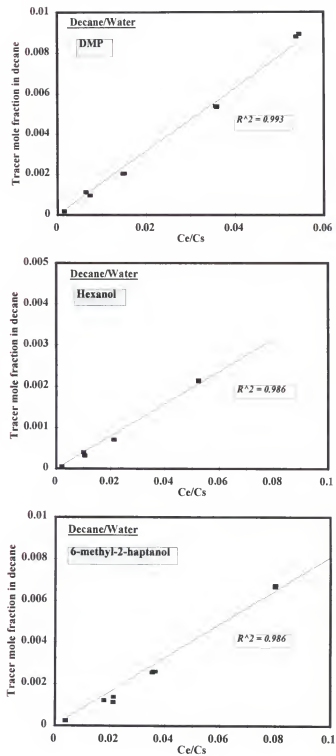

Figure 4-1. Partitioning isotherms for low aqueous concentration of tracers in decane/water system

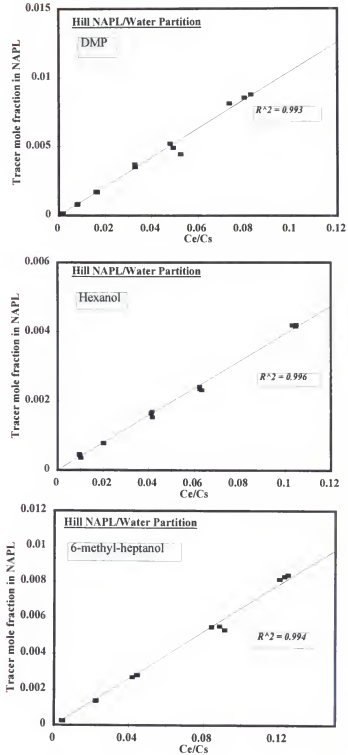

Figure 4-2. Partitioning isotherms for low aqueous concentrations of tracers in Hill AFB OU-1 NAPL/water system

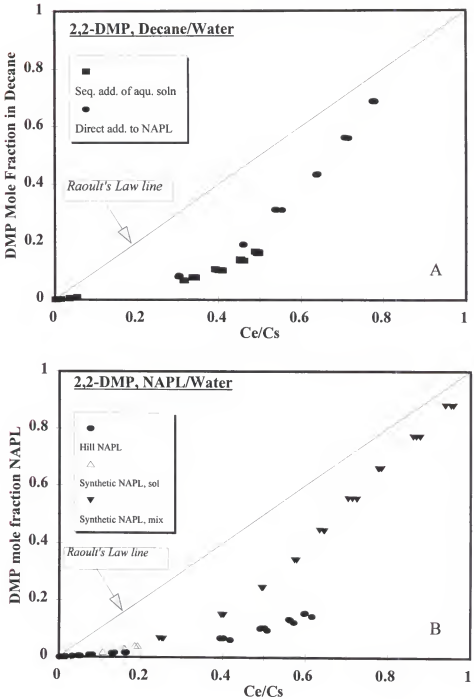

Figure 4-3. Non-linear isotherm of DMP partitioning from water into decane (A) and DMP NAPL/water partitioning (Hill NAPL and sythetic NAPL (B) open triangle: DMP partition from aqueous solution to NAPL; solid triangle: DMP direct added into NAPL

becomes the reference state. The activity coefficient then characterizes the non-ideality of the tracer in solution. The UNIFAC model can be used to predict the liquid phase activity coefficient.

Two sets of data are presented in Figure 4-3 for DMP partitioning in decane /water system. One isotherm is based on sequential addition of the nearly saturated DMP aqueous solution; the second isotherm is from initial mixing of known mole fraction of DMP with decane, then equilibrating with water. Several data points overlapped; thus, showing good agreement between the two experimental methods. These two methods achieved similarly higher mole fraction of tracers in NAPL. The sequential addition of aqueous DMP solutions achieved high mole fraction of DMP in the decane; suggesting that the pulse or frontal displacement technique used for input tracers solution during partitioning tracer tests likely resulted in higher mole fraction tracer in NAPL.

Effect of other solutes

Influence of co-tracers at low concentration Low levels of cooperative behavior in tracer partitioning is demonstrated for the multi-tracer batch experiment with all three tracers on Hill NAPL (Figure 4-4). The regressions for the linear part of the isotherms resulted in consistently higher partition coefficient (K_{NW}) values in the cases where co-tracers were present. A comparison of K_{NW} values from single- and multi-tracers tests is presented in Table 4-1. The enhancement of partitioning between the NAPL/aqueous phase in the multi-tracer system increases as the tracer concentration increases,and the cooperative partitioning is more significant for the higher molecular weight tracers. This cooperative behavior in the

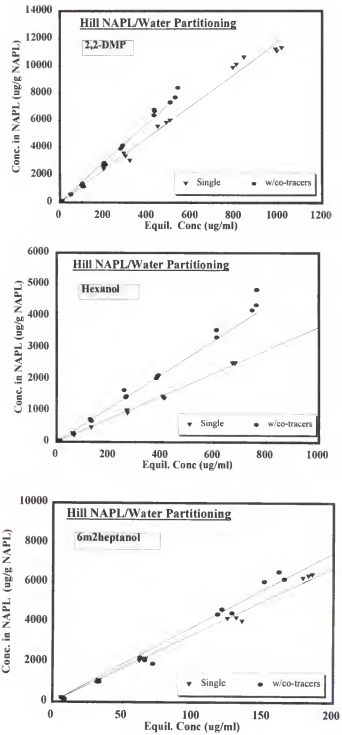

Figure 4-4. Effect of low concentration of co-tracers on the tracer partitioning in Hill NAPL/water system

Table 4-1. Comparison of tracers NAPL/water partition coefficient (K_N) measured in single-and multi-tracer aqueous

Alcohol Tracer	Partition Coefficient, K_N (ml/g)			
	Single	R^2	Mixed*	R^2
2,2-dimethyl-3-pentanol	11.7	0.989	14.3	0.994
n-hexanol	3.6	0.997	5.4	0.993
6-methyl-2-hepatanol	36.5	0.990	41.8	0.968

* mixture of four tracers (methanol, 2,2-dimethyl-3-pentanol, n-hexanol and 6-methyl-2-hepatanol).

multi-tracer system should be considered when batch-measured K_{NW} values are applied in quantifying NAPL content in the column and field partitioning tracer test. In order to obtain reasonable levels of retardation factor (R) values to estimate residual NAPL saturation (S_N), multi-tracers with a range of solubilities is commonly used in partitioning tracer tests. However, the degree of the enhancement in a dynamic flow system (column and field test) may not be similar to that measured in the batch equilibrium conditions, due to the chromatographic separation of the tracers in these flow systems. The tracer with a lower partition coefficient may move faster, and as a result, at some distance from the injection point, that tracer may experience less effect of the enhanced partitioning.

Influence of co-tracers at high concentration Presence of significant amount of another tracer in the system will change the composition of the original NAPL. As a result, it may impact tracer partitioning behavior. An extreme case of co-tracer is demonstrated in Figure 4-5 with octanol concentration as high as 30% in the synthetic NAPL mix. Since octanol is chemically and structurally similar to the tracer of interest, the tracer partitioning behavior becomes more ideal, and more linear, and will be much higher than that for octanol. The tracer partitioning isotherm with 30% octanol in the NAPL is very close to Raoult's law prediction (Figure 4-5). The impact of co-tracer on tracer partitioning behavior is an important factor that should be considered when tracer tests are used for estimation of NAPL residual saturation. This is especially true for those tests where cosolvent is used in remediation. If the residual alcohol solvent on/in NAPL is not extensively washed out by water, the partition coefficient of the tracers could be significant changed due to the presence of the residual alcohol.

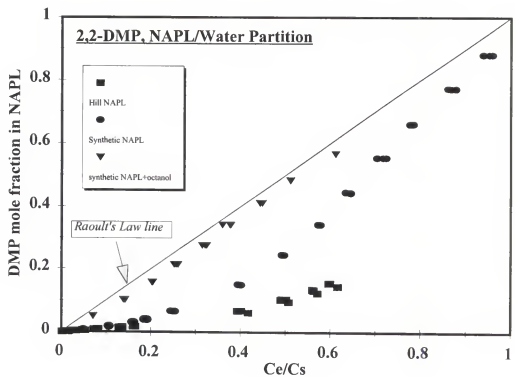

Figure 4-5. Partition isotherm of 2,2-dimethyl-3-pentanol in NAPL/water systems with 30 % of octanol present in the NAPL. Data for three NAPLs are shown: (1) Hill AFB NAPL; (2) Synthetic NAPLmixture; and (3) synthetic NAPL plus n-octanol.

Another important observation in Figure 4-5 is the deviation between the partition isotherm for the synthetic NAPL and the Hill NAPL. This deviation is not surprising since the synthetic NAPL only includes 15 identified components with several different functional groups; while the field NAPL is a very complex mixture with hundreds of unidentified components, and has been through years of the "aging" process. The tracer partitioning in the field NAPL mixture demonstrated an even stronger non-ideal behavior.

Influence of non-polar components on the isotherm. The partitioning behavior of the tracer should become more non-ideal due to increased fraction of components which are less polar and less similar in structure. Partitioning of DMP between synthetic NAPL and water with the presence of 0.05 mole fraction of a higher molecular weight alkane (Eicosane, $C_{20}H_{42}$) is shown in Figure 4-6B. As is the case for Hill NAPL after remediation, the tracer partitioning isotherm demonstrates greater deviation from the ideal line (Raoult's law prediction)

Prediction of the non-linear behavior

The UNIFAC model, originally proposed by Prausnitz et al. (1980), using group-interaction parameters is capable of predicting activity coefficients with reasonable accuracy. In this model, a mixture of different chemicals is treated as a mixture of functional groups constituting the components in the mixture. The interactions between the functional groups in the mixture, and the likely nonidealities resulting from such interactions, are calculated in order to estimate the activity coefficient of a chemical for a specified phase. The interaction parameters required in the UNIFAC model have been continuously reviewed and

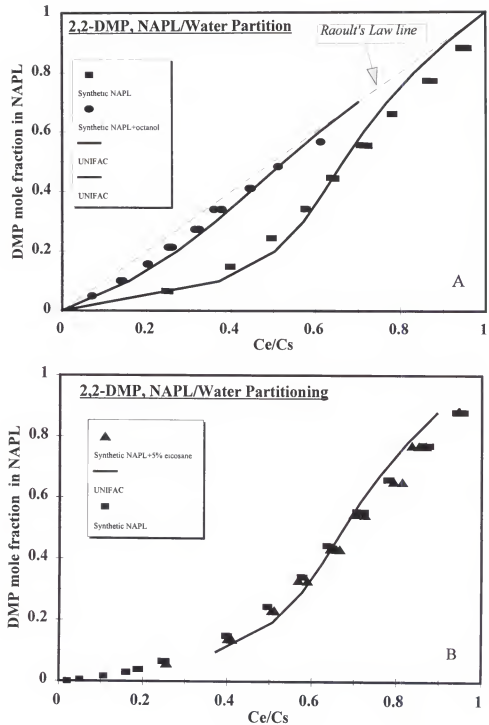

Figure 4-6. UNIFAC model simulation for 2,2-dimethyl-3-pentanol partitioning in NAPL/water systems with (A) octanol or (B) eicosane presented in NAPL

updated since the model was first introduced (Skjold et al., 1979; Magnussen et al., 1981; Gmehling et al., 1982; Alameida-Macedo et al., 1983; Hansen et al., 1991; Chen, 1992). By using this method, the activity coefficient, which characterizes the nonideality and nonlinearality of compound in the liquid solution, can be predicted.

The activity coefficient for DMP partitioning in decane-water or synthetic NAPL was predicted by the UNIFAC model. The synthetic NAPL mixture was made up with eleven target components and water in such a way that the mole fraction of each component was very close to that found in the field NAPL. Hexadecane was used to make up rest of the NAPL. To properly use UNIFAC, the functional subgroups for each compound are identified with types and quantities at a specific temperature and mole fraction (Chen, 1992). Then, the UNIFAC output data files provide the activity coefficient of tracers and NAPL or NAPL components. The activity of the partitioning racer in the aqueous and NAPL phases was calculated simply by multiplying the activity coefficient by the corresponding mole fraction.

The UNIFAC output data for all four cases of DMP partitioning are complied in Table 4-2 to 4-4. Results of the UNIFAC simulation along with the batch equilibrium partitioning data are shown in Figure 4-6. Excellent agreement between the experiment data and the UNIFAC-predicted results confirms the nonlinear behavior of the partition tracers and suggests nonlinearility may be predicted by the UNIFAC group- contribution method. However, more studies are needed to confirm this non-linear behaior in the column and field Partitioning tracer tests to more accurately estimate residual NAPL content.

Table 4-2. UNIFAC simulation output for 2,2-dimethyl-3-pentanol partitioning in decane/water system

Mole Fraction		Activity coefficient		Activity	
2,2-DMP	Decane	2,2-DMP	Decane	2,2-DMP	Decane
0.0	1.0	11.803	1.000	0.000	1.000
0.1	0.9	4.723	1.044	0.472	0.940
0.2	0.8	2.816	1.142	0.563	0.913
0.3	0.7	2.012	1.275	0.604	0.893
0.4	0.6	1.594	1.445	0.637	0.867
0.5	0.5	1.349	1.655	0.674	0.828
0.6	0.4	1.197	1.915	0.718	0.766
0.7	0.3	1.100	2.236	0.770	0.671
0.8	0.2	1.042	2.636	0.833	0.527
0.9	0.1	1.010	3.138	0.909	0.314
1.0	0.0	1.000	3.773	1.000	0.000

Table 4-3. UNIFAC simulation output for 2,2-dimethyl-3-pentanol partitioning in synthetic NAPL/water system with or without presence of octanol

Mole Fraction			Activity coefficient	Activity
2,2-DMP	Octanol	NAPL		
0.0	0.0	1.0	6.627	0.000
0.1	0.0	0.9	3.715	0.372
0.2	0.0	0.8	2.514	0.503
0.3	0.0	0.7	1.903	0.571
0.4	0.0	0.6	1.550	0.620
0.5	0.0	0.5	1.332	0.666
0.6	0.0	0.4	1.190	0.714
0.7	0.0	0.3	1.099	0.769
0.8	0.0	0.2	1.041	0.833
0.9	0.0	0.1	1.010	0.909
1.0	0.0	0.0	1.000	1.000
0.0	0.3	0.7	1.948	0.000
0.1	0.3	0.6	1.585	0.159
.2	0.3	0.5	1.358	0.272
0.3	0.3	0.4	1.211	0.363
0.4	0.3	0.3	1.124	0.445
0.5	0.3	0.2	1.052	0.526
0.6	0.3	0.1	1.016	0.609
0.7	0.3	0.0	1.001	0.700

Table 4-4. UNIFAC simulation output for 2,2-dimethyl-3-pentanol partitioning in synthetic NAPL/water system with or without presence of eicosane ($C_{20}H_{42}$)

Mole Fraction			Activity coefficient	Activity
2,2-DMP	Eicosane	NAPL		
0.0	0.0	1.0	6.627	0.000
0.1	0.0	0.9	3.715	0.372
0.2	0.0	0.8	2.514	0.503
0.3	0.0	0.7	1.903	0.571
0.4	0.0	0.6	1.550	0.620
0.5	0.0	0.5	1.332	0.666
0.6	0.0	0.4	1.190	0.714
0.7	0.0	0.3	1.099	0.769
0.8	0.0	0.2	1.041	0.833
0.9	0.0	0.1	1.010	0.909
1.0	0.0	0.0	1.000	1.000
0.0	0.3	0.7	1.948	0.000
0.1	0.3	0.6	1.585	0.159
0.2	0.3	0.5	1.358	0.272
0.3	0.3	0.4	1.211	0.363
0.4	0.3	0.3	1.124	0.445
0.5	0.3	0.2	1.052	0.526
0.6	0.3	0.1	1.016	0.609
0.7	0.3	0.0	1.001	0.700

Impacts of non-linearity of partition isotherms

The cooperative partitioning in the presence of co-tracers, and the tracer non-linear partition isotherms at high mole fraction in the aqueous solution or in the NAPL found in this study suggest that several factors should be considered when applying practicing partitioning tracer technique in estimating the residual NAPL content. Firstly, the batch equilibrium measurement of the partition coefficient, K_{NW} , should be conducted with the same combination of the tracers for column or field test, so that the cooperative affect may be minimized; Secondly, the non-linear partition behavior, which likely appears in the high aqueous concentration or high mole fraction of tracer in the NAPL, should be avoided by using low concentrations of the tracer and smaller pulse injection.

The initial and maximum concentrations of the partitioning tracers in two series of tests with the NAPL contaminated soil are listed in Table 4-5. These tests were described in Chapter 3, and the field tracer tests conducted at Hill AFB, UT were discussed by Jawitz et al. (1997). The ratio of maximum concentration of effluent to the aqueous solubility of the DMP was on the linear region of the isotherm (Figure 4-5) for most multi-level of sampling locations. Only at multi-level sample locations close to the injection (well 31 and 32) were the tracer concentrations large enough to be in the non-linear isotherm region, especially for the post-flushing partitioning tracer test. For partitioning tracer test in the columns, higher range of non-linear region was also found for the post-flushing tracer test. The tracer non-linear partitioning behavior may have resulted in an over estimation of NAPL residual saturation (S_N) in those cases. The partition coefficients used to estimate S_N were obtained from the linear region (low concentration) of partition, which would give lower value than that of the non-linear case (at the higher concentration region).

Table 4-5. Maximum effluent concentration of partitioning tracers and their relative aqueous concentration from selected sampling locations in a field test cell (Hill AFB) and lab columns

	[a] Location	Effluent maximum concentration		[b] Relative aqueous concentration (C_{max}/C_S)	
		2,2-DMP	6m2heptanol	2,2-DMP	6m2heptanol
Field Pre-SPME	31 red	483	129	0.079	0.087
	32 red	325	117	0.053	0.079
	33 red	147	44	0.024	0.030
	34 red	74	18	0.012	0.012
	53 red	210	70	0.034	0.047
Field Post-SPME	31 red	864	450	0.142	0.304(n)[c]
	32 red	671	274	0.110	0.185(n)
	33 red	307	135	0.050	0.091
	34 red	255	105	0.042	0.071
	53 red	253	93	0.041	0.063
Column Pre-flushing	Col 1	430	122	0.070	0.082
	Col 2	451	162	0.074	0.110
Column Post-flushing	Col 1	525	203	0.086	0.137(n)
	Col 2	693	284	0.114	0.192(n)

[a] From field cell multilevel sample well, at depth of 21 to 25 feet, number 31 is the closest sampling location to the injection well and 53 at the extraction well.
[b] Aqueous solubility of tracers (C_S) are: 6100 and 1480 mg/L for 2,2-dimethyl-3-pentanol and 6-methyl-2-heptanol, respectively.
[c] may be in the non-linear region.

Tracer sorption by contaminated soils

Alcohol tracers sorption by NAPL contaminated soils Figure 4-7 presents the BTCs for the alcohol tracers tests in columns packed with soils collected from the Hill AFB test cell before and after SPME flushing. The retardation of partitioning tracers in columns with SPME-flushed soil is significantly decreased since the residual NAPL has been microemulsified and diplaced during SPME flushing. The residual saturation (S_N) values calculated from these BTC data were 0.067 and 0.012 (average of three tracers) for pre- and post- flushing soil columns, respectively. The post-SPME soil was then re-contaminated by mixing a known amount of Hill NAPL. If the NAPL/water partitioning coefficient for pre- and post-SPME were assumed the same. The estimated residual NAPL saturation for this case was 0.0368 (Figure 4-7), which is slightly smaller than the expected $S_N = 0.0428$. The figures were calculated by summation of residual saturation from post-SPME and addition of the NAPL volumes (Table 4-6). The smaller residual saturation estimated by partitioning tracer test indicated that the part of residual NAPL or organic components, which partitioning with tracers from post-SPME soil may be covered by newly added NAPL and may not be accessible to the traces in this case. The remaining part of the organic phase (either soil organic matter or residual NAPL, which can not be removed by SPME, or the NAPL strongly associated with soil organic matter) may or may not have contributed to the partitioning of alcohol tracers, depending on whether they were exposed to the tracers or coated by NAPL not seen by the tracers.

However, the NAPL/water partition coefficients for post-SPME ($K_{NW,\,post}$) and for re-contaminated NAPL($K_{NW,\,mod}$) were different from that of pre-SPME ($K_{NW,\,pre}$) based on

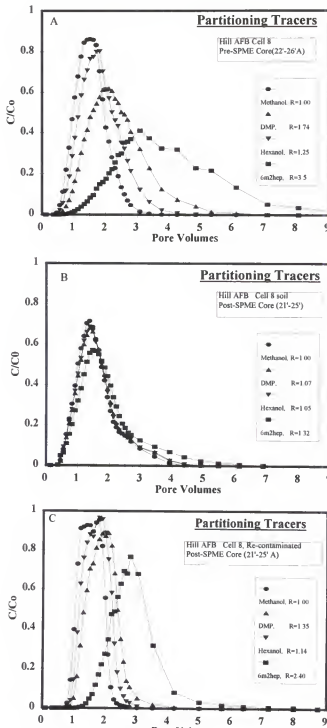

Figure 4-7. Alcohol tracer partitioning in lab columns packed with (A) pre-, (B) post-SPME flushing and (C) recontaminted NAPL contaminated soils from Hill AFB, UT

Table 4-6. The residual saturation NAPL (S_N) for pre-, post-flushing and recontaminated soil in lab column experiments

Tracers	Tracer Retardation (R)			NAPL-residual Saturation (S_N)		
	Pre-SPME	Post-SPME	Re-contaminated	Pre-SPME	Post-SPME	Re-contaminated
2,2-DMP	1.743	1.074	1.353	0.0649	0.0081	0.0314
Hexanol	1.247	1.053	1.138	0.0656	0.0176	0.0376
6-methyl-2-heptanol	3.500	1.319	2.404	0.0710	0.0114	0.0413
Average				0.0672	0.012	0.0368

* NAPL/water partitioning coefficient K_N for 2,2-dimethyl-3-pentanol, hexanol and 6-methyl-2-heptanol are 10.7, 3.52 and 32.7, respectively.

*Expected residual saturation for re-contaminated soil was 0.0428.
Re-contaminated soil was made by adding 0.0572 g of NAPL mixed with post-SPME soil packed in the column. Expected residual NAPL saturation calculated by sum of the part NAPL added in and residual saturation from post-SPME :

$$S_N = S_{Na} + S_{Nr} = \frac{\theta_N}{\theta_N + \theta_w} + S_{Nr}$$

where S_{Na} is the part of residual saturation contributed by addition of the NAPL and S_{Nr} is the residual saturation from the post-SPME soil. NAPL density assumed to be 0.9 g/ml. And θ_w is 2.00 ml/cm3.

the calculation from tracer retardations for post-SPME and for re-contaminated soil column, and as well as the pre-SPME NAPL/water partition coefficients for three partitioning tracers.

For post-SPME NAPL soil, the retardation factor can be expressed as:

$$R_{post} = 1 + \frac{K_{NW,post}\, S_{N,post}}{1 - S_{N,post}} \tag{4-6}$$

when the NAPL with a known $K_{NW,\,pre}$, was added to post-SPME soil (ΔS_N), then the retardation factor for the tracer became:

$$R_{post\,+\,\Delta S_N} = 1 + \frac{K_{NW,modi}\,(S_{N,post} + \Delta S_N)}{(1 - (S_{N,post} + \Delta S_N))} \tag{4-7}$$

and Based on Equation 2-3, we can propose a model for $K_{NW,\,modi}$ as:

$$K_{NW,modi} = \frac{S_{N,post} + \Delta S_N}{K_{NW,post}/S_{N,post} + K_{NW,pre}/\Delta S_N} \tag{4-8}$$

from equation 4-6 to 4-8, three unknowns ($K_{NW,\,post}$, $K_{NW,\,modi}$, and $S_{N,\,post}$) can be estimated based on measured post-SPME tracer retardation, R_{post}, re-contaminated retardation, $R_{post+\Delta SN}$, and measured pre-SPME NAPL/water partition coefficient, $K_{NW,\,pre}$ (Table 4-7).

The interfacial tracer test (Saripalli et al., 1996; Annable et al., 1997b) was conducted in lab columns packed with soil collected before and after SPME-flushing. The test resulted in similar NAPL/water interfacial area for both pre- and post- flushing soils (Figure 4-8). The NAPL-water interfacial area in both columns is essentially identical (~2500 cm^2/cm^3),

Table 4-7. Calculated NAPL/water partition coefficient for post-SPME soil ($K_{NW,\ post}$) re-contaminated soil ($K_{NW,\ modi}$), and residual NAPL saturation for post-SPME soil (S_N, post).

Tracers	$S_{N,\ post}$	$K_{NW,\ post}$	$K_{NW,\ modi}$	$K_{NW,\ pre}$
2,2-DMP	0.015	4.79	7.64	10.70
Hexanol	0.034	1.53	2.11	3.52
6-methyl-2-heptanol	0.009	35.13	35.21	32.07

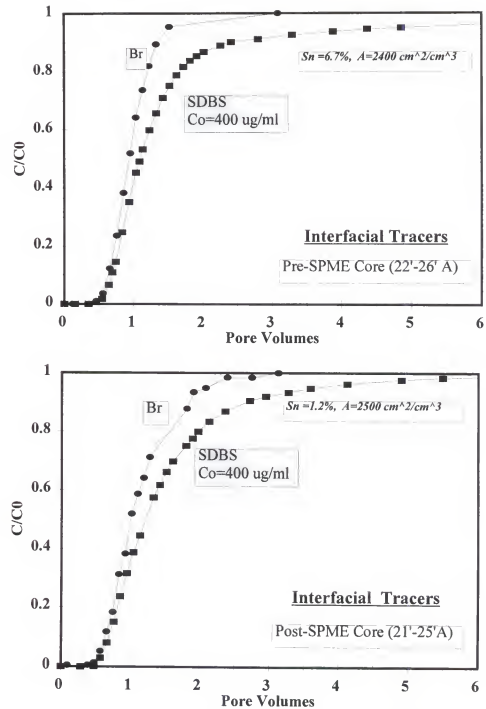

Figure 4-8. Breakthrough curves for Br and interfacial tracer (SDBS) on lab columns packed with pre- and post -SPME flushing soils.

even though the residual content was different by a factor of 6 (S_N ~6.7% and ~ 1.2%). These results suggest that removal of the NAPL only changed the thickness of the NAPL coatings. Assuming a uniform film, a 5-fold decrease in film thickness was achieved.

Pre- and post-cosolvent flushing (in column experiments, Chapter 3) partitioning tracer test data show that about 47% and 67% NAPL was removed by ethanol/water and ethanol/pentanol/water flushing. However, near-complete recovery (>95%) of all the target components was evident from pre- and post- flushing soil extractions. Similarly, for the field SPME test (Jawitz et al., 1997), less NAPL mass recovery was found from partitioning tracers estimation than based on recovery of NAPL components. Both estimation technique have their limitations. The Hill NAPL is a very complex mixture, consisting of hundreds of the extractable components. The recovery of target components may represent recovery of the components of interest. To accurately estimate the NAPL mass removal, other NAPL components, which were not identified in this study, should be considered. On the other hand, the partitioning tracer method is based on several assumptions (composition does not change through remediation process; the partitioning with soil organic matter is minimal, etc.,) which may not be applicable in many cases. Cosolvent flushing of the NAPL contaminated soil (Table 3-4) resulted in significant mass recovery, especially the xylenes and dichlorobenzene, (about 99% and 98%, respectively). For 70/30 ethanol/water flushing, however, only 48 % recovery on n-tridecane was achieved.

The Hill NAPL has been characterized as an oil equivalent to undecane to dodecane. If significant amounts of lower molecular weight and less hydrophobic components are removed, the remaining oil may become more hydrophobic and higher in molecular weight,

which on average, may be assumed to be like hexadecane. Experiments on tracer partitioning with several alkanes with different chain lengths (Figure 4-9) in this study showed that the alcohol partition coefficients (K_{NW} in ml/g) decreases with an increase in the alkane carbon number (Figure 4-10). Meyers et al (1997) extracted the Hill NAPLseveral times with 67% tert-butanol and 33% mixture, and then measured the alcohol partition coefficients. By comparing K_{NW} values with untreated NAPL, they found a decrease in the K_{NW}. The decrease in K_{NW} was about 30% for hexanol, K_{NW} = 3.12 for the untreated NAPL, 2.24 for the treated NAPL. For 6-methyl-2-heptanol, the K_{NW} decreased by ~60%; K_{NW} = 29 for untreated NAPL, 8 for the cosolvent treated NAPL. Meyers et al attributed this behavior to the cosolvent removing those most alcohol-like NAPL constituents; resulting in a NAPL with less alcohol-like components.

Benzene and PFBA on UT 586 Benzene BTCs for both methanol-washed and unwashed UT 586 coal tar contaminated soils are shown in Figure 4-11A, The retardation factor for washed soil was reduced as expected, since methanol had extensively washed away most of the PAHs and other tar components. PFBA BTC data indicate resulted in a retardation factor of 1 or close to 1 for both methanol-washed and unwashed soils (Figure 4-11B). Thus, PFBA behaved as a non-reactive tracer as expected. This sorption behavior of benzene and PFBA are generally expected.The contaminated soil from Hill AFB and UT586 coal tar contaminated soil both have simple background soil; the primary mineral was quartz. Figure 4-12, and 4-13 show soil particles from pre- and post- washing contaminated soils for Hill NAPL soil and UT586 coal tar soils, respectively. The difference in the NAPL coating on the particles can be easily identified.

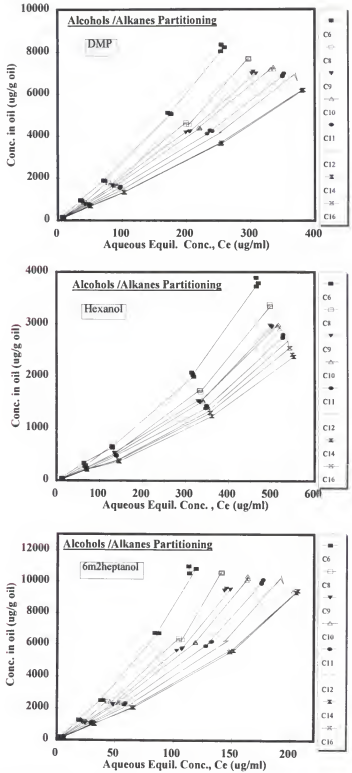

Figure 4-9. Partitioning isotherms in alkane/water system for several alkanes (C6 - C16)

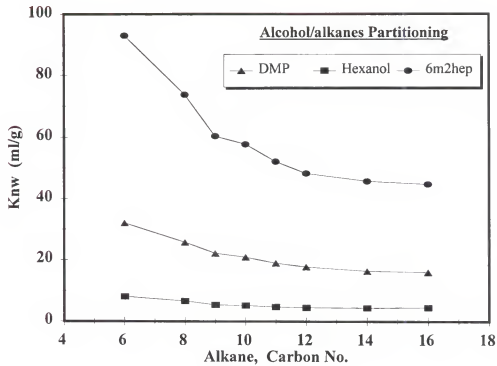

Figure 4-10. Relationship between alcohol tracer/alkane partition coefficient and carbon numbers of alkanes

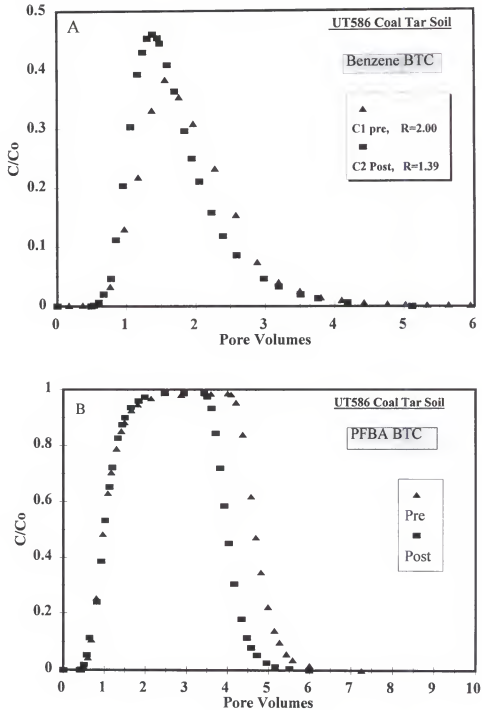

Figure 4-11. Benzene (A) and PFBA (B)BTC for UT586 coal tar contaminated soil (pre- and post-methanol wash)

A. pre-ethanol flushing

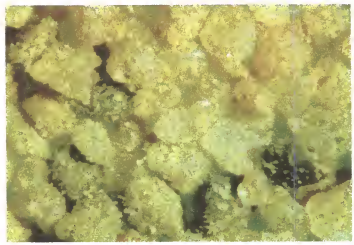

B. Post-ethanol flushing

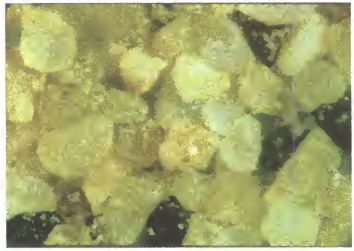

Figure 4-12. Optical Microscopy pictures for Hill AFB NAPL contaminated soil. (A) pre-cosolvent flushing; (B) post–cosolvent flushing.

A UT 586 coal tar soil pre methanol flushing

B UT 586 coal tar soil pre methanol flushing

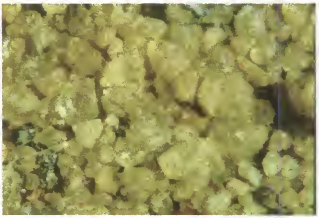

C. Pre-vs post–methanol flushing

Figure 4-13. Optical Microscopy photographs for UT 586 coal tar contaminated soil, (A) original contaminated; (B) methanol flushed; and (C) contaminated (right) and methanol flushed (left)

Some Special Cases of Partitioning Behavior

Increasing alcohol partitioning for methanol washed coal tar soil A total of 18 PAHs with concentration as high as 18700 mg/kg was measured for the coal tar contaminated Waterloo soil. It is a very sticky, black, oily soil. The alcohol tracer test on this contaminated soil indicated considerable retardation for all three tracers (Figure 4-14A). The soil was then flushed with more than 200 pore volumes of 90/10 methanol/water solution, followed by extensive flushing with water (about 500 pore volumes) to remove the residual methanol. However, residual methanol still remained in measurable amounts (~ 1000 mg/L) in the aqueous phase. The alcohol partition tracer test conducted on the soil after extensive cosolvent flushing followed by water flushing had significant increase in retardation for all three tracers (Figure 4-14B). The increase in retardation of 2,2- DMP was as much as 6.5 times that measured prior to cosolvent flushing. This increase in partitioning for treated contaminated soil was not expected. Waterloo soils were further investigated based on the component concentrations in methylene chloride /methanol (50/50 v/v) extracts. Methanol flushed the Waterloo soil resulted in considerable changes in the composition compared with that of the unwashed Waterloo soil (Table 4-7). Methanol flushing selectively removed lower molecular weight PAHs and more polar components, but left part of the coal tar components with higher molecular weight; thus, the residual NAPL is expected to be more hydrophobic. Results in Table 4-7 show the ratio of anthracene to naphthlene increases from 0.22 for the contaminated soil to 0.87 and 1.59 , respectively for the soil flushed with methanol/pentanol-/water (70/10/20) and methanol/water (90/10). UNIFAC simulation results demonstrated that the partition coefficient (K_{NW}) for 2,2-DMP

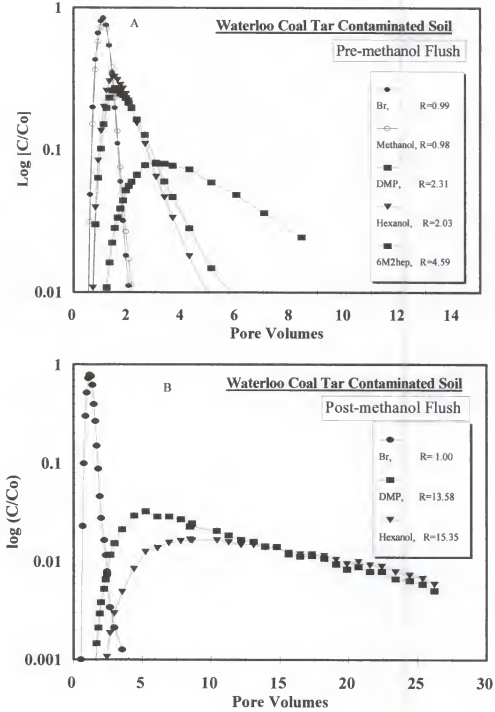

Figure 4-14. Alcohol partitioning tracer BTCs for coal tar contaminated Waterloo soil: (A) pre-methanol flushing; (B) post-methanol flushing

Table 4-8. Comparison relative PAH concentration of pre- and post alcohol flushing waterloo contaminated soil (PAHs concentrations are relative to naphthalene)

Compound	Concentration of PAHs* (mg/Kg of soil)			Relative concentration**		
	[a]pre-	[b]post-E	[c]post-EP	pre-	post-E	post-EP
naphthalene	2505.16	174.80	185.16	1.000	1.000	1.000
2-methylnaphthalene	1313.77	91.84	83.84	0.524	0.526	0.53
1-methylnaphthalene	827.32	40.32	25.18	0.330	0.230	0.136
acenapthylene	486.02	371.59	222.80	0.194	2.124	1.204
acenapthene	293.59	144.43	125.70	0.117	0.826	0.679
fluorene	740.06	115.60	99.67	0.294	0.661	0.538
phenanthrene	1388.52	280.26	165.43	0.554	1.602	0.894
anthracene	558.18	277.91	161.66	***0.223***	***1.588***	***0.873***
fluoranthene	1323.14	293.06	130.39	0.528	1.675	0.704
pyrene	1715.67	431.19	154.07	0.685	2.464	0.832
chrysene	770.30	293.55	131.69	0.307	1.678	0.711
1,2-benzantahracene	730.89	239.82	107.00	0.291	1.371	0.0.578
benz(b)fluoranthracene	534.88	196.37	115.52	0.213	1.123	0.624
benz(k)fluoranthracene	964.19	311.34	116.97	0.385	1.778	0.632
benzo(a)pyrene	465.45	282.60	128.18	0.186	1.615	0.692
Total PAHs	14617	3545	3022			

[a] Original contaminated Waterloo soil; [b] Waterloo soil flushed with methanol/water (90/10 v/v) for more than 200 column pore volumes; [c]Waterloo soil flushed with methanol/pentanol/water (70/10/20 v/v/v) for more than 200 pore volumes

*soil extracted with Methylene chloride /Methanol (50/50 V/V) at 1/8 soil to solvent ratio

** concentration of PAH divided by concentration of naphthalene

partitioning into PAHs actually decreased with an increase of the number of rings on PAHs (Figure 4-15). This is consistent with the findings for alcohol partitioning into alkanes. With increased NAPL hydrophobicity, the alcohol tracer partition coefficient decreased; therefore, selective removal of the low molecular weight PAHs, may not be the reason for increase in tracer retardation.

The coal tar is composed of several hundred or more organic compounds, including water-insoluble comounds, like high molecular weight hydrocarbons and asphaltenes, and relatively more soluble aromatics (e.g., xylenes) and PAH compounds, such as naphthalene , methylnaphthalene, etc. Luthy et al.(1993) found that a semirigid, skin-like film developed at a coal tar-water interface over a period of 3 days. Interfacial films have been reported for crude oil-water systems, in which film formation is generally attributed to the presence of large and complex molecules in the organic phase (Nelson et al., 1996). A review of the petroleum literature suggested that interfacial film formation may occur in the case of complex multi-component NAPLs composed of high molecular weight organic compounds. For the heavily contaminated Waterloo coal tar soil, the original coal tar-water interface had prolonged exposure to water. That interface may have developed the similar skim-like film as the one described above; limiting coal tar components transport from the inner film to water, also limiting other components, such as alcohol tracers, to access the component inside the coating. Methanol wash dissolved and removed the film; unmasking the relatively fresh coal tar inside the film.

Furthermore, methanol flushing washed away the tar and exposed inner coal tar particles which may increase the coal tar-water interfacial area. As a result, the alcohol

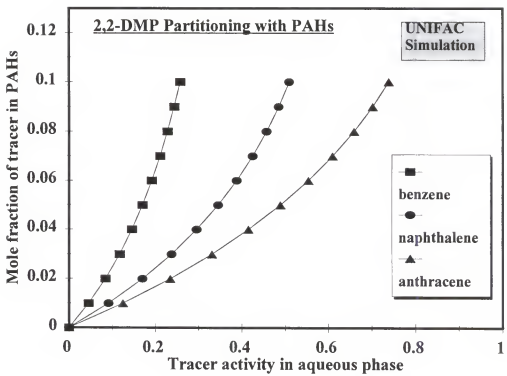

Figure 4-15. UNIFAC model simulation for 2,2-dimethyl-3-pentanol partitioning into PAH compounds

partition in this washed coal tar soil may have increased. The interfacial area measurements were attempted on both pre and post flushing soils with interfacial tracer method (IFT). The pre-flushing IFT indicates retardation of SDBS (sodium dodecylbenzene sulfonate). However, for post-methanol flushing soil, the SDBS was so strongly retarded and the concentration of the SDBS tracer pulse so spread out that SDBS concentration could be detected in the effluent when using the same analytical method as that used for the pre-flushing analysis. Thus, these date indicat that a significant amount of coal tar /water interfacial area was presented. Sufficient amount of methanol partitioning into the coal tar phase altered the coal tar composition, and with presence of methanol in the coal tar, the partition coefficient and partitioning behavior of the alcohol tracers may have significantly changed as indicated early in the chapter. Therefore, the exposure of inner surface, which was originally coated by thick coal tar oil, increased reactive interface; and the presencet of methanol in coal tar phase may have contributed to the increasing in the retardation of the alcohol tracers for post methanol flushing waterloo soil.

Change in sorption behavior. Benzene (as a reactive tracer) BTCs for UT690 coal tar soil initially indicated in retardation factor of 4.13 and 4.62 for C_o concentrations of 800 mg/L and 80 mg/L, respectively, for ^{14}C benzene in 30/70 methanol/water in column experiment (Figure 4-16). Significant nonlinear sorption behavior was not observed for benzene sorption in this concentration range. The BTCs for tritium and PFBA, both normally used as non-reactive tracers, showed no retardation on the original UT690 coal tar soil (Figure 4-17). However, when the soil was extensively flushed with 500 pore volumes of methanol, the effluent color changed from yellowish brown to clear, and no detectable amounts of naphthalene were found in methanol effluent.

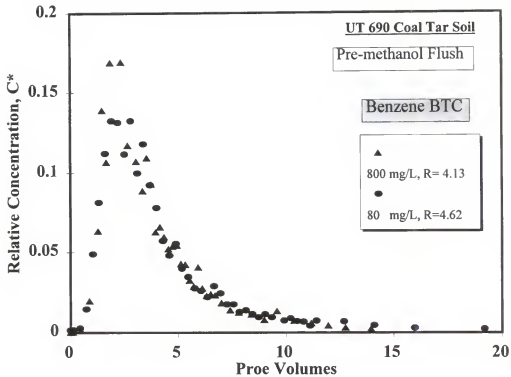

Figure 4-16. Benzene sorption BTC for original UT690 coal tar contaminated soil

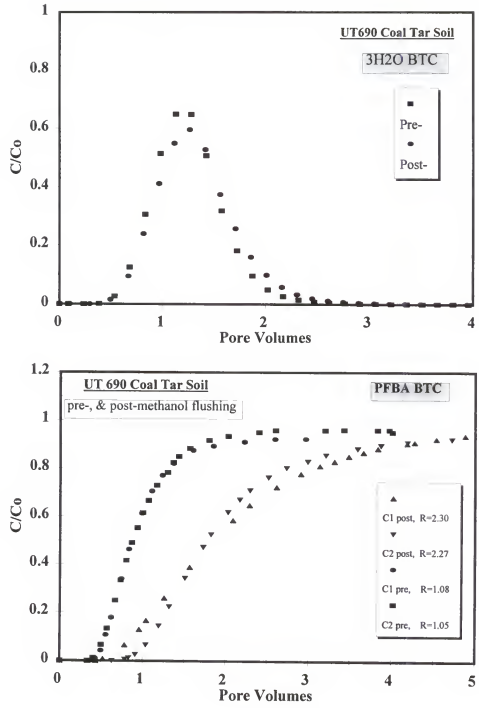

Figure 4-17. Tritium (A) and PFBA (B) retention in pre- and post-methanol washed UT690 coal tar contaminated soil columns (C1= column 1; C2= column 2).

Figure 4-18 shows particles of UT 690 coal tar soil. For post-flushing soil, 4 different type of particles can be easily separated by their colors: red, white crystal like, white bone like, and black particles. These black particles were separated by a small hand magnet as anonmagnetic and relatively magnetic fractions. X-ray diffraction and Scanning Electron Microscopy - Energy Dispersive X-ray (SEM-EDX) analysis identified these particles as follows: 1) the red color particles were mainly quartz, with Si and C as the dominant elements and high amount of Al and O and the presence of Ca and Fe (Figure 4-19), which possibly indicates Al-oxide and Ca-AL-oxide; 2) the white-bone like particles showed a quartz-like pattern from XRD analysis (Figure 4-20); 3) the magnetic fraction of the black particles was identified as an iron oxide ($Fe_3 O_4$) (Figure 4-21); 4) the black non-magnetic particles appeared the result of high temperature treatment and depressions, porous on the surface could be observed on the electron-microscopy (Figure 4-22). The XRD showed no specific pattern, indicating that it may not be crystal-like material, and SEM-EDXA identified carbon as the primary element, with the presence of some Al, Ca, Fe, O (Figure 4-23). These carbon-like particles were not only very porous on the surface, but inside the pores were heterogeneous (Figure 4-24). Methanol washed away the coal-tar coatings on the soil particles and unmasked such complex mineral and organic sorption surface. This resulted in a significant change in sorption behavior of the nonreactive and partitioning tracers. Thus, benzene retardation increased from 4.67 to 7.43 in 30/70 methanol/water solution with initial concentrations (C_o) 2900 to 44 mg/L. Benzene sorption in this methanol flushed coal tar soil appeared to depend on the initial benzene concentration in the solution; increasing retardation was found with decreasing C_o concentration (Figure 4-25). The

Figure 4-18. Optical Microscopy picture for sandy fraction of UT 690 coal tar contaminated soil, post-methanol flushing and after ultra-sonication

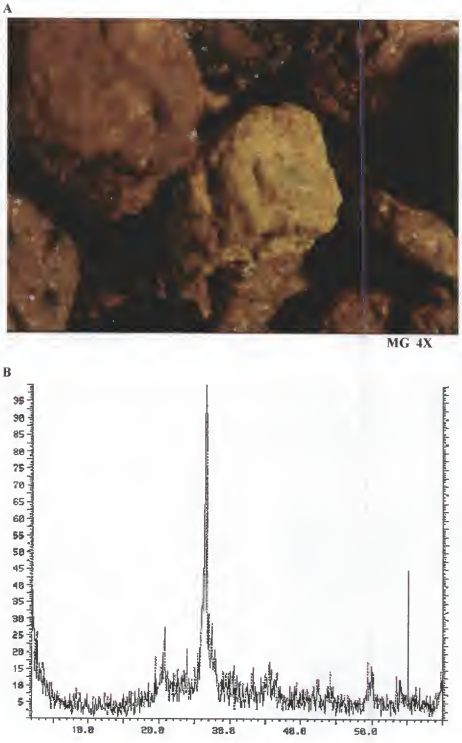

Figure 4-19. Optical Microscopy photograph (A) and X-ray Diffraction pattern (B) of sorted red pieces of UT 690 coal tar soil

A

B

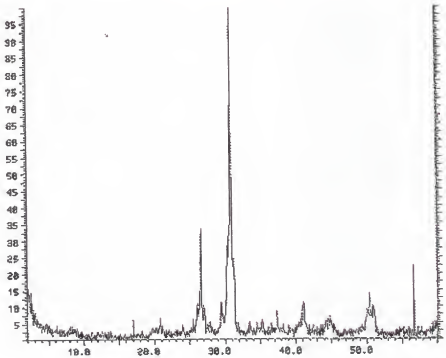

Figure 4-20. Optical Microscopy photograph (A) and X-ray Diffraction pattern (B) of sorted white pieces of UT 690 coal tar soil

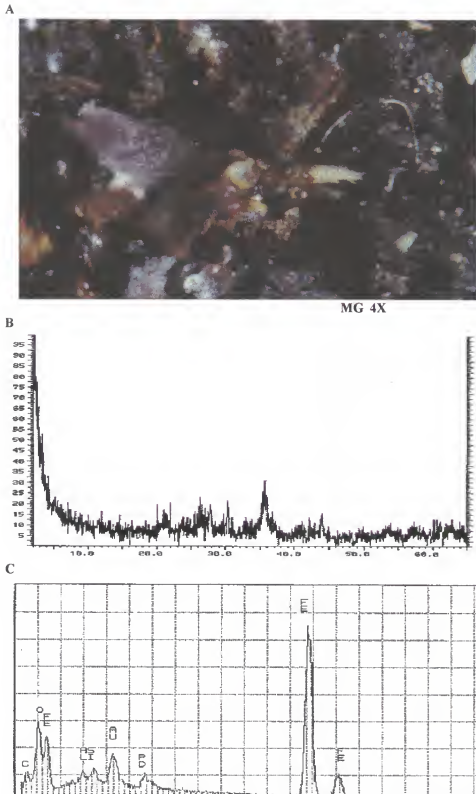

Figure 4-21. Optical Microscopy picture (A) and X-ray Diffraction pattern (B) and EDX (C) of sorted magnetic pieces of UT 690 tar soil

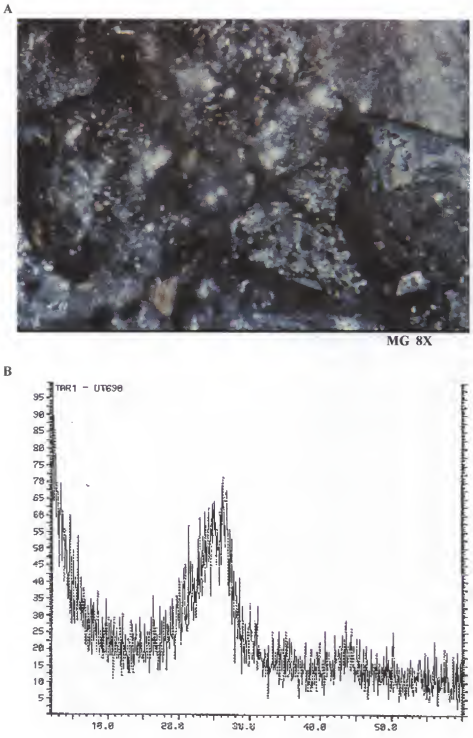

Figure 4-22. Optical Microscopy photograph (A) and X-ray Diffraction pattern (B) of sorted black pieces of UT 690 coal tar soil

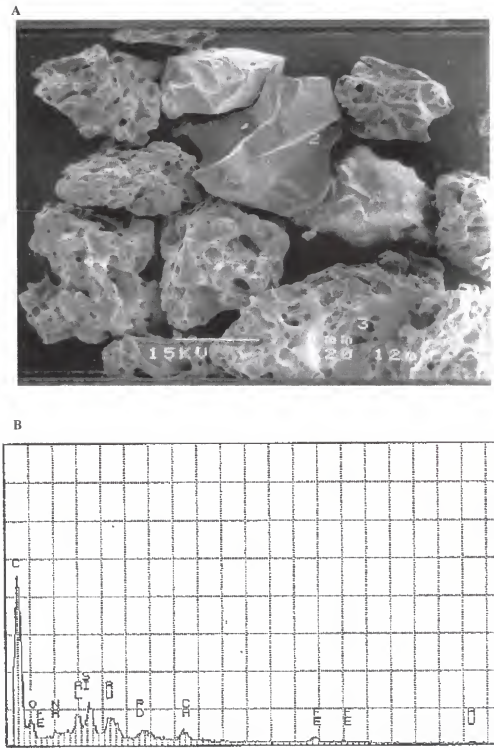

Figure 4-23. Scan Electron Microscopic photograph (A) and EDX (B) of sorted black pieces of UT 690 coal tar soil

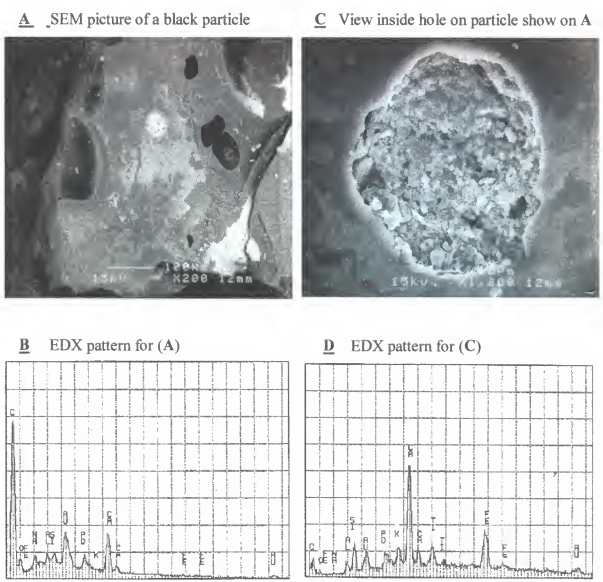

Figure 4-24. Scan Electron Microscopic photograph (A and C) and EDX (B and D) of zoomed in a piece from sorted black pieces of UT 690 coal tar soil

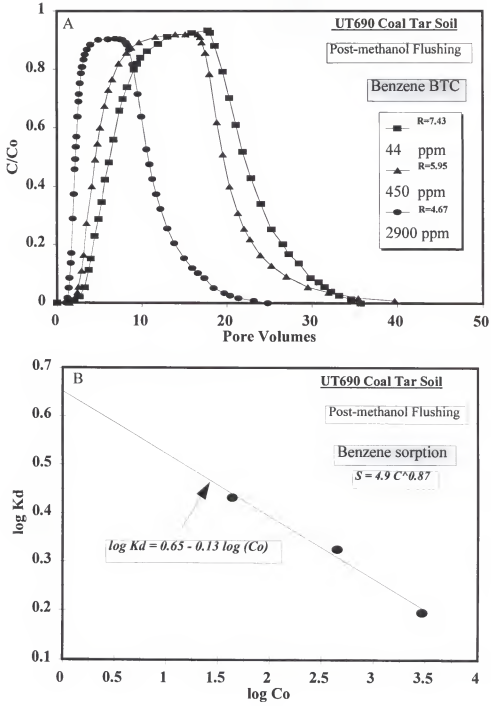

Figure 4-25. Benzene sorption behavior in column packed with post-methanol-flushing UT 690 coal tar contaminated soil (A) sorption BTC at different Co concentrations; (B) relation of sorption coefficients versus initial concentrations.

sorption coefficient K_d was estimated with equation:

$$R = 1 + \frac{K_d \rho}{\theta} \qquad (4\text{-}9)$$

where R is the retardation factor calculated from the normalized first moment of benzene BTC, θ is the volumetric water content of the column, and ρ is the bulk density of the soil in the column. Thus, K_d for different benzene C_o concentrations was calculated. The nonlinear sorption behavior of benzene can be described by Freundlich type non-linear sorption isotherm with a N value of 0.87 (Figure 4-25B).

In addition to the non-linear sorption behavior of benzene, PFBA was considerablly sorbed in this post methanol washed UT690 coal tar soil (Figure 4- 17B). PFBA naturally is an organic acid, existing in dissociated form (negative charge) at neutral pH and has a pK_a value of 2.7 (Bowman et al., 1992). There may be two possibilities for PFBA sorption in the soil: 1) PFBA exist in a non-ionic form due to change of pH in the soil; and 2)exposure of the soil mineral surface, which was originally coated by coal tar oil. Thesenewly exposed mineral surfaces may be associated with some charge species reacting with PFBA. There should be a significant pH change to allow the partitioning of neutral PFBA. This may not be the case in a dynamic column experiment with all the fluid in a 0.01 N $CaCl_2$ solution. Therefore, it is very likely that PFBA sorption on post-flushing soil is due to the exposure of the mineral surface. Similarly, selective removal and exposure of chemicals strongly associated with soil minerals (inaccessible beneath coal tar coatings), as well as these black carbon particles, may cause increasing benzene sorption and sorption non-linearity. Due to the limited quantity of

the contaminated soil, characterization and further analysis of the separated particles could not be conducted to verify the exact cause for the nonlinear and increased sorption of benzene and the sorption of PFBA on the methanol washed UT 690 coal tar contaminated soil.

Conclusions

The partitioning of alcohol tracers between NAPL and water may exhibit cooperative behavior in the presence of the other tracers (co-tracer). This cooperative effect may increase the partitioning coefficient (K_N) 1.5 to 5 times for the three partitioning tracers we investigated. The partitioning of tracers was found to be non-ideal at low concentrations, and non-linear in higher relative aqueous concentration range, and higher mole fraction in the NAPL. This non-ideal and non-linear partitioning behavior can be minimized through the use of structurally similar co-tracers in the batch equilibrium studies, and may be predicted using the UNIFAC simulations. Non-linear partitioning and co-tracer effect on tracer partition isotherm may over or under estimate on residual NAPL saturation through the partitioning tracer method if higher initial concentration or mixed tracers are used.

Cosolvent flushing of tar-contaminated soil may dissolve the "oil" film initially formed by long exposure to water of the coal tar-water interface, thus exposing new coal tar coating, or unmasking the soil mineral particles. These new sorbent surfaces may have a significant impact on the tracer partitioning behavior. An increase in the retardation of benzene and the sorption of an organic acid (PFBA) have been found for the methanol-washed coal-tar soil with complex soil background. About a seven-fold increase in partition

coefficient for alcohol tracers was found for extensively methanol-flushed contaminated Waterloo coal tar soil. These changes in tracer partitioning behavior, as a result of cosolvent flushing, have important implications for assessing soil cleanup based on partitioning tracer techniques.

CHAPTER 5
SUMMARY AND CONCLUSIONS

Prediction of solubility in aqueous solutions is necessary for defining the source loading function that controls the characteristics of the dissolved contaminant plume at disposal sites. Aqueous solubility and the effect of cosolvent on solubility of several hydrophobic organic contaminants were investigated and predicted using the log-linear relationship between solubility and volume fraction cosolvent. The measured and estimated solubility and partitioning data were then used to evaluate the behavior of the components in NAPL mixtures. The primary conclusions based on the obtained results are:

1. Aqueous solubility of hydrophobic solutes with large molecular weight and low solubility can be estimated by log-linear extrapolation of their solubility measured in cosolvent mixtures. Measued solubilities and partition coefficients for polycyclic aromatic hydrocarbons and other alkyl- or chloro-substituted aromatic compounds were in good agreement with values predicted using Raoult's law. Deviation from the Raoult's law prediction were found to be more significant for long-chain alkanes (>C10) in a complex NAPL mixture (collected from a contaminated aquifer at Hill AFB, Utah). The possible factors to this deviation include: (1) structural similarity

of components in a mixture; (2) solute-NAPL compatibility; and (3) effects of NAPL (lower molecular weight solutes) dissolved in water on solute (higher molecular weight, more hydrophobic) aqueous solubility.

2. Addition of higher molecular weight alcohol (pentanol) into ethanol/water mixture significantly increased the NAPL component solubility compared to the solubility enhancement measured in ethanol-water binary mixtures. NAPL solubility enhanced by pentanol addition to ethanol/water mixtures appears more for fraction ethanol at lower basis (0.4) than at higher ethanol basis (0.7).
3. In the log K_{oc} versus log K_{ow} plots, the partition coefficient for contaminants in soil can be bound at the upper end by their partition coefficients in pure coal tar (or other complex NAPL) and on the lower end by the partition coefficients for a "clean" uncontaminated soil.

Cosolvent mixtures such as ethanol/water and ethanol/pentanol/water increase the solubility and decease the partitioning and sorption of NAPL contaminants. These factors are favorable for enhanced remediation of NAPL sites. Results from this study (experimental data and model simulation) have shown that cosolvents are very effective additives to solubilize and remove organic constituents of complex NAPLs in contaminated soils or aquifers, as indicated by following:

1. The average NAPL removal effectiveness was 98.6% for 70/10/20 ethanol/pentanol/water flushing, and; 86.98% for ethanol/water flushing for NAPL contaminated soil columns. The removal of contaminants by cosolvent flushing was

much more effective with addition of (10 %) higher molecular weight alcohol (pentanol).

2. The contaminant dissolution from NAPLs by cosolvent flushing can be predicted by the numerical model based on the bicontinuum approach. The model simulated effluent profiles for several NAPL components agreed very well with the NAPL constituent concentration profiles measured in column effluent during cosolvent flushing.

3. Dissolution from NAPLs is a rate-limited process. For dissolution from multi-component NAPL and NAPL contaminated soil, diffusion through the organic phase could be the primary rate limiting step. The rate-limitations for dissolution from the multi-component Hill AFB NAPL contaminated soil may be described as similar process as those from aged tar-contaminated soils.

The partitioning tracer techniques provide an attractive tool to estimate the residual NAPL saturation, and has been used to evaluate the effectiveness of remediation of NAPL contaminated soils. However, several factors were found to affect the tracer partitioning behavior, thus, the estimation of the residual NAPL content. These factors were:

1. The partitioning of alcohol tracers between NAPL and water may exhibit cooperative behavior in the presence of the other tracers (co-tracer). This cooperative effect may increase the partitioning coefficient (K_N) 1.5 to 5 times for the three partitioning tracers investigated.

2. The partitioning of tracers was found to be non-ideal at low concentrations, and non-

linear in higher relative aqueous concentration range, and higher mole fraction in the NAPL. This non-ideal and non-linear partitioning behavior can be minimized through the use of structurally similar co-tracers in the batch equilibrium studies, and may be predicted using the UNIFAC simulations. Non-linear partitioning and co-tracer effect on tracer partition isotherm may have some impact on the estimation of residual NAPL saturation through the partitioning tracer method if higher initial concentration or mixed tracers are used.

3. Cosolvent flushing of contaminated soil may dissolve the NAPL film and expose new NAPL coatings, or unmask the soil durface that remain coated in contaminated soils. These mineral or organic interfaces may have a significant impact on the tracer partitioning behavior. An increase in the retardation of benzene and the sorption of an organic acid (PFBA) have been found for a methanol-washed coal-tar soil with complex soil background. Alcohol tracer partition coefficients were found to increase about 7 times increase after extensively flushing a tar-contaminated Waterloo soil. These changes in tracer partitioning behavior as a result of cosolvent flushing have important implications for assessing the extent of soil cleanup based on partitioning tracer techniques.

APPENDIX A

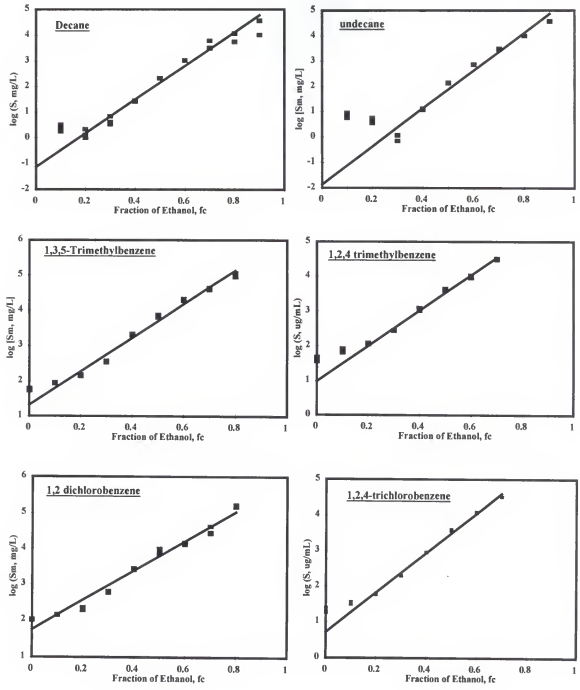

Figure A-1. Relationship between log solubility of organic chemicals versus volume fraction of ethanol in ethanol/ water solution (single NAPLs)

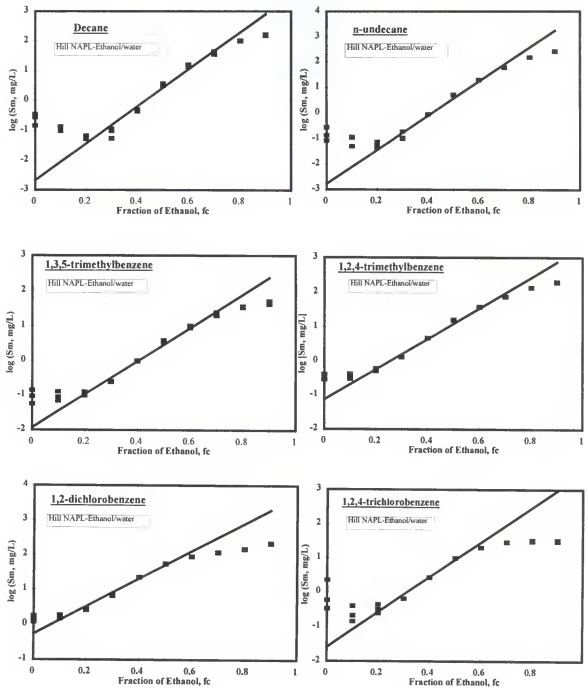

Figure A-2. Solubility of NAPL target components from Hill OU-1 cell NAPL in ethanol/water solution (a)

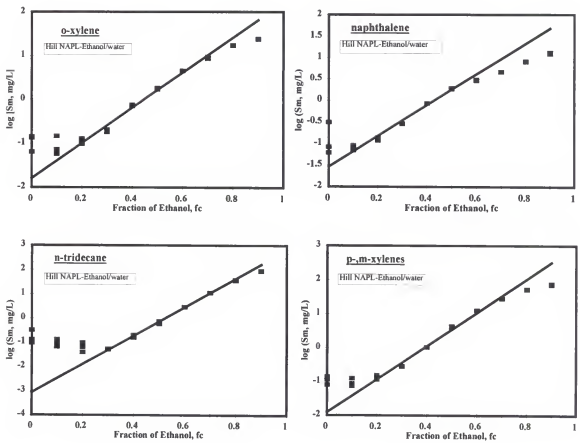

Figure A-2. Solubility of NAPL target components from Hill AFB NAPL in ethanol/water solution (b)

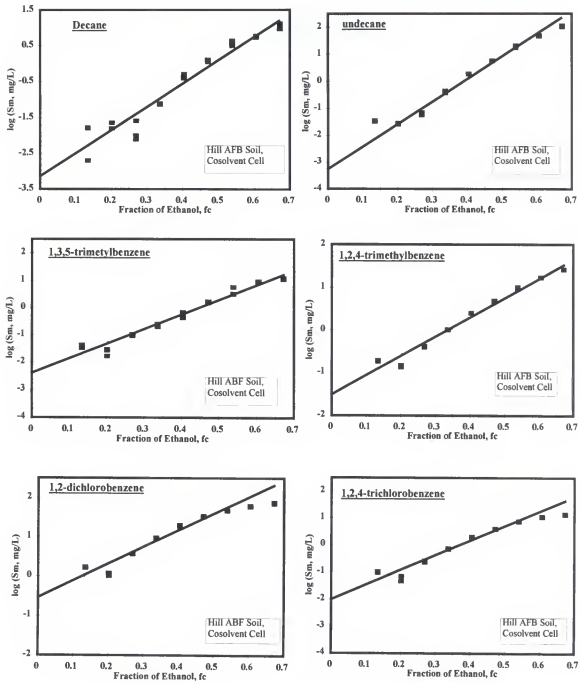

Figure A-3. Linear relationship between log solubility of target components versus volume fraction of ethanol for NAPL contaminated soil (Hill AFB) in ethanol/water solution(a)

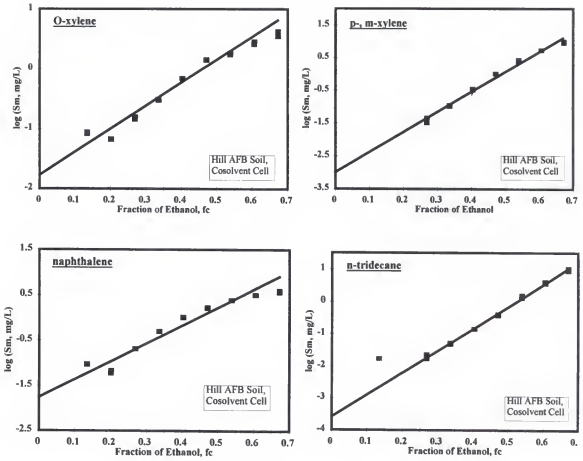

Figure A-3. Linear relationship between log solubility of target components versus volume fraction of ethanol for NAPL contaminated soil (Hill AFB) in ethanol/water solution (b)

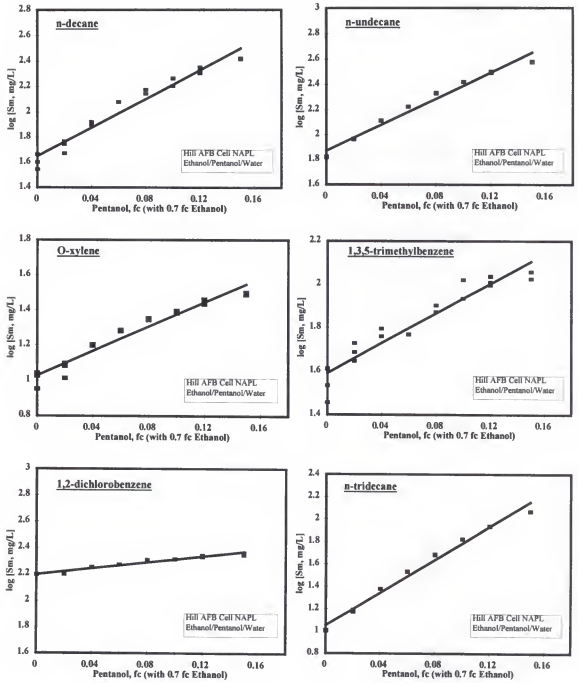

Figure A-4. log Sm of target components versus pentanol fraction with 0.7 fc ethanol in NAPL-ethanol/pentanol/water system

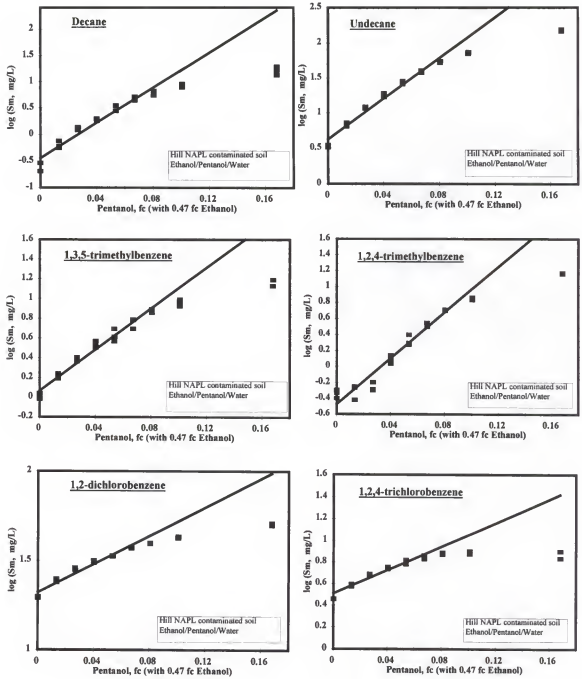

Figure A-5. Examples of log Sm versus fraction of pentanol with 0.47 fraction of ethanol in the NAPL contaminated soil and Ethanol/pentanol/water system

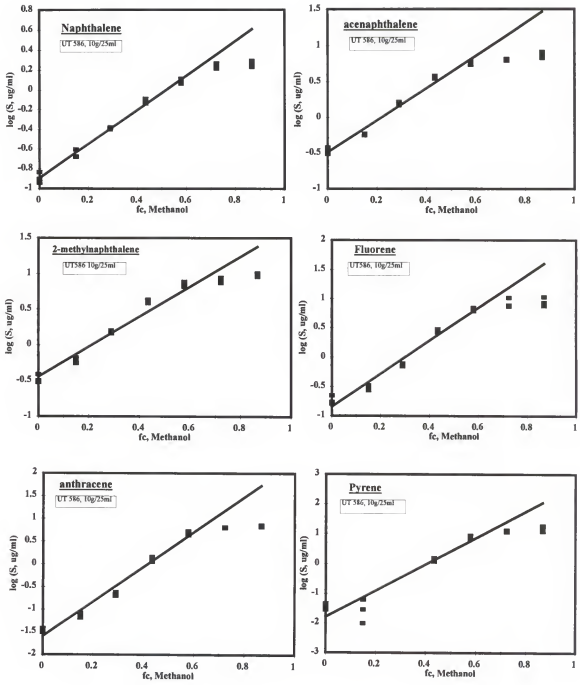

Figure 6-A. Linear relationship between log solubility of PAHs versus volume fraction of methanol for coal tar contaminated soils in methanol/water solution (a)

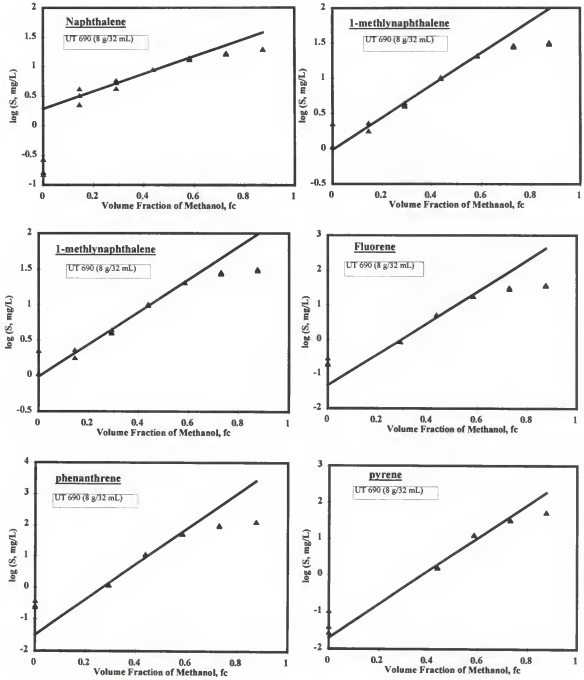

Figure A-6. Linear relationship between log solubility of PAHs versus volume fraction of methanol for coal tar contaminated soils in methanol/water solution (b)

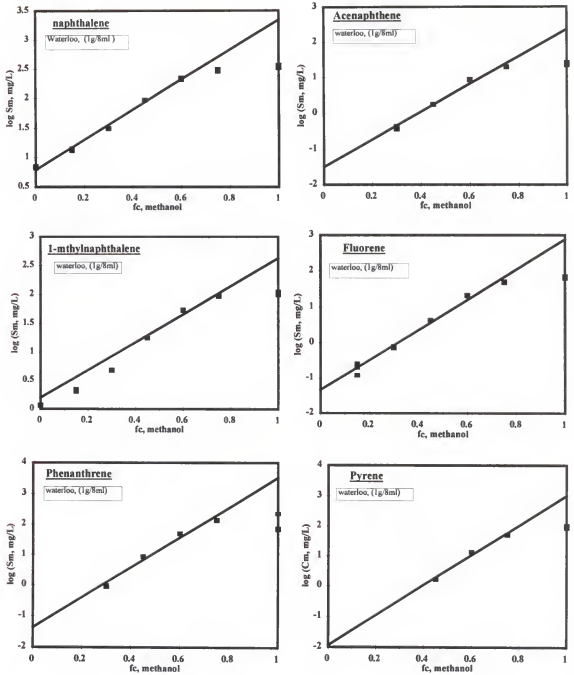

Figure A-6. Linear relationship between log solubility of PAHs versus volume fraction methanol for coal tar contaminated soils in methanol/water solution (c)

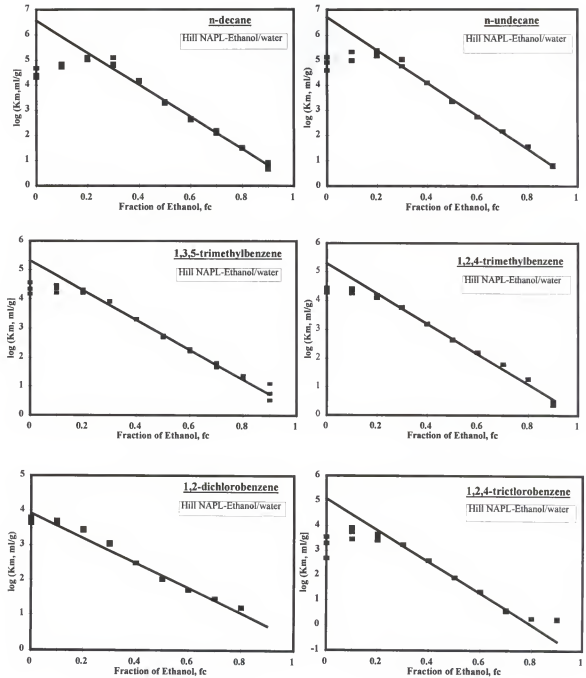

Figure A-7. Inverse linear relationship between log partition coefficient for target components versus volume fration of ethanol in NAPL-ethanol/water system (a)

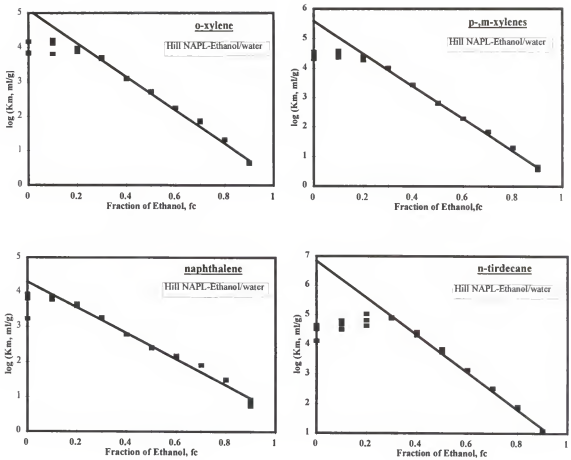

Figure A-7. Inverse linear relationship between log partition coefficient for target components versus volume fration of ethanol in NAPL-ethanol/water system (b)

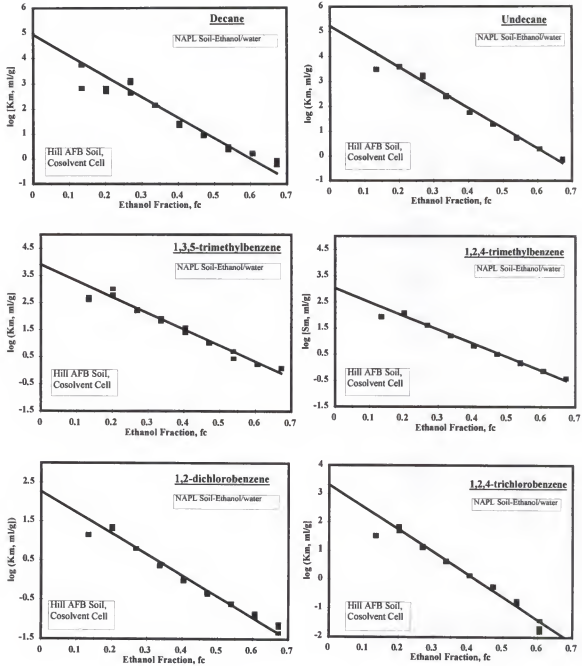

Figure A-8. Inverse linear relationship between log partition coefficient for target components versus volume fration of ethanol in NAPLcontaminated soil-ethnaol/water system (a)

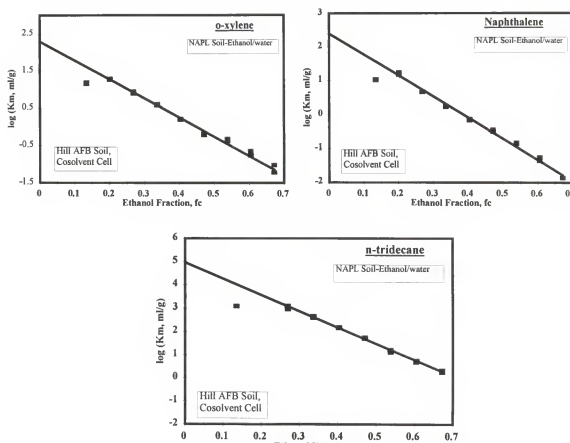

Figure A-8. Inverse linear relationship between log partition coefficient for target components versus volume fration of ethanol in NAPLcontaminated soil-ethnaol/water system (b)

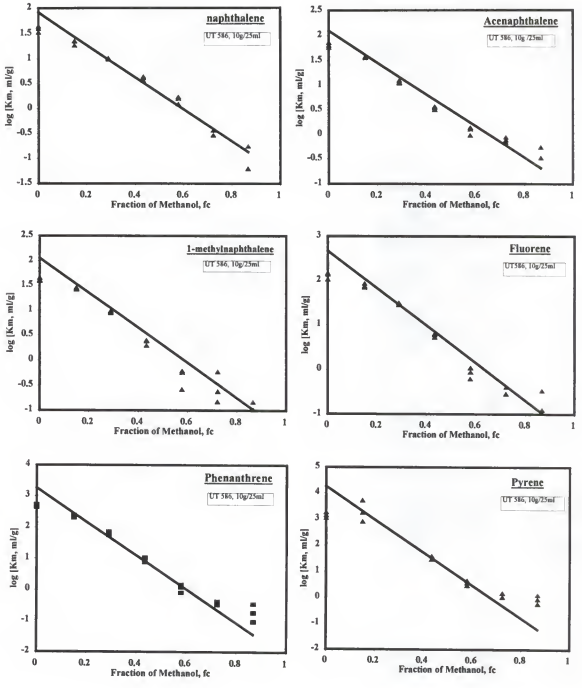

Figure 9-A. Inverse linear relationship between log partition coefficient , log Km of PAHs versus volumne fraction of methanol for coal tar contaminated soil in methanol/water solution (a)

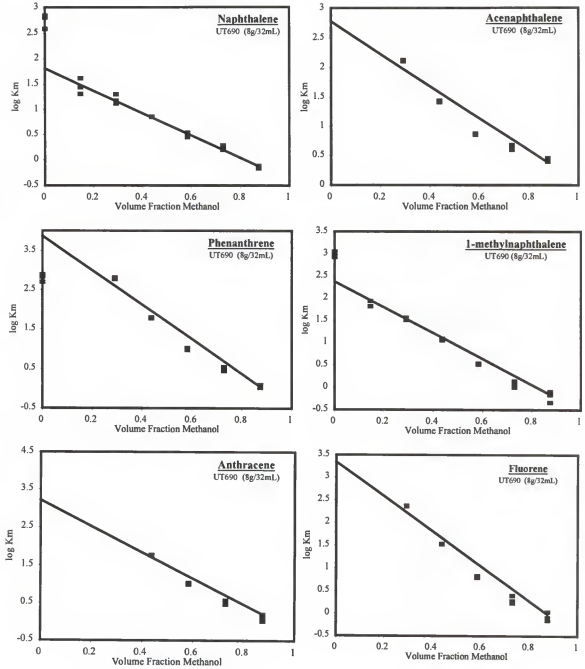

Figure A-9. Inverse linear relationship between log partition coefficient, log Km of PAHs versus volumne fraction of methanol for coal tar contaminated soil in methanol/water solution (b)

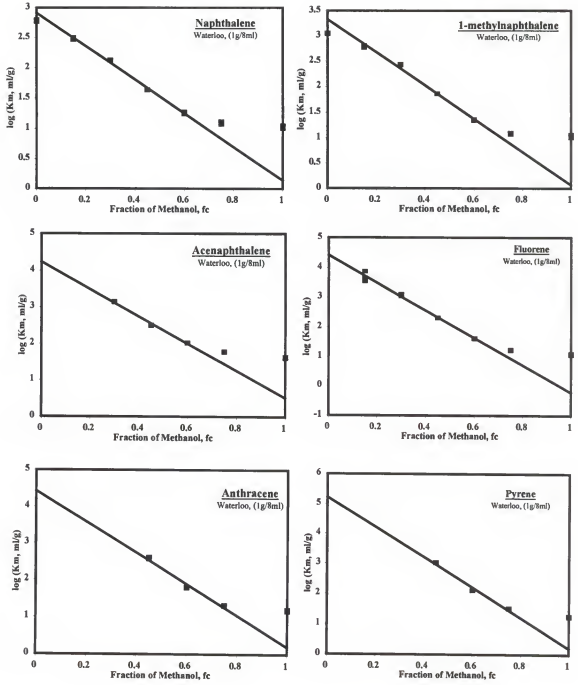

Figure A-9. Inverse linear relationship between log partition coefficient, log Km of PAHs versus volumne fraction of methanol for coal tar contaminated soil in methanol/water solution (c)

Table A-1. Hill AFB OU-1 NAPL Solubility in Ethanol/Water cosolvent Mixtures

Ethanol	log (Ce, mg/L)										
fc	P-xylene	O-xylene	1,3,5 TMB	Decane	1,2,4 TMB	1,2 DCB	Undecane	Dodecane	1,2,4TCB	Naphthale	Tirdecane
0	-0.943	-0.845	-1.252	-0.466	-0.539	0.248	-0.866	-0.750	0.349	-0.506	-0.883
0	-1.092	-1.187	-1.032	-0.564	-0.550	0.082	-0.554	-0.514	-0.483	-1.208	-0.491
0	-0.851	-0.866	-0.860	-0.842	-0.396	0.155	-1.076	-0.975	-0.233	-1.076	-1.009
0.1	-0.903	-0.833	-0.900	-0.873	-0.372	0.265	-0.955	-0.896	-0.397	-1.041	-1.036
0.1	-1.056	-1.137	-1.051	-1.013	-0.449	0.233	-1.292	-1.041	-0.678	-1.119	-1.167
0.1	-1.125	-1.237	-1.161	-0.914	-0.526	0.171	-0.928	-0.848	-0.842	-1.149	-0.866
0.2	-0.870	-0.963	-0.928	-1.208	-0.235	0.453	-1.284	-0.873	-0.495	-0.873	-1.174
0.2	-0.804	-0.893	-0.900	-1.284	-0.215	0.457	-1.347	-1.004	-0.352	-0.857	-1.398
0.2	-0.939	-1.009	-1.009	-1.174	-0.294	0.408	-1.119	-0.839	-0.609	-0.924	-0.991
0.3	-0.553	-0.740	-0.616	-1.013	0.115	0.810	-0.963	-0.590	-0.192	-0.542	-1.284
0.3	-0.542	-0.699	-0.618	-0.943	0.124	0.848	-0.714	-0.609	-0.188	-0.536	-1.252
0.3	-0.545	-0.684	-0.597	-1.268	0.115	0.811	-1.000	-0.627	-0.188	-0.539	-1.268
0.4	0.017	-0.152	-0.018	-0.304	0.675	1.351	-0.055	-0.026	0.430	-0.070	-0.678
0.4	0.024	-0.117	-0.001	-0.367	0.682	1.354	-0.047	-0.017	0.434	-0.067	-0.777
0.4	0.014	-0.139	-0.016	-0.338	0.677	1.349	-0.049	-0.029	0.425	-0.068	-0.790
0.5	0.608	0.227	0.532	0.564	1.195	1.731	0.697	0.636	0.999	0.263	-0.225
0.5	0.633	0.258	0.588	0.481	1.210	1.745	0.711	0.647	0.996	0.289	-0.121
0.5	0.639	0.255	0.547	0.568	1.208	1.741	0.691	0.635	1.000	0.271	-0.135
0.6	1.102	0.656	1.007	1.125	1.590	1.953	1.293	1.050	1.312	0.489	0.470
0.6	1.107	0.653	0.950	1.189	1.580	1.943	1.288	1.040	1.303	0.464	0.466
0.6	1.104	0.654	0.952	1.180	1.584	1.955	1.283	1.042	1.307	0.472	0.464
0.7	1.441	0.936	1.389	1.539	1.880	2.068	1.777	1.404	1.466	0.667	1.052
0.7	1.449	0.969	1.335	1.608	1.881	2.069	1.779	1.395	1.460	0.662	1.057
0.7	1.454	0.974	1.298	1.646	1.883	2.074	1.779	1.401	1.473	0.666	1.058
0.8	1.715	1.241	1.552	1.999	2.143	2.165	2.177	1.792	1.494	0.903	1.555
0.8	1.724	1.234	1.532	2.016	2.144	2.169	2.179	1.795	1.521	0.914	1.579
0.8	1.715	1.242	1.562	1.987	2.140	2.172	2.174	1.793	1.526	0.906	1.574
0.9	1.852	1.380	1.714	2.177	2.292	2.333	2.409	2.076	1.490	1.105	1.947
0.9	1.861	1.385	1.626	2.223	2.292	2.330	2.408	2.076	1.527	1.087	1.945
0.9	1.874	1.389	1.699	2.210	2.308	2.346	2.422	2.087	1.503	1.124	1.953
Methylene Chloride Extraction (1:18 NAPL : Solution)											
log Cmax	1.907	1.429	1.729	2.260	2.345	2.354	2.485	2.162	1.486	1.191	2.060
	1.920	1.424	1.657	2.300	2.348	2.357	2.489	2.167	1.533	1.187	2.061
	1.926	1.413	1.596	2.318	2.347	2.356	2.488	2.169	1.534	1.154	2.073
Avg.	1.918	1.422	1.661	2.293	2.346	2.356	2.487	2.166	1.518	1.177	2.065

Table A-2. Hill AFB OU-1 NAPL Partitioning in Ethanol/Water cosolvent Mixtures

Ethanol	log (Kp, ml/g)										
fc	P-xylene	O-xylene	1,3,5 TMB	Decane	1,2,4 TMB	1,2 DCB	Undecane	Dodecane	1,2,4TCB	Naphthale	Tirdecane
0	4.408	3.833	4.566	4.297	4.423	3.636	4.907	4.469	2.692	3.234	4.513
0	4.557	4.177	4.346	4.395	4.434	3.803	4.595	4.234	3.551	3.943	4.121
0	4.316	3.855	4.174	4.673	4.280	3.730	5.116	4.695	3.297	3.810	4.639
0.1	4.368	3.821	4.214	4.705	4.256	3.619	4.995	4.616	3.464	3.776	4.667
0.1	4.521	4.127	4.365	4.845	4.333	3.651	5.333	4.761	3.748	3.854	4.798
0.1	4.590	4.227	4.476	4.745	4.410	3.714	4.969	4.568	3.912	3.884	4.497
0.2	4.335	3.952	4.242	5.039	4.119	3.429	5.325	4.593	3.563	3.606	4.805
0.2	4.269	3.882	4.214	5.116	4.098	3.425	5.387	4.725	3.418	3.590	5.029
0.2	4.405	3.998	4.323	5.006	4.178	3.475	5.160	4.559	3.678	3.658	4.622
0.3	4.017	3.728	3.929	4.845	3.767	3.065	5.003	4.310	3.256	3.271	4.915
0.3	4.006	3.687	3.931	4.775	3.758	3.025	4.755	4.329	3.252	3.265	4.883
0.3	4.009	3.672	3.910	5.099	3.767	3.063	5.041	4.347	3.251	3.268	4.898
0.4	3.443	3.131	3.326	4.134	3.199	2.487	4.094	3.744	2.604	2.781	4.308
0.4	3.436	3.095	3.308	4.197	3.193	2.485	4.086	3.734	2.601	2.779	4.408
0.4	3.446	3.118	3.323	4.169	3.198	2.489	4.088	3.746	2.610	2.779	4.421
0.5	2.835	2.736	2.756	3.259	2.656	2.030	3.336	3.071	1.915	2.418	3.854
0.5	2.809	2.703	2.696	3.344	2.641	2.012	3.322	3.060	1.921	2.389	3.749
0.5	2.803	2.706	2.740	3.255	2.643	2.017	3.342	3.073	1.913	2.409	3.764
0.6	2.292	2.258	2.225	2.675	2.210	1.706	2.719	2.636	1.350	2.152	3.150
0.6	2.283	2.258	2.290	2.605	2.218	1.712	2.723	2.645	1.347	2.179	3.154
0.6	2.289	2.260	2.290	2.616	2.216	1.701	2.729	2.645	1.360	2.172	3.156
0.7	1.839	1.885	1.676	2.203	1.808	1.465	2.166	2.232	0.550	1.906	2.535
0.7	1.826	1.834	1.768	2.116	1.805	1.460	2.163	2.243	0.607	1.913	2.529
0.7	1.827	1.834	1.833	2.071	1.810	1.467	2.167	2.238	0.604	1.914	2.530
0.8	1.306	1.305	1.341	1.506	1.281	1.225	1.568	1.688	0.266	1.508	1.920
0.8	1.283	1.325	1.392	1.469	1.279	1.210	1.565	1.683	NM	1.484	1.884
0.8	1.307	1.302	1.311	1.529	1.289	1.199	1.574	1.685	NM	1.500	1.892
0.9	0.665	0.644	0.532	0.941	0.426	NM	0.805	0.880	0.257	0.805	1.075
0.9	0.625	0.631	1.107	0.655	0.492	NM	0.832	0.905	NM	0.936	1.096
0.9	0.562	0.659	0.768	0.810	0.365	NM	0.783	0.879	0.213	0.744	1.085

APPENDIX B

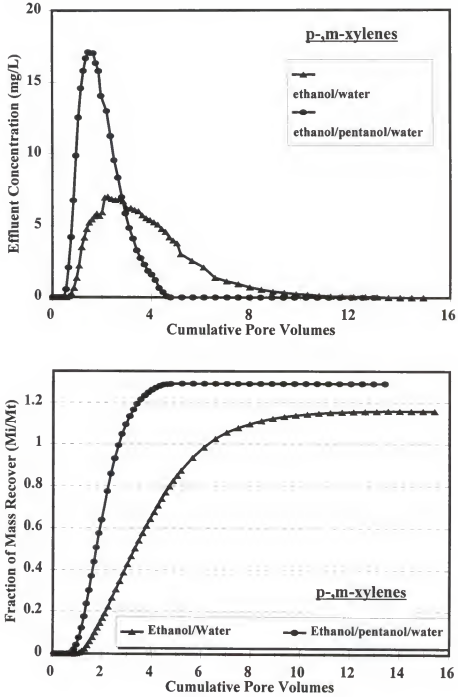

Figure B-1. Comparison of ethanol/water and ethanol/pentanol/water flushing on effleunt concentration and fraction of mass recover for p&m-xylenes on NAPL contaminated soil from Hill AFB, UT.

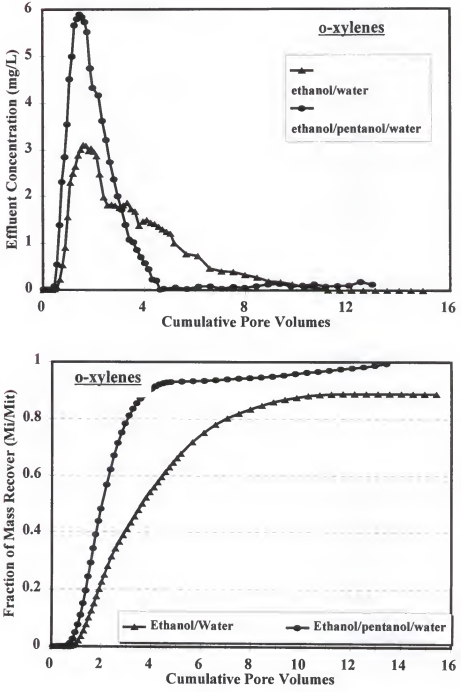

Figure B-2. Comparison of ethanol/water and ethanol/pentanol/water flushing on effleunt concentration and fraction of mass recovery for o-xylene on NAPL contaminated soil from Hill AFB, UT.

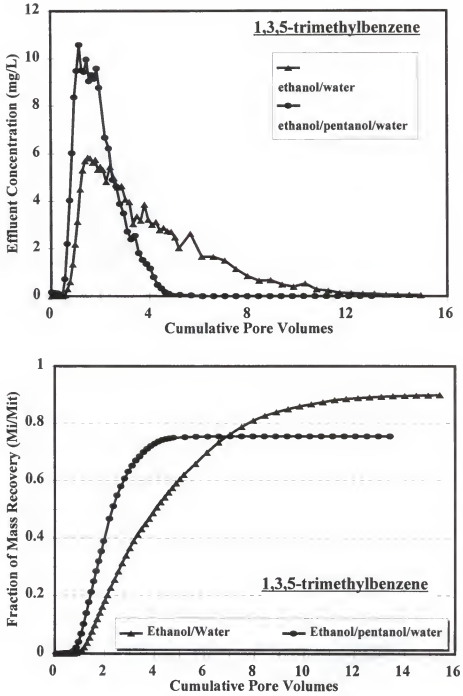

Figure B-3. Comparison of ethanol/water and ethanol/pentanol/water flushing on effleunt concentration and fraction of mass recovery for 1,3,5-trimethylbenzene on NAPL contaminated soil from Hill AFB, UT.

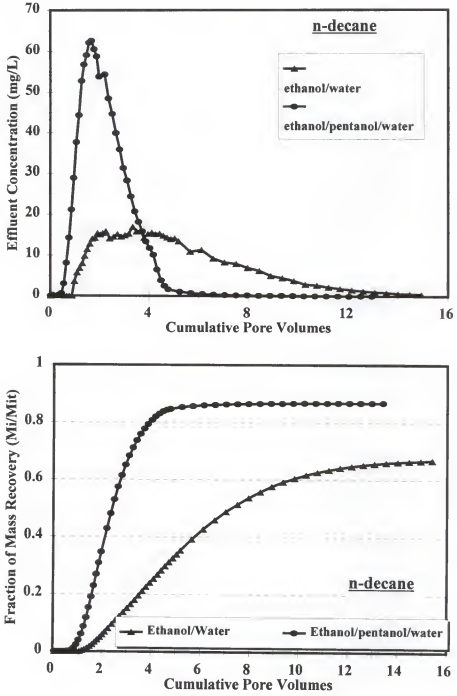

Figure B-4. Comparison of ethanol/water and ethanol/pentanol/water flushing on effleunt concentration and fraction of mass recovery for Decane on NAPL contaminated soil from Hill AFB, UT.

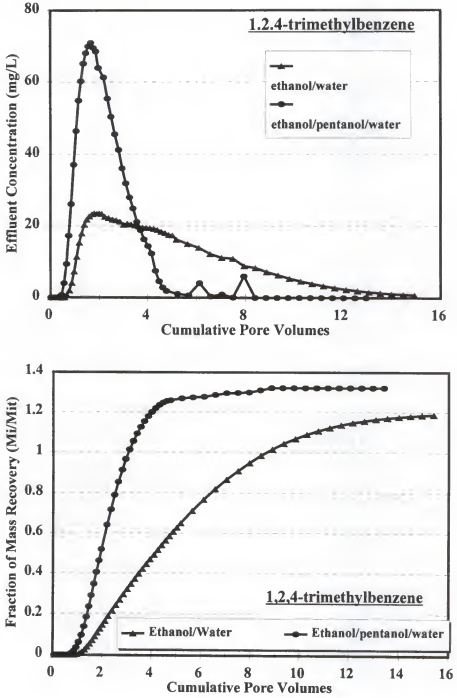

Figure B-5. Comparison of ethanol/water and ethanol/pentanol/water flushing on effleunt concentration and fraction of mass recovery for 1,2,4-trimethylbenzene on NAPL contaminated soil from Hill AFB, UT.

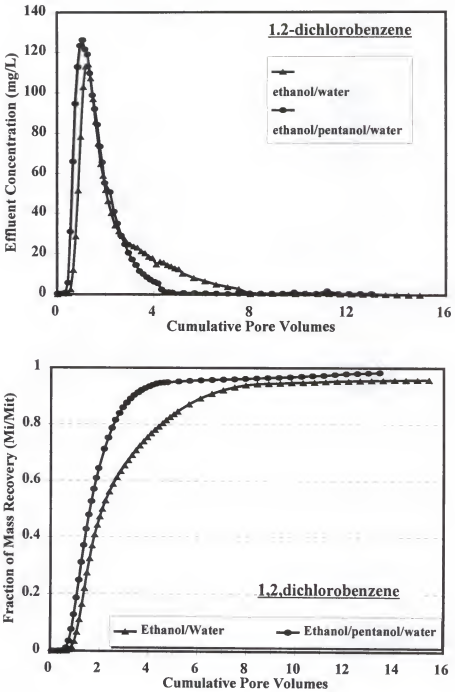

Figure B-6. Comparison of ethanol/water and ethanol/pentanol/water flushing on effleunt concentration and fraction of mass recovery for 1,2-chlorobenzene on NAPL contaminated soil from Hill AFB, UT.

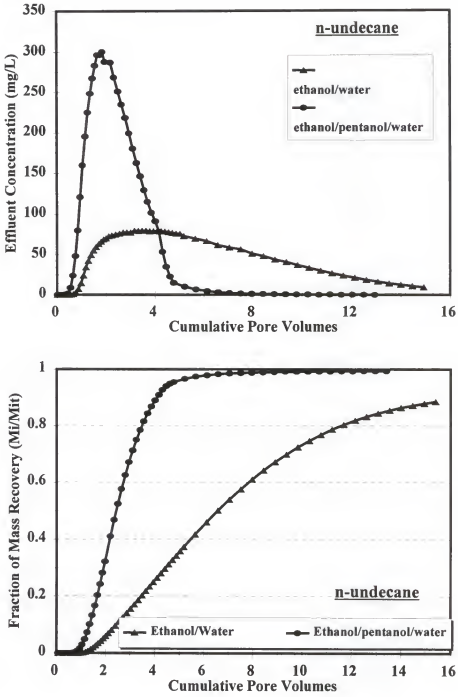

Figure B-7. Comparison of ethanol/water and ethanol/pentanol/water flushing on effleunt concentration and fraction of mass recovery for n-undecane on NAPL contaminated soil from Hill AFB, UT.

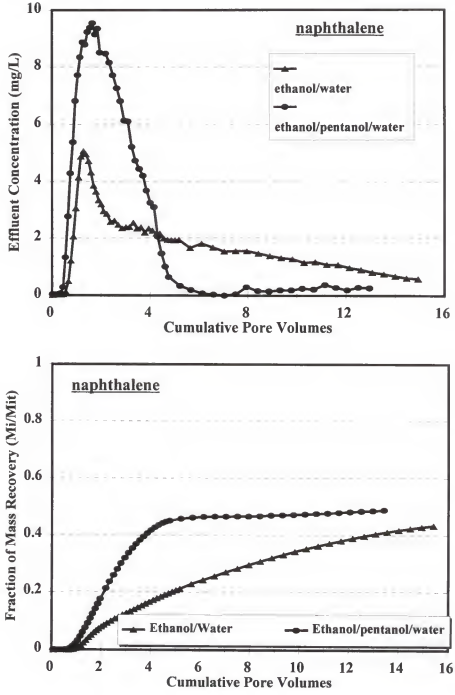

Figure B-8. Comparison of ethanol/water and ethanol/pentanol/water flushing on effleunt concentration and fraction of mass recovery for naphthalene on NAPL contaminated soil from Hill AFB, UT.

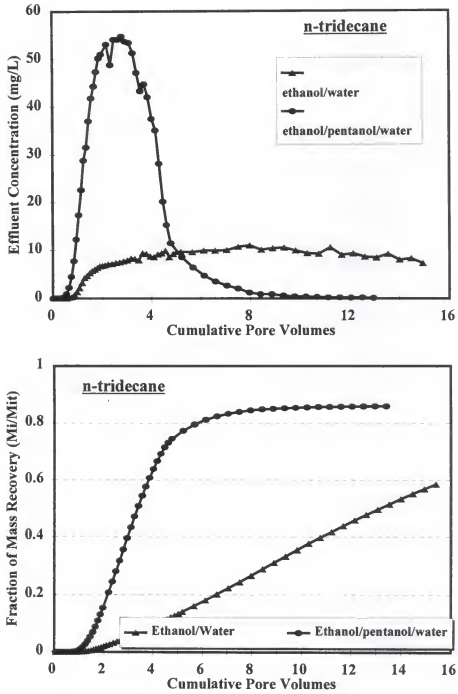

Figure B-9. Comparison of ethanol/water and ethanol/pentanol/water flushing on effleunt concentration and fraction of mass recovery for n-tridecane on NAPL contaminated soil from Hill AFB, UT.

REFERENCE

Annable, M.D., P.S.C. Rao, R.K. Sillan, D. Dai, A.L Wood and C.G. Enfield. 1997a. Evaluation of In-situ Cosolvent Flushing using partitioning tracers. Submitted to Water Resources Research.

Annable, M.D., J.W. Jawitz, P.S.C. Rao, D.P. Dai, H.K.Kim and A.L. Wood. 1997b. Field evaluation of interfacial and partitioning tracers for characterization of effective NAPL-water contract area. Submitted to Ground Water,

Annable, M.D., P.S.C. Rao, K. Hatfield, W.D. Graham, A.L Wood and C.G. Enfield. 1995. Use of partitioning tracers for measuring residual NAPL: Preliminary Results from a field-scale test. Proceedings from the 2nd Tracer workshop, Austin, TX.

Almeida Macedo, E., U. Weidlich, J. Gmehling, and P.A. Rasmussen. 1983. Vapor-liquid equilibria by UNIFAC group contribution. Revision and Extension. 3, Ind. Eng. Chem. Process Des. Dev., 22:676-678.

Augustijn, D.C.M. 1993. Chemodynamics of complex waste mixtures: Applications to contamination and remediation of soils and aquifer media. Ph.D Dissertation. University of Florida.

Augustijn, D.C.M., D. Dai, P.S.C Rao and A.L. Wood. 1994. Solvent flushing dynamics in contaminated soils. In Transport and Reactive Processes in Aquifers. A.A Balkema/Rotterdam.Brookfield. pp. 557-562.

Baker, E.G. 1967. Fundamental Aspects of Petroleum Geochemistry, B. Nagy and U. Columbo, Eds. (Elsevier, Amsterdam), p299

Banerjee, S. 1984. Solubility of organic mixtures in water. Environ. Sci. Technol., 18(8):587-591.

Banerjee, S., S.H. Yalkowsky and S.V. Valvani. 1980. Water solubility and octanol/water partition coefficient of organics. Limitations of the solubility-partition coefficient correlation. American Chemical Society, 14, 10:1227-1229.

Bowman, R.S., and J.F. Gibbens. 1992. Difluorobenzoates as nonreactive tracers in soil and groundwater. Water Resources, 30(1):8-14.

Boyd, S.A. and S. Sun. 1990. Residual petroleum and polychlorobiphenyl oils as sorptive phases for organic contaminants in soils. Environ. Sci. Technol., 24(1):142-144.

Briggs, G.G. 1981. Theoretical and experimental relationships between soil adsorption, octoanol/water partition coefficients, water solubilities, bioconcentration factors, and the parachor. J. Agric. Food Chem., 29: 1050.

Brusseau, M.L., P.S.C. Rao, R.E., Jessup, and J.M. Davidson. 1989. Flow interruption: A method for investigating sorption nonequilibrium. J.Contam. Hydrol. 4:233-240

Brusseau, M.L., and P.S.C. Rao. 1989. Sorption nonideality during organic contaminated transport in porous media. CRC Critical Reviews in Environ. Control 19:33-99

Brusseau, M.L., A.L. Wood, and P.S.C. Rao. 1991. Influence of organic cosolvents on the sorption kinetics of hydrophobic organic chemicals. Environ. Sci. Technol. 25:903-910.

Brusseau, M.L., 1993. Complex mixtures and groundwater quality. Environmental Research Brief. EPA/600/S-93/004, pp15

Campbell, R.R., R.G. Luthy, and M.J.T. Carrondo. 1983. Measurement and prediction of distribution coefficients for wastewater aromatic solutes. Environ. Sci. Technol., 17, 582-590.

Chen, F. 1992. Manual for program gamma: Calculation of activity coefficients by means of UNIFAC. National Environmental Research Institute.

Chiou C.T and D .W.Schmedding. 1982. Partition of organic compounds in octanol-water systems. Environ. Sci. Technol. 16, 4-10.

Chiou, C.T. and J.H. Block. 1986. Parameters affecting the partition-coefficient of organic compounds in solvent-water and lipid-water systems. IN: Partition Coefficient. Determination and Estimation. W.J. Dunn III, J.H. Block, and R.S. Pearlman (Eds.) Pergamon Press, Inc., New York, pp.37-60.

Choi, J. and S. Aomine. 1974. Adsorption of pentachlorophenol by soils. Soil Sci. Plant Nutr., 20(2):135-144.

Cline, P.V., J.J. Delfino, and P.S.C. Rao. 1991. Partitioning of aromatic constituents into water from gasoline and other complex solvent mixtures. Environ. Sci. Technol. 25: 914-920.

Coyle, G.T.,T.C.Harmon, and I.H. Suffet. 1997. Aqueous solubility depression for hydrophobic organic chemicals in the presence of partially miscible organic solvents. Environ. Sci. Technol., 31(2):384-389.

EPRI. 1992. Estimating Release of Polycyclic Aromatic Hydrocarbons From Coal Tar at Manufactured-Gas Plant Sites. EPRI-RP2879-07.

EPRI. 1993. Chemical and physical characteristics of coal tar from selected manufactured gas plant (MGP) sites. EPRI-RP2879-01, 12 EPRI, Washington, DC.

Falta, R.W., S.E. Brame, C.M. Lee, J.T. Coates, C. Wright, S. Price, P. Haskell, and E. Roeder. 1996. A Field est of NAPL removal by high molecular weight alcohol injection. IN: Non-Aqueous Phase Liquids (NAPLs) in Subsurface Environment: Assessment and Remediation. ASCE, New York. pp:254-269.

Fu, J., and R.G. Luthy. 1986a. Aromatic compound solubility in solvent/water mixtures. J. Environ. Eng. 112:328-345.

Fu, J., and R.G. Luthy. 1986b. Effect of organic solvent on sorption of aromatic solutes on to soils. J. Environ. Eng. 112:3346-366.

Garbarini, D.R. and L.W. Lion. 1986. Influence of the nature of soil organics on the sorption of toluene and trichloroethylene. Environ. Sci. Technol., 20(12):1263-1269.

Gerstl, Z.. 1990. Estimation of organic chemical sorption by soils. J. Contam. Hydrol. 6:357-375

Gmehling, J., P.Rasmussen, and A. Fredenslund. 1982. Vapor-liquid equilibria by UNIFAC group contribution. Revision and Extension. 2. Ind. Eng. Chem. Process Des. Dev., 21:118-127.

Gschwend, P.M. and S.C. Wu. 1985. On the constancy of sediment-water partition coefficients of hydrophobic organic pollutants. Environ. Sci. Technol., 19(1):90-96.

Guerin, M.R. 1978. Energy sources of polycyclic aromatic hydrocarbons. IN: Polycyclic Hydrocarbons and Cancer. H.V. Gelboin and P.O.P Tso (Eds.). Academic Press, New York, Vol I., pp 3-42.

Haag, W.R. and T. Mill. 1988. Effect of a subsurface sediment on hydrolysis of haloalkanes and epoxides. Environ. Sci. Technol., 22(6):658-663.

Hagwall, M. 1992. Partitioning of aromatic constitutes into water from diesel fuel. Master's Thesis, The Royal Institute of Technology, Stockholm, Sweden.

Hansch, C. 1969. A quantitative approach to biochemical structure-activity relationships. Acc. Chem. Res., 2:232-235.

Hansch, C., and W.J. Dunn. 1972. Linear relationships between lipophilic character and biological activity of drugs. J. Pharm. Sci., 61:1-6.

Hansch, C., and A. Leo. 1979. Solubility Constants for Correlation Analysis in Chemistry and Biology, Wiley, New York.

Hansen, H.K., P. Rasmussen, and A. Fredenslund. 1991. Decomposition of dichlorodifluoromethane on BPO_4. Ind. Eng. Chem. Res., 30: 2355.

Hassett, J.J., W.L. Banwart, S.G. Wood, and J.C. Means. 1981. Sorption of α-naphthol: Implications concerning the limits of hydrophobic sorption. Soil Sci. Soc. Amer. J., 45: 38-42

Heyse. E., D.Dai, P.S.C Rao and J.J Delfino. 1997. Development of a continuously stirred flow cell for investigating sorption mass transfer. J. of Contaminant hydrology, 25:337-355.

Hunt J.R., N. Sitar, and K.S. Udell. 1988. Nonaqueous phase transport and cleanup, 1. Analysis of mechanisms. Water resour. Res. 24:1247-1258.

Imhoff., P.T., S.N. Gleyzer, J.F. McBride, L.A. Vancho, I.Okuda, and C.T. Miller. 1995. Cosolvent-enhanced remediation of residual dense nonaqueous phase liquids: Experimental investigation. Environ. Sci. Technol., 29(8): 1966-1976.

Jawitz, J. W., M.D. Annable, P.S.C Rao and R.D. Rhue. 1997. Field Implementation of a Winsor Type I surfactant/alcohol mixutre for in-situ solubilization of a complex LNAPL as a single-phase microemulsion. Submitted to: Environ. Sci. Technol.,

Jawitz, J.W. 1997. Personal Research Notes.

Jin, M., M. Delshad, V. Dwarakanath, D.C. McKinney, G.A. Pope, K. Sepehrnoori, C. Tilburg, and R.E. Jackon. 1995. Partitioning tracer test for detection, estimation, and remediation performance assessment of subsurface nonaqueous phase liquids. Water Resources Research, 31 (5): 1201-1211.

Karickhoff, S.W., 1981. Semi-empirical estimation of sorption of hydrophobic pollutants on natural sediments and soils. Chemospheere, 10:833-846.

Karickhoff, S.W., D.S. Brown, and T.A., Scott. 1979. Sorption of hydrophobic pollutants on natural sediments. Water Res. 13:241-248.

Kenega, E.E. and C.A.I. Goring. 1980. Relationship between water solubility, soil sporption, octanol-water partitioning, and concentration of chemicals in biota. IN: Aquatic toxicology. J.G. Eaton, P.R. Parrish, and A.C. Hendricks (Eds.) Special Technical Publication 707; American Society for testing of Materials: Philadelphia, PA. Pp. 78-115

Lane, W.F., and R.C. Loehr. 1992. Estimation the equilibrium aqueous concentrations of polynuclear aromatic hydrocarbons in complex mixtures. Environ. Sci. Technol. 26:983-990.

Lee, L.S., C.A. Bellin, R. Pinal, and P.S.C Rao. 1993. Cosolvent effects on sorption of organic acids by soils from mixed-solvents. Envir. Sci. Tech., 27: 165-171.

Lee, L.S., M, Hagwell, J.J. Delfino, and Rao, P.S.C. 1992a. Partitioning of polycyclic aromatic hydrocarbons Diesel Fuel into water. Environ. Sci. Technol., 26(11):2104-2110.

Lee, L.S., Rao, P.S.C., and I. Okuda. 1992b. Equilibrium partitioning of polycyclic aromatic hydrocarbons from coal tar into water. Environ. Sci. Technol., 26(11):2110-2115.

Leinonen, P.J., D. Mackay and C.R.Phillips , 1971. A Correlation for the solubility of Hydrocarbons in Water. Can. J. Chem. Eng. , 49: 288-290.

Leinonen, P.J., D. Mackay 1973. The multicomponent solubility of hydrocarbons in water Can. J. Chem. Eng. , 51, 230-233.

Leo, A. and C. Hansch. 1971. Linear free-energy relationships between partitioning solvent systems. J. Org. Chem., 36(11):1539-1544.

Lettinga, G., W. DeZeeuw, and E. Ouborg. 1981. Anaerobic treatment of wastes containing methanol and higher alcohols, Water Res., 15:171-178.

Lion, L.W., Stauffer, T.B., and W.G. MacIntyre. 1990. Sorption of hydrophobic compounds on aquifer materials: analysis methods and the effect of organic carbon. J. Cont. Hyd., 5(3):215-234.

Luthy, R.G., A. Ramaswaml, S. Ghoshal, and W. Merkel. 1993. Interfacial film in coal tar nonaqueous-phase liquid-water systems. Environ. Sci. Technol. 27:2914-2918.

Macedo, E.A., Weidlich, U., Gmehling, J., and P. Rasmussen. 1983. Vapor-liquid equilibria by UNIFAC group contribution. Revision and Extension. 3 Ind. Eng. Chem. Process Des. Dev., 22:678-681.

Mackay, D., W.Y. Shiu, A. Maijanen and S. Feenstra. 1991. Dissolution of non-aqueous phase liquids in groundwater. J. Cont. Hyd., 8:23-42.

Mackay, D.M., J.A. Cherry. 1989. Groundwater contamination: Pump-and-treat remediation. Environ. Sci. Technol. 23:630-636.

Mackay, D., W.Y. Shiu. 1977. Aqueous solubility of Polynuclear Aromatic Hydrocarbons. J. Chem. Eng. Data, 22, 4:399-402.

Magnussen, T., Rasmussen, P., and A. Fredenslund. 1981. UNIFAC parameter table for prediction of liquid-liquid equilibria. Ind. Eng. Chem. Process Des. Dev., 20:331-339.

Maruya, K.A., Risebrough, R.W., and A.J. Horne. 1996. Partitioning of polynuclear aromatic hydrocarbons between sediments from San Francisco Bay and their pore waters. Environ. Sci. Technol., 30(10):2942-2947.

Meyers S.L., C.L. Wright, C.M. Lee, R.W. Falta, and J.T. Coates. 1997. Effect of co-solvent flooding on partitioning tracer behavior, 213th ACS National Meeting San Francisco, California. 37(1):249

Miller, M.M., P. Wasik, G-L. Huang, W.-Y Shiu, and D. Mackay. 1985. Relationships between octanol-water partition coefficients and aqueous solubility. Envir. Sci. Tech., 19:522-529.

McAcliffe, C. 1967. Solubility in water of normal C9 and C10 alkane hydrocarbons. Science, Vol. 163: 478-479.

Morris, K.R., R. Abramowits, R. Pinal, P. Davis, and S.H. Yalkowsky. 1988. Solubility of aromatic pollutants in mixed solvents. Chemosphere 17: 285-298

Mukherji, S., Peters, C.A., and W.J. Weber. 1997. Mass transfer of polynuclear aromatic hydrocarbons from complex DNAPL mixtures. Environ. Sci. Technol., 31:416-423.

Munz, C. and P.V. Roberts. 1986. Effects of solute concentration and cosolvents on the aqueous activity coefficient of halogenated hydrocarbons. Environ. Sci. Technol., 20(8):830-836.

Nelson, E.D., S. Ghoshal, J.C. Edwards, G.X. Marsh, and R.G. Luthy. 1996. Chemical characterization of coal tar-water interfacial filem. Environ. Sci. Technol., 30: 1014-1022.

Nkedi-Kizza, P., P.S.C., Rao, and A.G. Hornsby. 1987. Influence of organic cosolvents on leaching of hydophobic organic chemicals through soils. Environ. Sci. Technol. 21:1107-1111.

Nkedi-Kizza, P., P.S.C., Rao, and A.G. Hornsby. 1985. Influence of organic cosolvents on sorption of hydophobic organic chemicals by soils. Environ. Sci. Technol. 19:975-979.

Novak, J.T., C.D. Goldsmith, R.E. Benoit, and J.H. O'Brien. 1985. Biodegradation of methanol and tertiary butyl alcohol in subsurface systems. In: Degradation, Retention, and Dispersion of Pollutants in Ground Water. Inter. Assoc. Water Pollution Control Research, Great Britain, pp. 71-85.

National Research council (NRC). 1994. Alternatives for Groundwater cleanup. Washington, D.C.: National Academy Press.

National Research council (NRC). 1997. Innovations in Ground Water and Soil Cleanup. Washington, D.C.: National Academy Press.

Picel, K.C., Stamoudis, V.C., and M.S. Simmons. 1988. Distribution coefficients for chemical components of a coal-oil/water system. Water Res., 22(9):1189-1199.

Pinal, R., P.S.C. Rao, L.S. Lee and P.V. Cline. 1990. Cosolvency of partially miscible organic solvents on the solubility of hydrophobic organic chemicals. Environ. Sci. Technol. 24: 639-647.

Pope, G.A., M. Jin, V. Dwarakanath, B.A. Rouse, and K. Sepehrnori. 1995. Partitioning tracer test to characterize organic contaminants. Proceeding of the 2nd Tracers Workshop, Austin TX.

Pope, G.A., K. Sepehrnoori, B.A. Rouse, V. Dwarakanath, M. Jin, A. Abubakar, and M.H. Lim. 1994. Laboratory experiments for NAPL partitioning tracer test in OU1 test cell at Hill Air Force Base, Utah. EPA Contract Report.

Power, S.E., L.M. Abriola, and W.J Weber. 1992. An experimental investigation of nonaqueous phase liquid dissolution in saturated subsurface systems: steady stat mass transfer rates. Water Resour. Res. 28:2691-2705.

Prausnitz, J.M., T.F. Anderson, E.A. Grens, C.A. Eckert, R. Hseieh, and J.P. O'connell. 1980. Computer calculations for Multicomponent vapor-liquid and Liquid-Liquid equilibria, Inc. Englewood Cliffs, N.J.

Puig, J.E., L.E. Scriven, H.T. Davis, and W.G. Miller. 1982. Fluid microstructures and enhanced oil recovery. In: Interfacial Phenomena in Enhanced Oil Recovery, D. Wasan and A. Payatakes, eds., Amer. Inst. Chem. Eng., New York, NY. pp. 1-27

Rao, P.S.C., M.D. Annable, R.K. Sillan, and D. Dai, K.H. Hatfield, W.D. Graham, A.L Wood and C.G. Enfield. 1997. Field-scale evaluation of in-situ cosolvent flushing for remediation of an unconfined aquifer contaminated with a complex LNAPL. Water Resources Research.

Rao, P.S.C., L.S. Lee and R. Pinal. 1990. Cosolvency and sorption of hydrophobic organic chemicals. Environ. Sci. Technol. 24:647-654.

Rao. P.S.C., A.G. Hornsby, D.P Kilcrease and P.J. Nkedi-Kizza. 1985. Sorption and transport of hydrophobic organic chemicals in aqueous and mixed solvent systems: Model development and preliminary evaluation. J. Environ. Qual. 14:376-383.

Rubino, J.T., S.H. Yalkowsky. 1987a. Cosolvency and cosovent polarity. Pharmaceutical Research, 4(3):220-230.

Rubino, J.T., S.H. Yalkowsky. 1987b. Cosolvency and deviations from log-linear solubilization. Pharmaceutical Research, 4(3):231-236.

Rubino, J.T., S.H. Yalkowsky. 1987c. Solubility by cosolvents IV: Benzocaine, diszepam and phenytoin in aprotic sovent-water mixtures. J. Parrenteral Sci. & Tech., 41: 172-176.

Rubino, J.T., S.H. Yalkowsky. 1985. Solubilization by cosolvents III: Diazepam and Benzocaine in binary solvents. J. Parent. Sci. Technol., 39 (3): 106-111.

Rubino, J.T., S.H. Yalkowsky. 1984. Solubilization by cosolvents II: Phenyton in binary and ternary solvents. J. Parent. Sci. Technol., 38 (6): 215-221.

Sanemasa, I.; Miyazaki, Y.; Arakawa, S.; Kumamaru, M.; Degughi, T. The solubility of benzene-hydrocarbon binary-mixtures in water. Bull. Chem. Soc. Jpn. 1987, 60, 517-523.

Saripalli, K.P., 1996. Use of Interfacial Tracers For characterization of Nonaqueous Phase Liquid (NAPL) Distribution in Porous Media. Dissertation University of Florida, pp 201.

Sawheny, B.L., J.J. Pignatello, and S.M. Steinberg. 1988. Determination of 1,2-dibromoethane (EDB) in field soils: implications for volatile organic compounds. J. Environ. Qual., 17:149-156.

Schellenberg, K., Leuenberger, C., and R.P. Schwerzenbach. 1984. Sorption of chlorinated phenols by natural sediments and aquifer materials. Environ. Sci. Technol., 18(9):652-657

Schwarzenbach, R.P., P.M. Gschwend and D.M. Imdoden. 1992. Environmental Organic Chemistry. pp. 76-108. John Wiley & Sons, Inc

Schwarzenbach, R.P., and J. Westall, 1981. Transport of nonpolar organic compounds from surface water to groundwater: Laboratory sorption studies. Environ, Sci. Technol.,15,1360-1367

Schwille, F. 1988. Dense Chlorinated Solvents in Porous and Facutured Media. Lewis (Chelsea, MI) 146 pp.

Sillan, R.K., P.S.C. Rao, M.D. Annable,. and D. Dai, K.H. Hatfield, W.D. Graham and A.L Wood. Evaluation of in-situ cosolvent flushing dynamics using a network of spatially-distributed multi-level samples. Water Resour. Res.

Skjold, S., B. Kolbe, J. Gmehling, and P. Ramusen. 1979. Vapor-liquid equilibria by UNIFAC group contribution. Revision and extension. Ind. Eng. Chem. Precess Des. Den. Sci. Technol., 19:522-529.

Van der Warden, M., A.L.A.M. Bridié, and W.M. Groenewoud. 1971. Transport of mineral oil components to groundwater, 1. Model experiments on the transfer of hydrocarbon from a residual oil zone to trickling water. Water Res. 5:213-226.

Verschueren, K. 1983. Handbook of Environmental Data of Organic Chemicals, 2nd ed. Van Nostrand Reinhold Company, New York, NY

Wilson, J. L., S. H. Conrad, W.R. Mason, W. Peplinski, and E. Hagan. 1990. Laboratory Investigation of Residual Organics from Spills, Leaks, and the Disposal of Hazardous Wastes in Groundwater. EPA/600/6-90/004 U.S. EPA 267 pp.

Wilson, R.D., and Mackay, D.M., 1995. Direct detection of residual nonaqueous phase liquid in the saturated nonaqueous phase liquid in the saturated zone using SF6 as a partitioning tracer. Envir. Sci. Tech., 29 (5): 1255-1258

Wise, W. 1997. NAPL Characterization via partitioning tracer tests: Quantifying effects of partitioning nonlinearities. Submitted to Journal of Contaminant Hydrology.

Wise, W., and E.A. Fitzpatrick. 1997. NAPL Characterization via partitioning tracer tests:: A modified langmuir relation to describe partitioning nonlinearities. Submitted to Journal of Contaminant Hydrology.

Wood, A.L., Bouvhard, M.L. Brusseau, and P.S.C Rao. 1990. Cosolvent effect on sorption and mobility of organic contaminants in soils. Chemosphere, 21: 575-587

Yalkowsky, S.H. and S. Banerjee. 1992. Aqueous Solubility Methods of Estimation for Organic Compounds. Marcel Dekker, INC. New York. pp 41-124.

Yalkowsky, S.H. 1987. Solubility of organic solutes in mixed aqueous solvents. Project Completion report, CR# 812581-01. U.S. Environmental Protection Agency, Ada. OK.

Yalkowsky, S.H. 1985. Solubility of organic solutes in mixed aqueous solvents. Project Completion report, CR# 811852-01. U.S. Environmental Protection Agency, Ada. OK.

Yalkowsky, S.H. and J.T. Rubino. 1984. Solubilization by coslvents I: Organic solutes in propylene glycol-water mixtures. J. of Pharm. Sci.. 74:416-421.

Yalkowsky, S.H. and T. Roseman. 1981. Solubilization of drugs by cosolvents IN: Techniques of solubilization of Drugs, S.H. Yalkowsky (Ed.). Marcel Dekker, Inc., New York, NY, pp 91-134.

Yalkowsky, S.H. and S.C. Valvani. 1980. Solubility and partitioning I: solubility of nonelectrolytes in water. J. Pharm. Sci., 69: 912-922.

BIOGRAPHICAL SKETCH

Dongping Dai was born on August 26, 1961, in Hangzhou, China. In 1983, she received a B.S. degree in Soil and Agro-chemistry from Zhejiang Agricultural University in Hangzhou, China. Right after graduation, she began to work as an Assistant Researcher in the Institute of Soil and Fertilizer, Zhejiang Academy of Agriculture. In January 1990, she started her graduate study in Agronomy and Soil Science Department at the University of Hawaii. She was married in May 1990 to Xiaokuang Lai. Later that year, she moved to Gainesville, Florida, and continued her graduate study in Soil and Water Science Department, University of Florida and completed a master's degree in science in May 1993. She has one lovely daughter, Diana Lai, born in 1994.

After receiving her master's degree, Dongping worked as a Senior Chemist and Lab Manager in Dr. Rao's lab in Soil and Water Science Department at UF. On a half-time basis, she initiated and studied in a Ph.D program in environmental chemistry and in an Interdisciplinary Graduate Program in Hydrologic Science.

I certify that I have read this study and that in my opinion it conforms to acceptable standards of scholarly presentation and is fully adequate, in scope and quality, as a dissertation for the degree of Doctor of Philosophy.

P. Suresh C. Rao, Chair
Graduate Research Professor of
Soil and Water Science

I certify that I have read this study and that in my opinion it conforms to acceptable standards of scholarly presentation and is fully adequate, in scope and quality, as a dissertation for the degree of Doctor of Philosophy.

R. Dean Rhue
Professor of
Soil and Water Science

I certify that I have read this study and that in my opinion it conforms to acceptable standards of scholarly presentation and is fully adequate, in scope and quality, as a dissertation for the degree of Doctor of Philosophy.

Willie G. Harris
Professor of
Soil and Water Science

I certify that I have read this study and that in my opinion it conforms to acceptable standards of scholarly presentation and is fully adequate, in scope and quality, as a dissertation for the degree of Doctor of Philosophy.

Michael D. Annable
Assistant Professor of
Environmental Engineering Sciences

I certify that I have read this study and that in my opinion it conforms to acceptable standards of scholarly presentation and is fully adequate, in scope and quality, as a dissertation for the degree of Doctor of Philosophy.

Robert T. Kennedy
Associate Professor of
Chemistry

This dissertation was submitted to the Graduate Faculty of the College of Agriculture and to the Graduate School and was accepted as partial fulfillment of the requirements for the degree of Doctor of Philosophy.

December 1997

Dean, College of Agriculture

Dean, Graduate School